Fast, Large, and Accurate 3D Printing

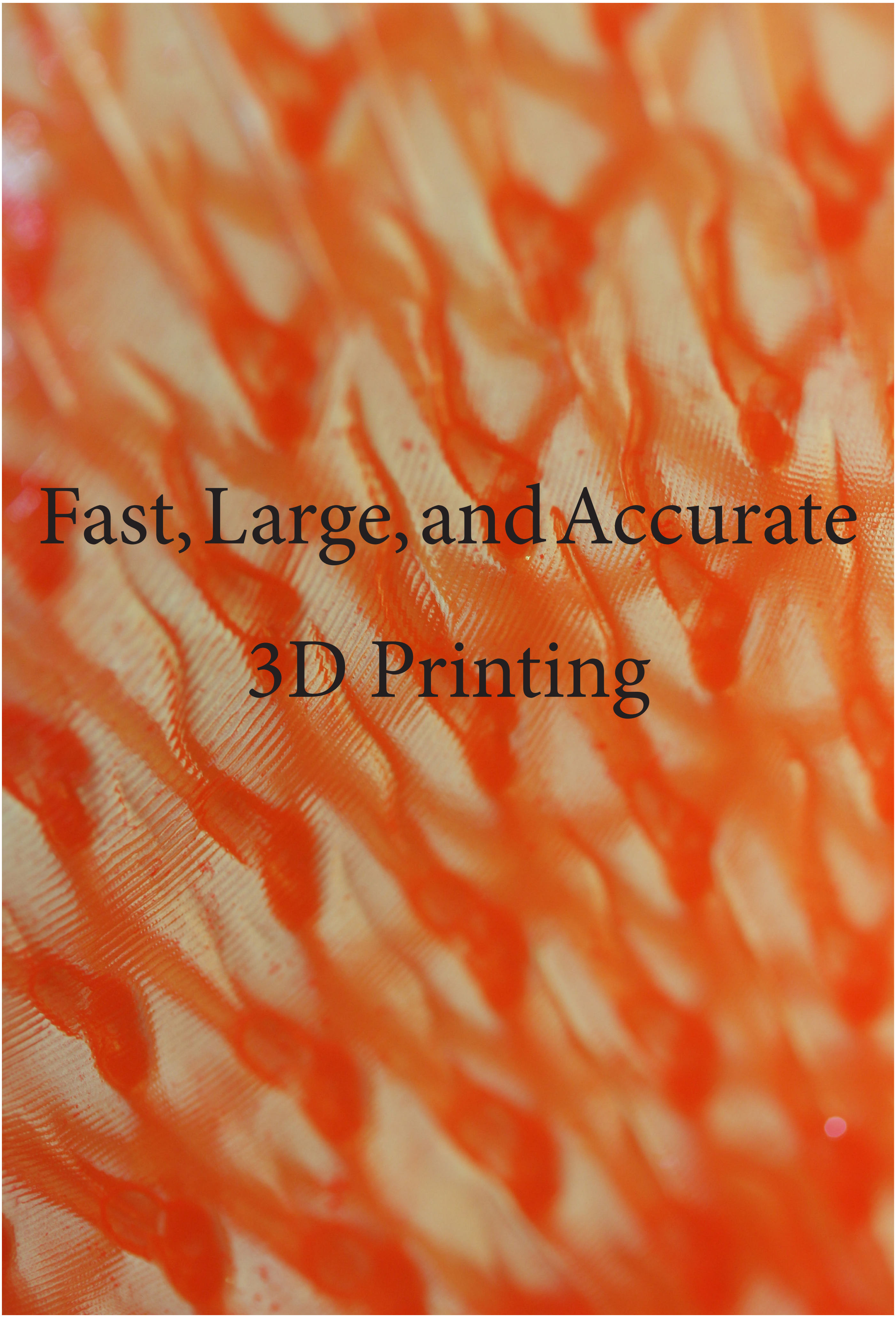

Fast, Large, and Accurate 3D Printing

Jesse Kilpatrick

A 90 point thesis submitted in fulfilment of the requirements for the degree of Master of Design Innovation

Victoria University of Wellington
School of Design

2022

Acknowledgements

First, I'd like to thank my supervisors. Ross Stevens - for putting me on the cutting edge of 3D printing in New Zealand. Simon Fraser - for depth of insight and weight of experience.

I would also like to thank Katie O'Brien, for being so patient with my Adobe problems; Tyler Harlen and Zach Challies for getting me past some serious stumbling blocks in Grasshopper.

Finally, I'd like to thank the rest of my Industrial Design cohort, without whose camaraderie I would have been overwhelmed.

Abstract

To achieve the goal of fast and large 3D printing at high resolutions, certain other criteria must be met. First, the method of printing should have good baselines for printing speed, build volume, and resolution. This excludes FDM printing, (slow, poor z-axis resolution) SLA printing (slow, small build volume in commercial-grade printers) and SLS/SLM methods (slow). Niche methods can be similarly counted out. What remains is DLP printing - specifically top-down DLP printing using multiple projectors, because that enables continuous printing over a wide area.

Second, the limitations of DLP need to be mitigated. These limitations primarily stem from problems associated with resin flow and overzealous curing. Printing thick features requires resin to move further over the already-printed surface; when it fails to do so this results in resin starvation, which is a print failure. Printing thin is a solution.

However, printing thin has its own issues: DLP printing sets the form of the object, but the partially cured resin remains soft and flexible, meaning it can warp during the print (due to thermal contraction), especially if the print is large – again causing print failure. To solve this problem, this research is focusing on co-opting a strength of DLP printing – printing lattice structures. By attaching a conforming lattice to one side of a thin surface, the argument is that this will reinforce it enough to give it the strength it would have if printed slower and thicker, prevent print failures, and maintain maximum print speeds. As such, this solution is related to design for additive manufacturing best practice.

Rhino and Grasshopper have been utilised to develop an algorithm which can apply reinforcement to a surface, with the traits of that reinforcement being manipulable by the user. Test prints using basic surfaces have been used to determine the printability of a series of different reinforcement structures. The optimal reinforcement techniques have then been applied to case study objects to demonstrate the ones that can be printed fast, large, and accurately – and potentially improved by structural reinforcement.

Contents

Introduction

This research portfolio is a record of the development of a prototypical technique intended to enable 3D printing that simultaneously satisfies three usually mutually exclusive criteria: Fast, Large, and Accurate 3D printing. In order to do that, a printing method that can already satisfy each of the criteria individually, or any two at once, was used - DLP printing. DLP (Digital Light Processing) is an acronym derived from the use of an eponymous component within projectors used by the type of printers in question. The technique developed was reached by introducing a restrictive criterion: the printed objects must be thin (in terms of cross-sectional area), and therefore derive rigidity from designed structure rather than mass. Besides the desirability of printing large objects quickly, at undiminished resolutions, this method has serendipitous auxiliary benefits, such as reduced material consumption.

The technique can be considered a software solution to a hardware problem. That problem is printing objects with large dimensions quickly, without sacrificing z-axis resolution. The reason the solution is a software one is because it relies on the application of a digital algorithm. The problem is a hardware one because it stems from physical constraints imposed by the current capabilities of 3D printing and additive manufacturing machines, and by the laws of physics they (and everything) necessarily obey.

This thesis is divided into three parts, by the methodology used within that part. The first part, methodologically research on design, therefore consists primarily of background research. Here, DLP printing is explained in detail, along with a comparison of it with other 3D printing methods in order to demonstrate the reasoning behind its particular use in this scenario. Additionally, it has a rundown of lattice structures, in order to make evident the logic behind the selection of the reinforcement structures used. Finally, this section has a chapter explaining why the Rhino 3D modelling program's Grasshopper plugin was used to develop the digital algorithm for applying structural reinforcement to a surface, and how related things have been done previously elsewhere. also

The second part includes a brief discussion of the resin used for DLP printing, and the limitations and opportunities provided by its many quirks and characteristics. It focuses on a report on and discussion of the conception and design of the algorithm used and evolution of the software required to develop and digitally apply reinforcement structures to a selected extant or newly designed surface. Written (or rather, drawn) using the Rhino plugin Grasshopper, the algorithm allows for the use of surfaces with a variety of forms, shapes, and number of edges, enabling the reinforcement of widely varied objects. It also enables limited customisation of the reinforcement structure, via manipulation of its type, density, and amplitude. This second section is methodologically research for design.

The third part is devoted to application of the technique. By using the algorithm to generate different reinforcement structures on different surfaces, and printing these, certain qualities and limitations become evident. The discovery and evaluation of these, along with the problems associated with getting them and presented by them, form the basis of this section. The methodology behind this third part is research through design.

Methodology

Collectively, this thesis is predicated on research on, for and through design - in that specific order. First, research on design to construct an overview of 3D printing status quo was conducted, to establish a foundational body of primarily qualitative, but also quantitative where appropriate, knowledge from which to work. It was also used to support the subordinate hypothesis that DLP printing was the best route to take for implementing the primary concept of a technique for simultaneously fast, large, and accurate 3D printing. With the establishment of that body of knowledge, comparison of 3D printing methods, focused on their strengths and, importantly, weaknesses with regard to that triumvirate of desirable traits, became a viable method to determine the suitability of DLP printing, and the avenues of opportunity it provided for the development of a new technique.

Once DLP printing was substantiated, essentially by process of elimination, as the best route to take, research into how the new technique could function was necessary. This revolved around gathering and evaluating information about one of the strengths of many methods of 3D printing and additive manufacturing - the fact that "complexity is free" (Lipson, 2012), and therefore lattices and lattice-type structures are at least feasible and even preferable. On the basis that DLP printing was included among printing methods that excel at producing lattice-type structures, with precedent lattice structures being printed by companies like Carbon as paragons of the virtue of their technology ("Rethinking foam—Carbon's lattice innovation," n.d.), research was conducted into those structures. The idea of using supports to enable viable 3D printed or additively manufactured objects was explored as a source of precedence for procedurally generated structural reinforcement.

The next two stages focused on research for design in the form material research, specifically into the kinds of UV-reactive resin used in DLP printing, and software research to determine which program would be best suited to the design of a tool to add structural reinforcement to the surface of an object.

Software research for design was an extended period of discovery and learning, used to generate and iterate increasingly complex and feature-rich algorithms in Grasshopper, which could then be applied in Rhino. These were designed towards a maximally efficient prototypical technique or proof of concept. It became apparent that Rhino and Grasshopper, while useful for the design phase of file generation, were not able to generate files the printing software could tolerate to an acceptable degree. Therefore, the use of additional software was required - specifically Meshmixer and Netfabb.

With files the printer could use, research through design began in earnest. This consisted of a series of 3D prints, reaching towards the maximum level of complexity the software and hardware available could handle. Each print was then evaluated and the lessons learned taken on board for modification of the design of the object, its file, the lattice structure, or the Grasshopper algorithm if necessary or appropriate.

PART 1: Research On Design

1a) 3D Printing Context Research

The 3D printer or additive manufacturing machine field and marketplace are both large, rapidly growing, and continually evolving. Unfortunately, this means that extensive surveys of all options - commercially available printers and materials - and their capabilities rapidly become obsolete. It is also beyond the scope of this thesis to exhaustively detail the exact specifications as required for such lists, which are available online, for example in the journal Chemical Reviews (Ligon, Liska, Stampfl, Gurr, & Mülhaupt, 2017). For these reasons, a few printers that are archetypal of, or best-in-field for their specific method will be used as exemplars for the purposes of comparison - as a way to establish relativity of the universal key traits. In this way the fundamental processes of each, many of which carry over into similar printing methods, can be shown along with relevant inherent strengths and limitations of those processes. Some 3D printers which possess extraordinary traits in a specific category will also be mentioned. The comparisons happen in the context of the pertinent chapter discussing that individual trait. By contrast, because this thesis specifically deals with it, DLP printing is carefully described in the following chapter to ensure a coherent and valid argument can be made.

Chapter 1) DLP

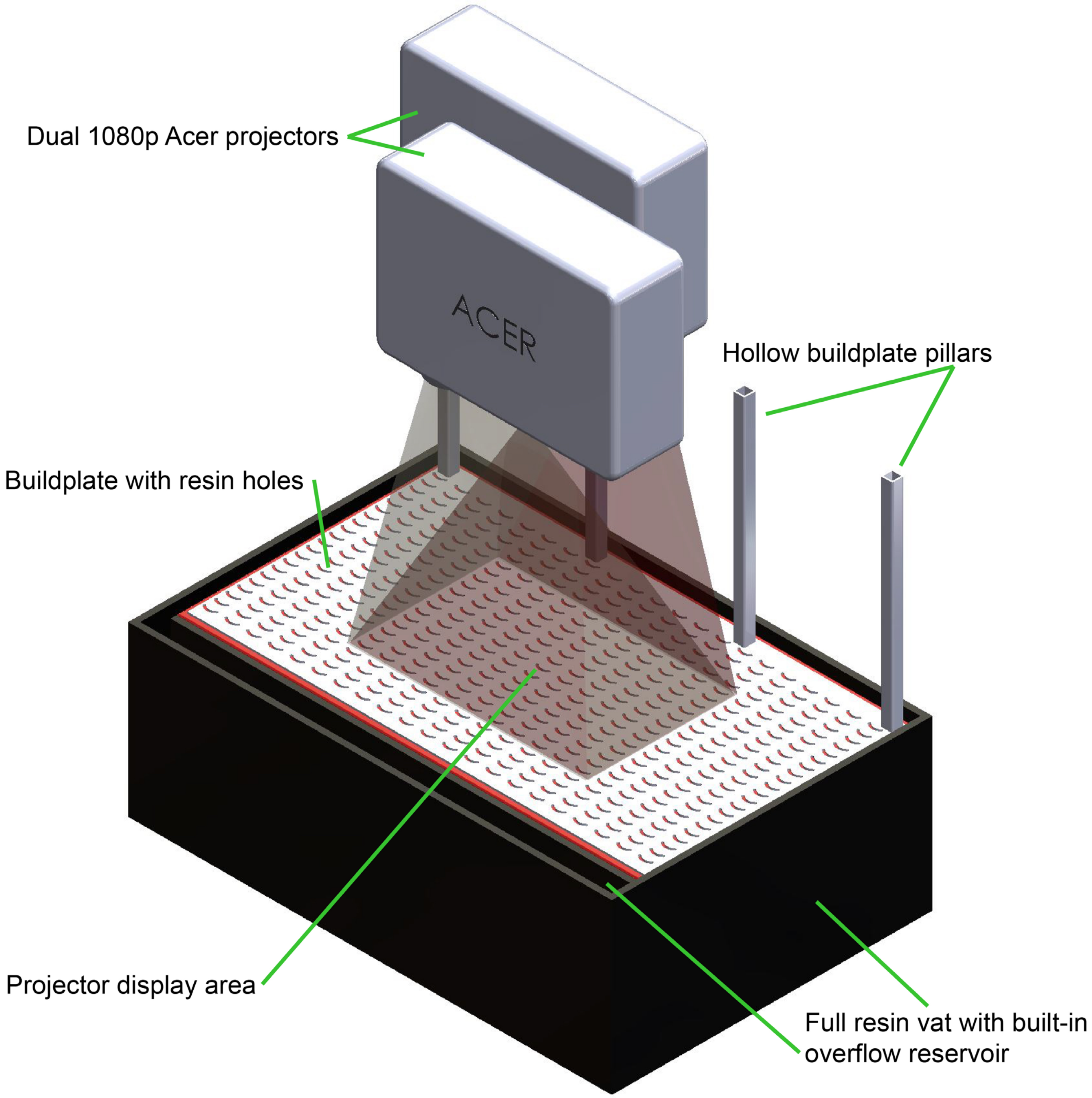

Figure 1: Isometric representation of a Gizimax Ultimate set up with a medium vat.

Figure 2: The first layer is displayed and attaches to the buildplate. UV light, shown in purple, triggers photopolymerisation of the resin where they intersect. This causes it to transform from a liquid to a solid. Liquid resin flows through holes in the buildplate, and into the buildplate pillars, which are hollow to minimise their displacement.

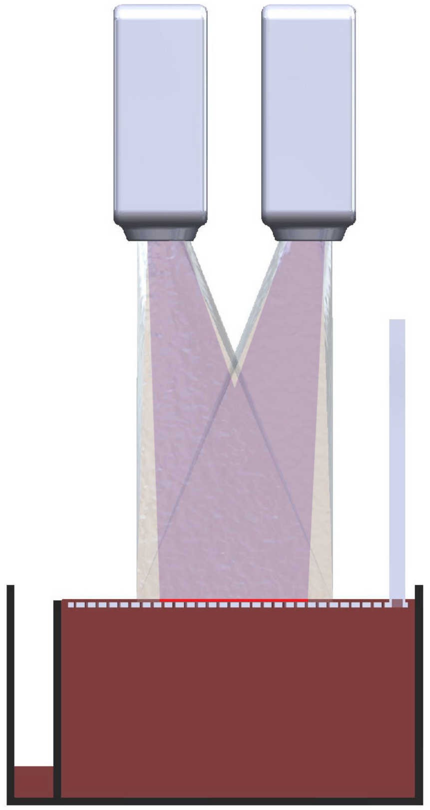

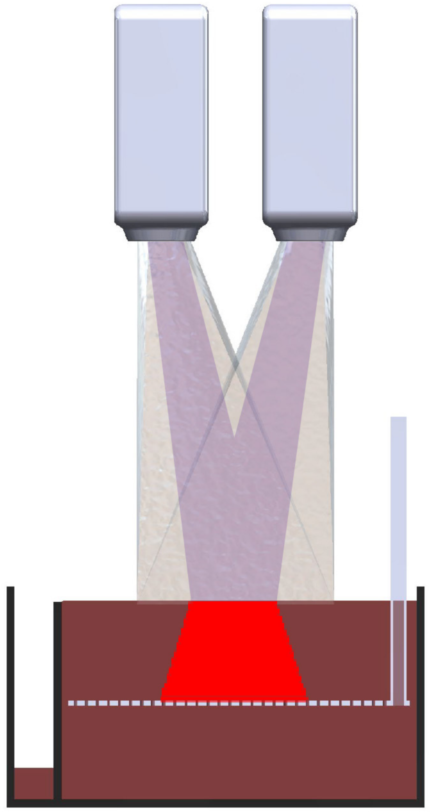

Figure 3: The buildplate descends into the vat as the print progresses. Consecutive layers are displayed and harden on top of the previous layer. The rest of the display area, though lit, does not contain UV light and therefore does not cause the resin to react.

Figure 4: As the buildplate and the printed layers descend, liquid resin flows over the surface, hardening when it contacts the displayed UV image.The resin level stays the same throughout the print, because any displacement caused by the buildplate pillars is negated by the fact that the displaced resin can overflow into the overflow reservoir.

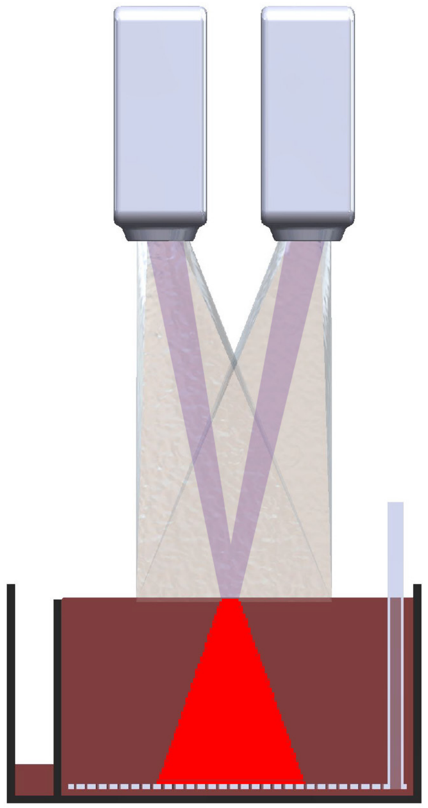

DLP printers typically come in one of two arrangements, referred to as bottom-up and top-down. Both orientations feature in the original stereolithography patent (US4575330A, 1986). The type detailed in the diagrams above is the latter, meaning the buildplate starts at the top of the resin and moves down into it during the printing process. These, and Figure 5, below, are of the Gizmo3D Gizimax Ultimate ("Gizmo 3D Printers," n.d.), at the School of Architecture and Design at Victoria University of Wellington.

The enclosure and UV post-curing box seen in Figure 5 are aftermarket additions made in house at the School of Design. The enclosure has active extraction. This particular model is no longer available to purchase, but came with three vat sizes and two off-the-shelf Acer 1080p projectors ("H6510BD," n.d.). The small vat can utilise only one of the projectors. The medium vat, shown in Figure 1-Figure 5, can use both. The large vat has the same width (x axis) and depth (y axis) dimensions as the medium vat, but is 800mm high (z axis) and also uses both projectors.

Newer versions (as seen on the website at time of writing) use a single powerful dedicated UV projector, rather than an alignment of two full spectrum projectors. When printing, the two projectors display the same image at the same time, effectively doubling the amount of UV light hitting the resin. Because each slice of the file being printed is displayed in its entirety to solidify each layer, the projectors are essentially projecting an animation of the object, like a CAT scan, with a very slow frame rate. As seen in Figure 6, each slice is actually a PNG image file, with the cross-section of that particular layer in white and the remainder in black.

Figure 5: Gizimax Ultimate with medium vat equipped; large vat to the right to show size. The UV post-curing box sits in the space the large vat would occupy were it in use.

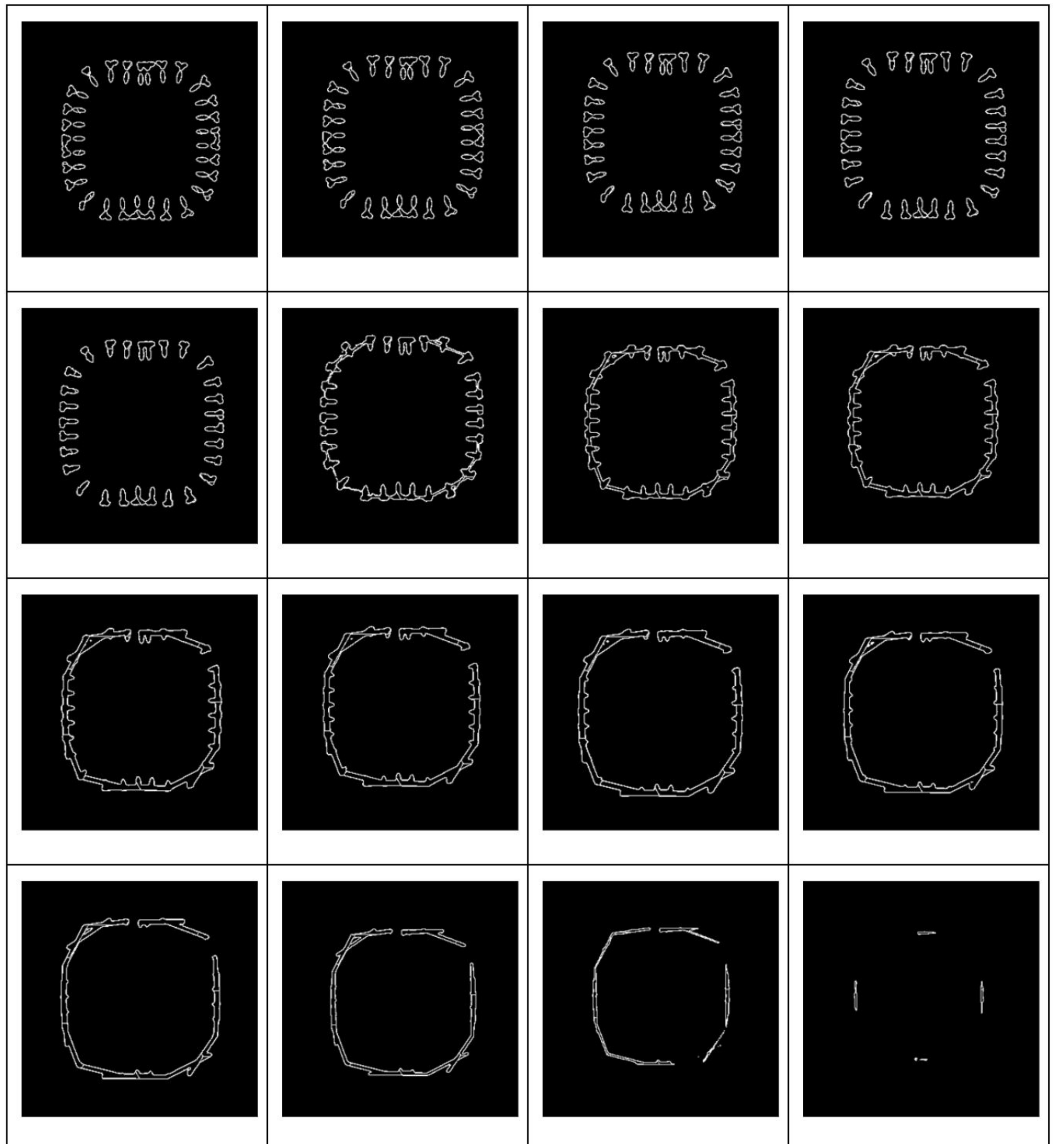

Figure 6: The final 16 slices/images displayed of a 50μm z-axis resolution print.

Chapter 2) Fast

Figure 7: SLA diagram showing print in progress, with laser, mirror, vat, and partially completed layer attached to vat bottom.

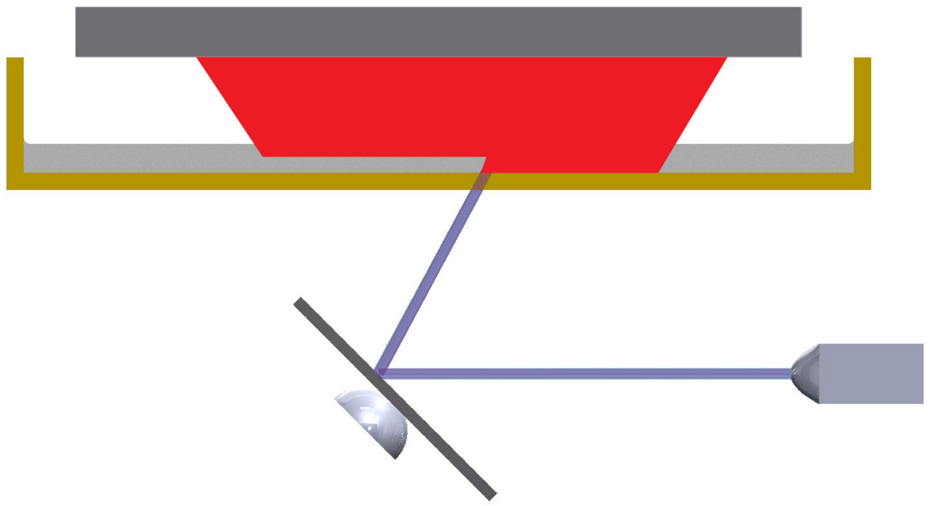

Figure 8: CLIP schematic showing 'Digital Light Synthesis engine' projector, oxygenated resin 'dead zone' and entire layer being cured.

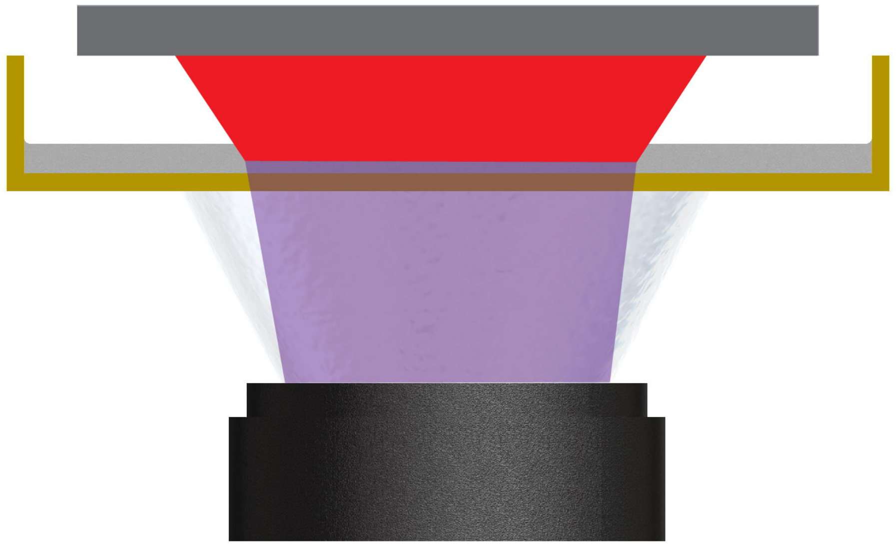

What speed refers to in the context of 3D printing is the rate at which matter can be transformed from its raw material state of polymer (for example) feedstock, whether that be a reel of plastic, a vat or tray of liquid resin, or a bed of powdered plastic, into the ordered form of a digitally designated object. All of the common methods of additively producing a three dimensional object work by building up an object layer by layer. DLP printing has the capability to be fundamentally faster than most other methods of 3D printing/additive manufacturing due to the nature of the print process.

FDM (Fused Deposition Modelling) works by drawing each layer with plastic extruded from a nozzle - a point-based process. As a benchmark for FDM, the Tiertime UP! Box+, which is the most common 3D printer at Victoria, has a maximum print speed of 100mm/s and a nozzle diameter of 0.4mm ("Tiertime UP BOX+ 3D Printer," n.d.). With these numbers it can be calculated that the maximum volume of plastic that the printer can extrude while printing is 12.57mm3/s, which seems like a lot until you realise it's only 45.252mL/hr.

Similarly, SLA (Stereolithography Apparatus), as seen in Figure 7, SLS (Selective Laser Sintering) and SLM (Selective Laser Melting) processes draw each layer with a laser - more point-based methods. As a benchmark for SLA, the Formlabs Form 2 can print 1-3cm/hr on the z-axis at 100μm layer heights ("Frequently Asked Questions | Formlabs," n.d.). While a laser can scan much faster than a nozzle can move, the Form 2 is limited by the fact that, because it is a resin-based bottom-up type machine, each layer must be peeled off the bottom of the resin tray and fresh resin wiped across it. Similarly in SLS and SLM, which are powder-based top-down methods, fresh powder must be rolled onto the previous layer ready to be sintered for the next one. Line-based methods, such as polyjet and binder-jetting methods suffer from similar penalties. For example, for each layer in an Objet Connex 3D printer, such as the one at the School of Design, the print head must make at least two passes (left-right, and then right-left to return); more passes must be made if the objects being printed cover more area on the build tray than the head can cover with the first pair.

These extra steps between layer building are time-consuming and present limiting factors in these methods, drastically lengthening their respective printing times. On the other hand, Carbon's process, as seen in Figure 8 ("Process," n.d.), what they call CLIP (Continuous Liquid Interface Production), uses a projector and avoids the peeling/wiping penalty despite being a bottom-up method (Tumbleston et al., 2015). It is the continuity of actual printing, uninterrupted by detachment or resin refreshment steps, coupled with the ability to cure an entire layer at once, that make these printing methods so much faster.

CLIP is an equivalent of top-down continuous DLP

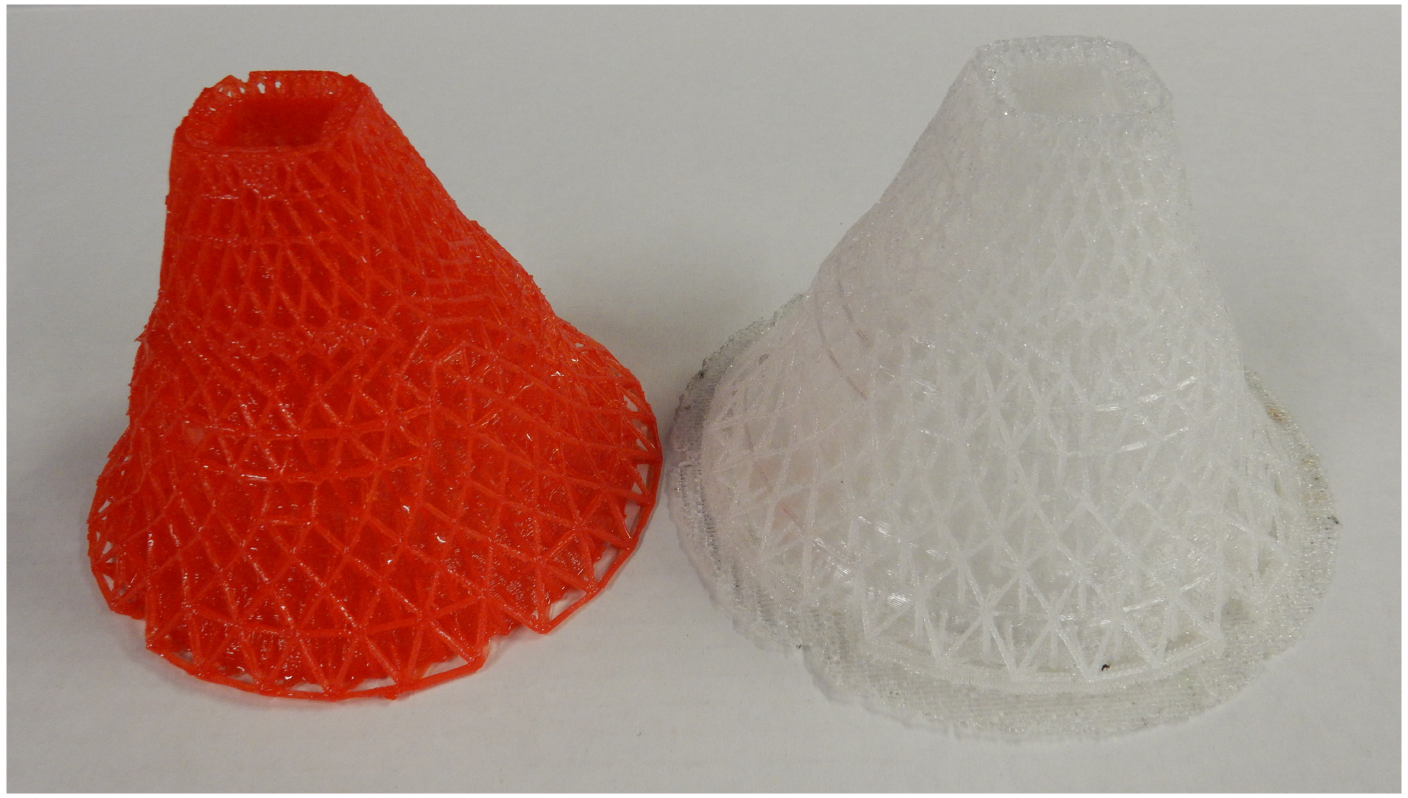

Figure 9: A DLP print (left) and an FDM print, of the same digital model. The DLP print was printed at ***0.05mm*** *z-axis resolution in* ***1.5 hours****. The FDM print was printed at* ***0.25mm*** *z-axis resolution and took* ***6.5 hours****.*

printing, like the continuous mode on the Gizimax, and currently has a speed advantage. It can be posited that this is due to the suction effect of the printed part moving up, drawing fresh resin into the space it occupied as it moves (Tumbleston et al., 2015, p. 1349). However, there are several issues with that argument due to the problematic nature of the suction effect. Coupled with the requirement to maintain a curing-inhibiting oxygenated resin 'dead zone' that is only "tens of micrometers" thick (Tumbleston et al., 2015, p. 1349) between the object being printed and the window below to prevent attachment to the "Teflon AF film" (Ligon, Liska, Stampfl, Gurr, & Mülhaupt, 2017, p. 10219) that window consists of, the suction effect may prove to be a hurdle for future hardware development that the top-down method can avoid. Companies using similar bottom-up continuous methods have begun to surface, without the requirement of an oxygen-permeable membrane to enable the 'dead zone'. This indicates Carbon may not hold the fastest commercially available printer crown for long. Newpro3D and Sprybuild are examples of these companies ("NewPro 3D," n.d., "Sprybuild," n.d.).

Top-down continuous DLP does not have any suction effect to pull resin to where it needs to be, which gives one of two predominant factors limiting its speed. First, there is the rate at which fresh resin can flow across the previously cured layer as the print descends into the resin; second, the speed at which it cures once exposed to UV. The former means that resins with lower viscosity and surface tension enable faster printing, because they will flow more rapidly and a form a shallower, weaker meniscus. Ligon et al. describe "[v]iscosity and wetting behavior of the resin onto the solidified part [as] both of critical importance" (2017, p. 10221). They also note that these resin traits can be improved through the use of diluents (Ligon, Liska, Stampfl, Gurr, & Mülhaupt, 2017, p. 10223), for example as produced by 3Dresyn ("Thinner 3Dresyn H 'Hard diluent,'" n.d.). Additionally, it should be mentioned that Tauböck, Tarle, Marovic, & Attin note that heating resin can reduce viscosity in addition to other beneficial effects (2015, p. 1358). During the course of this thesis ambient printer room temperature was maintained at 19ºC and no resin heater was used, due to University safety protocols and for consistency.

Curing speed of resin is an important limiting factor for continuous printing because it necessitates a Goldilocks-esque balance between high curing rate and resin flow through areas exposed to UV. A faster curing rate logically requires shorter image display times and therefore enables faster prints, but if it's too high, rather than just right, the resin will cure before or as it flows to its destination. This can cause a dam effect and is one of the problems associated with DLP printing that lead to resin starvation holes in the print. Resin starvation is a print failure where, because of the aforementioned dam effect, premature or over-zealous curing due to resin viscosity or

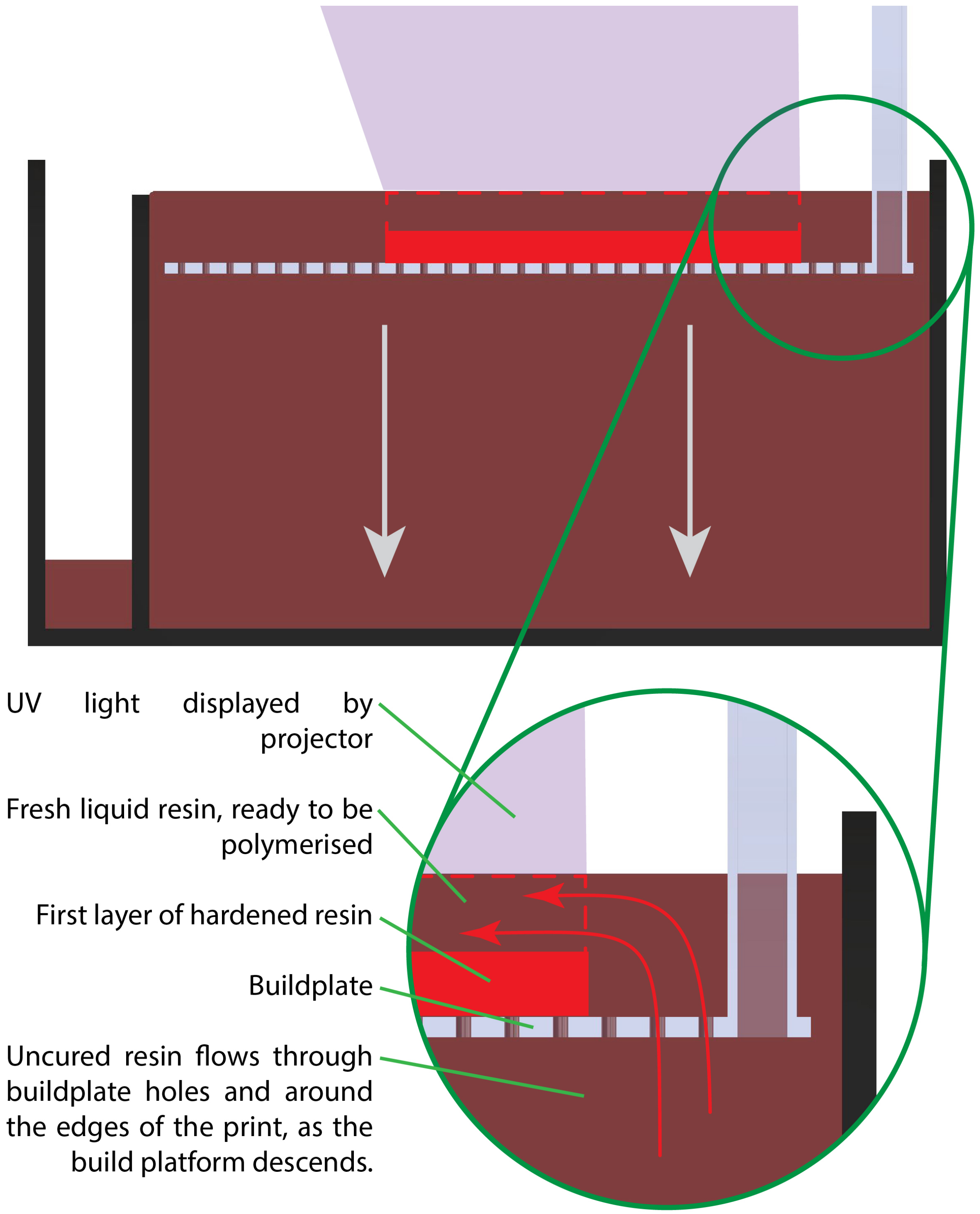

Figure 10: Resin flow during a print.

projector settings, the topography or orientation of the print, or insufficient z-axis motion, liquid resin cannot reach its intended location. See Figure 11 for a diagram of one type of resin starvation.

In summation, methods of 3D printing that can produce an entire layer at once, and do so continuously, are fundamentally faster than those that are point-based or line-based, and methods that involve peeling/wiping stages which interrupt actual printing. Resin properties and behaviour also have a prominent effect on speed.

Chapter 3) Large

For 3D printers, the size they can print at is often the primary marketing specification, used as a mark of distinction, and the initial statistic used as a point of comparison (“Compare 3D Printers,” n.d.). It is generally calculated by maximum build volume. That is, the area of the build platform, multiplied by the distance that the build platform or the printing apparatus can travel. In other words, width x depth x height, or r2 x height for 3D printers with circular build platforms.

FDM-style printers can be very large - big enough to print buildings, using concrete slurries in place of reels of plastic. The BigRep One, at the School of Design, which is a dual-headed plastic FDM printer, has a build volume of over one cubic meter (“BigRep ONE,” n.d.). Similarly, industrial-grade SLA machines can have very large build volumes. Because volume when printing is a function of xy area multiplied by height, printers with a small build area can still have enormous build volumes if the range of motion of the build platform is very high. Bottom-up printers have an advantage here, since their resin vats can remain very shallow and self-refilling. FDM printers can also take advantage of a tall z-stage.

Commercial-grade machines, ones that are suitable for an office or University environment, for example, tend to be a lot smaller. The Gizimax Ultimate, while somewhat problematic for those environments due to resin odor issues, actually has a maximum build volume on par with large industrial grade DLP machines (“ProMaker L7000 D,” n.d.), thanks to the height of its large vat. That particular Prodways machine also features two DLP heads, although it uses them in a different way and they are a different type, using LEDs. This is the key to large printing, however: scale, and modularity. The Gizimax Ultimate at the School of Design has two projectors already, as mentioned earlier and shown in Figures 1-5. Gizmo3D’s co-founder, Kobus du Toit, holds a patent, which describes a method for aligning images from “a plurality” of projectors to improve 3D printing (WO2016179661A1, 2016).

Having switched to using more powerful UV projectors, the obvious way to scale up in a modular way would be by splitting an image into parts and having multiple projectors aligned in parallel, to each display a section of every layer. This option for future development will not work with bottom-up technology that requires a 100µm thick membrane display window (Ligon, Liska, Stampfl, Gurr, & Mülhaupt, 2017, p. 10219), which must be maintained at significant tension with a tensioning ring (WO2014126837A2, 2014). Sagging in the membrane can cause optical distortion of the displayed image.

The volume of resin required to fill a vat suitable for such a printer would be very expensive, although existing industrial-grade top-down machines do so. However, due to the popularity of 3D printing in hobbyist circles, many users of top-down machines are exploring methods of floating the resin in a vat on another, cheaper and denser fluid, such as glycerine or a saturated salt solution (Brigante Design, n.d.). Kobus has also conducted some preliminary research on this front ("Testing of Glycerin/Glycerol/Glycerine," n.d.).

Unfortunately, the volume-based metric used to calculate the build volume a printer is capable of can be very misleading, and is more of a theoretical maximum, because most printers will struggle to take full advantage of those apparent dimensions. This is for a variety of reasons, which differ based on the type of printing in question.

One near-universal problem involved with printing large objects, and with objects that have a large mass in particular, is shrinkage caused by thermal contraction. Heat is either used, as in FDM and SLS, for example, or generated, such as during photopolymerisation, throughout the duration of most printing processes. Due to the thermodynamic action of this heat, thermal contraction forces present in each layer build up over the course of a print and can cause warping and cracking, which are print failures (Bartolo, 2007, p. 480, and Kantaros & Karalekas, 2013, p. 44). These forces can be monumental, especially in materials with qualities such as high thermal capacity or low coefficient of thermal expansion that predispose them to such issues, and depending on the printing process, can be compounded by higher z-axis resolutions, that is, thinner layers (D'Amico, Debaie, & Peterson, 2017, p. 944).

Having already discussed resin flow problems in the previous chapter, it is nonetheless important to note that size - that is, cross-sectional area of a layer - is a common source of resin renewal problems. This is because uncured resin must travel from the edges of a cured area to the centre of that area in order to be there to be cured into the next layer, as shown in Figure 10 and in more detail in Figure 11. This can also be seen in the looped animation of a print in progress on Carbon's website ("Process," n.d.), although they don't show the starvation. It is primarily a problem associated with continuous DLP printing, since continuous printing is a result of a lack of intermediate steps between layer display. One of those steps, for example in the Form 2, is a wiping of fresh resin across the tray bottom after the previous layer has been detached from it. The previously mentioned suction effect is Carbon's solution, but its limit is acknowledged by Tumbleston et al. (2015, p. 1351-1352), and is one of the reasons the Carbon printers build volumes are so small. Currently, there is no method to enable simultaneity of continuous printing and resin renewal with the Gizimax Ultimate. Therefore, top-down DLP printing is unable to continuously print large surface areas. However, this thesis will show that large surface areas are not a prerequisite for large prints, and will demonstrate a novel technique

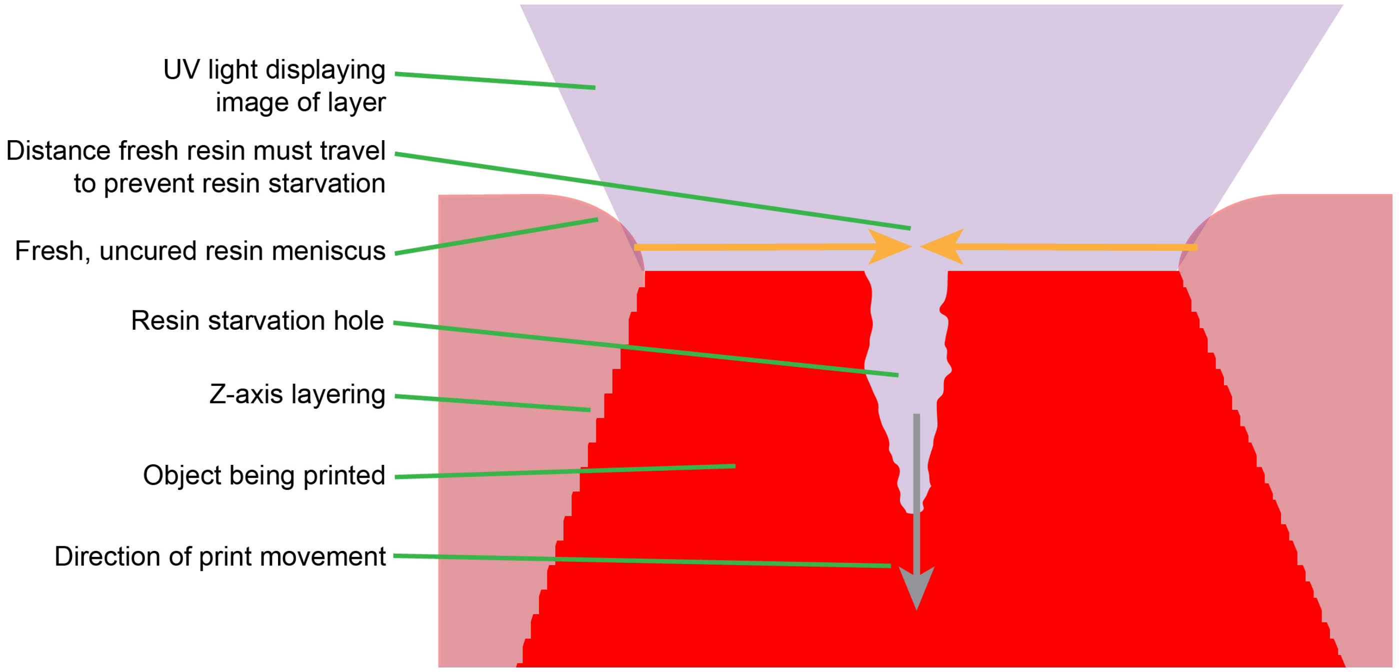

Figure 11: Diagram showing the formation of a meniscus between the surface of uncured resin and the object being printed, and the distance uncured resin must move for each layer to be complete.

designed to avoid such limitations.

So, multiple methods of 3D printing can print large, but nearly all of them are impaired by thermodynamic complications, and the vat polymerisation printers also suffer from problems resulting from issues with resin flow when printing large objects, especially at high speed.

Chapter 4) Accurate

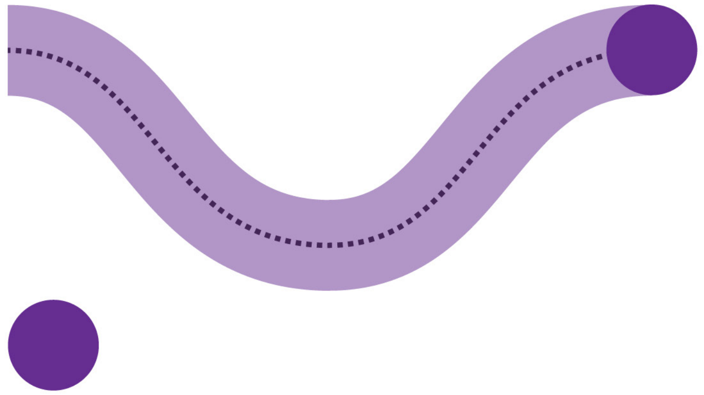

Figure 12: xy-axis view of an SLA laser path and minimum spot size.

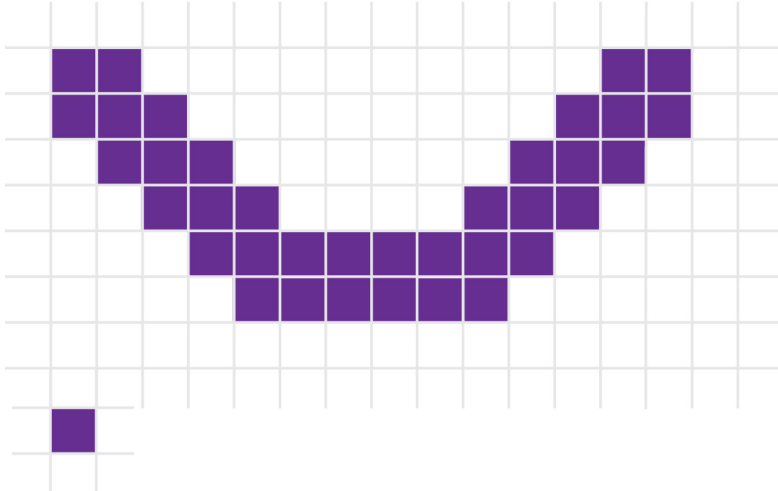

Figure 13: xy-axis view of a DLP layer being cured and minimum pixel size, with projector(s) at distance d from resin surface.

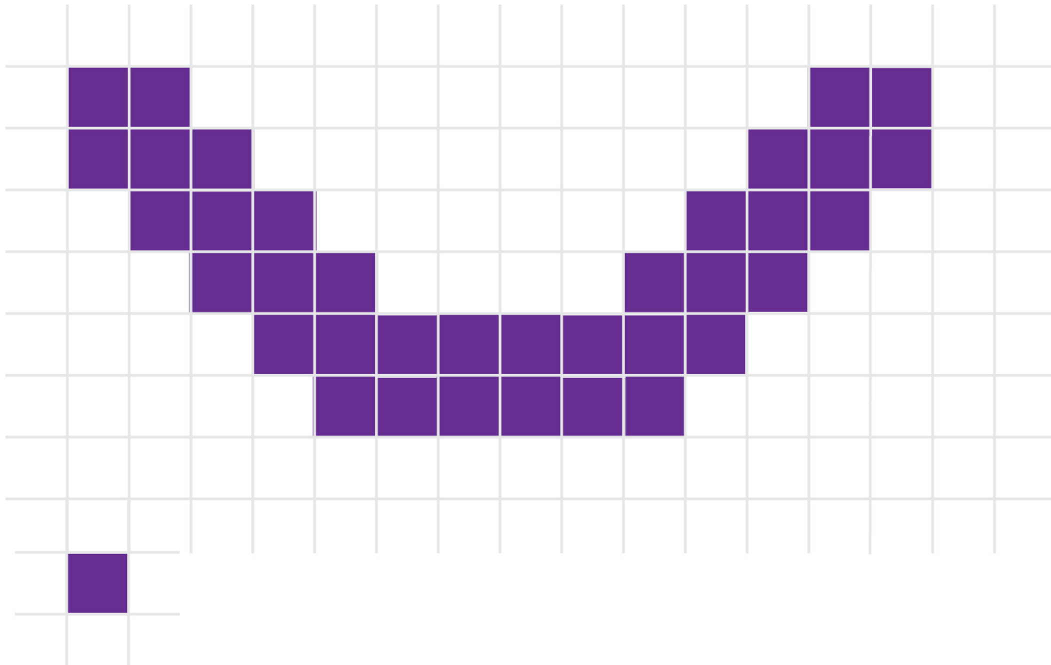

Figure 14: xy-axis view, with the projector(s) at distance d+n from the resin surface to allow a larger display area, at the expense of large pixels and consequently lower xy resolution. Based on a diagram from Formlabs ("3D Printing Technology Comparison," n.d.).

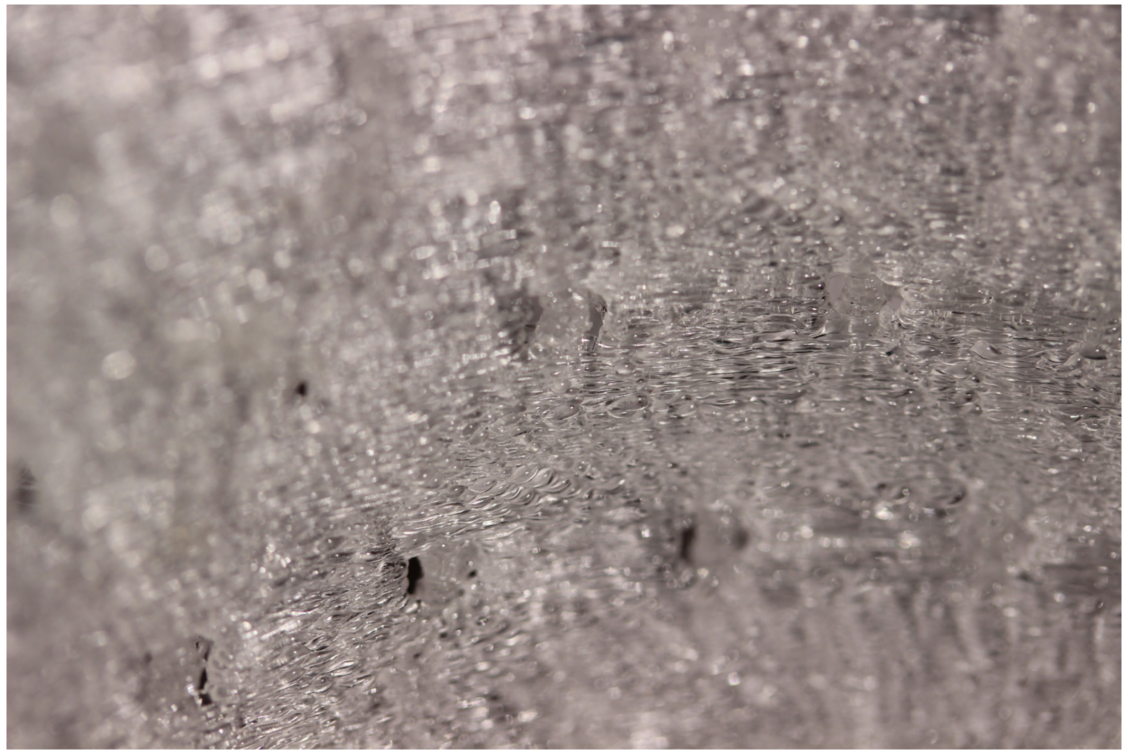

Figure 15: Z-layering seen in an FDM print with a z-axis resolution of 0.25mm/250µm.

Figure 16: The interaction of xy-banding and z-axis layering creates a fine stippling effect.

Accuracy, in the context of 3D printing, can be defined as the fidelity of the printed object to the dimensions specified in the digital model. There are two measurements used to quantify accuracy. The first is z-axis resolution. This refers to how thick each layer is, usually measured in micrometers/microns (µm). Z-axis resolution is visible as the layering effect, which becomes more apparent the lower that resolution is, as seen in Figure 15. As such, it is highly visible in FDM prints, especially before post-processing. The Form 2 software limits z-axis resolution to a selection of 25, 50, or 100µm ("Tech Specs for the Form 2 | Formlabs," n.d.) while Carbon can technically print at a 0.4µm z-axis resolution, effectively eliminating z-axis layering and thus enabling "isotropic mechanical properties" (Janusziewicz, Tumbleston, Quintanilla, Mecham, & DeSimone, 2016, p. 11705), although their M2 printer is quoted at ~25µm by a printing bureau that uses them ("Carbon M1 & M2 Build Specs," n.d.). The Gizimax at the School of Design can print at 10µm. The UP Box+ can manage 100µm (0.1mm) at best ("UP BOX+," n.d.).

The second measurement is xy-axis resolution. For point-based printers like the UP Box+ and Form 2, this is the diameter of that point - 400µm, or 0.4mm ("Tiertime UP BOX+ 3D Printer," n.d.), and 140µm ("Tech Specs for the Form 2 | Formlabs," n.d.), respectively.

For printers that use projectors, pixel resolution is materialised as xy-axis banding. This looks like z-axis layering lines, only perpendicular to them - that is, vertically rather than horizontally, with respect to the orientation the object was printed in. The Carbon M2's DLS Light Engine has a pixel resolution of 75µm ("Carbon M1 & M2 Build Specs," n.d.), although Carbon printers have been able to print features as fine as 50µm across previously, as noted by Tumbleston et al. (2015, p. 1351), who quote pixel resolutions as being "typically between 10 and 100µm" (Tumbleston et al., 2015, p. 1350). The projectors in the Gizimax at the School of Design, and the UV projectors that come with newer versions, have 1080p resolution, meaning a grid of 1920 x 1080 pixels. As shown in Figure 13 and Figure 14, the distance between the projector(s) and the resin surface can have a significant effect on pixel size. This is another argument for using a scalable, modular array of projectors: print resolution can be maintained at a high level by keeping the projectors close to the resin surface.

It should be noted that companies are "modifying for 3D printing" 4K UV projectors ("mUVe 3D DLP ULTIPro 4K Printer and Upgrade Kit," 2017). 4K resolution is 3840 x 2160 pixels. This means that for every pixel from a 1080p projector, a 4K projector has four. Increasing the number of pixels for a given display area in this way is one way of increasing xy resolution.

Another way is by using "pixel-shifting and

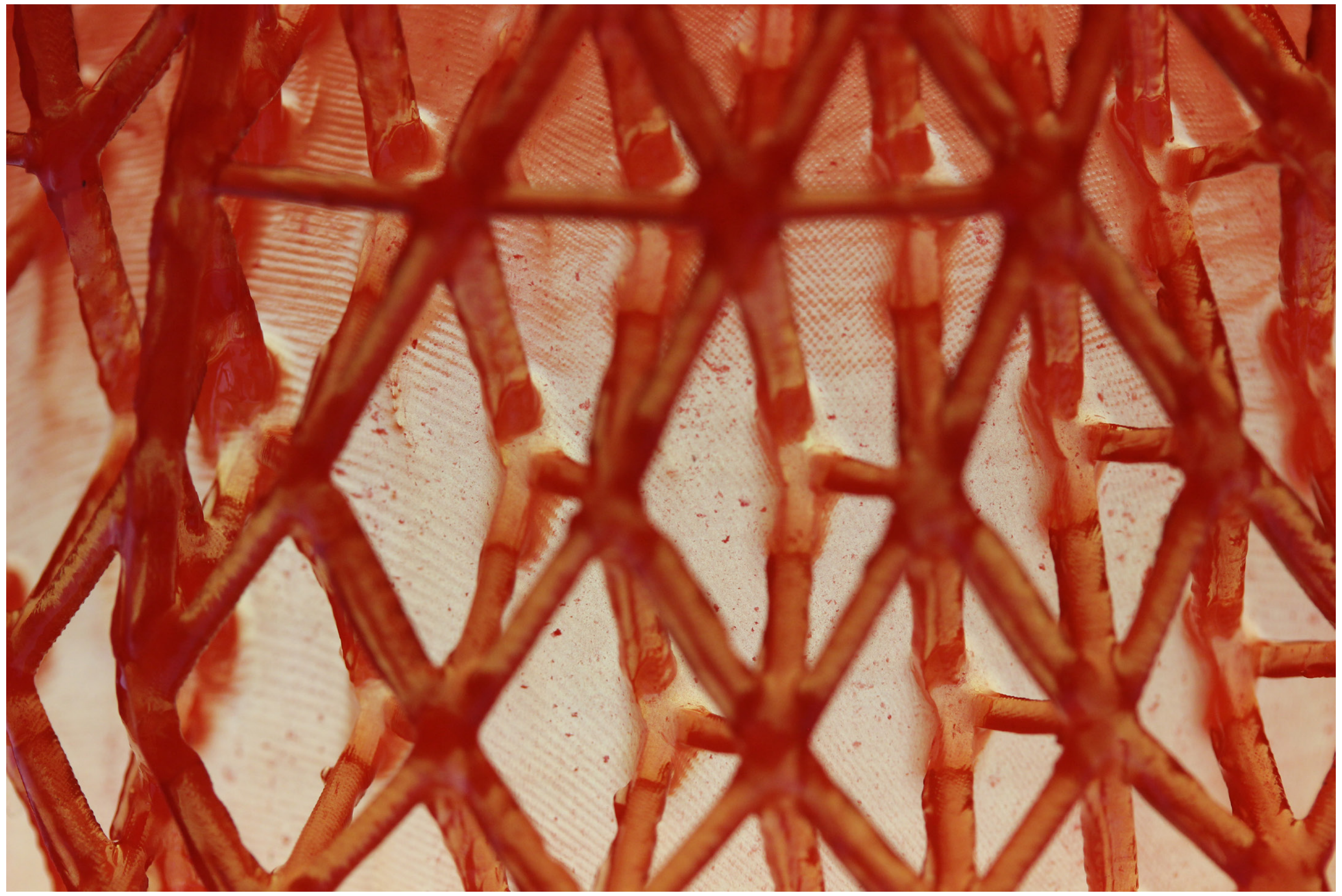

Figure 17: Curved xy-banding visible on the external, lattice-reinforced surface of an object.

greyscaling technologies" to "harmoniously anti-alias 3D objects" ("Understanding Our Advanced DLP | 3D Printing," 2017, p. 2). Commonly used in computer animation, pixel-shifting does just that - shifts pixels by a very small, predetermined distance, in order to approximate higher resolution. Greyscaling works in conjunction with pixel-shifting, by modulating the amount of energy displayed in specific pixels, and thereby modifying curing.

A third way is by including both a DLP projector and an SLA laser in a single printer. This has been done in both top-down (Zhou, Ye, & Zhang, 2015) and bottom-up (Busetti, Lutzer, & Stampfl, 2018) orientations. With this method, in either orientation, the DLP projector cures the bulk of the layer, while the laser contours the edges, in order to negate xy pixelation. The use of a laser precludes continuous printing, however, since the object being printed would move in the z-axis while the laser is scanning in the xy-axis.

To summarise, resolution of a 3D print is measured in two ways, made distinct by the axis they are represented in. There are certain limits imposed by the particular technology used, but for DLP at least there are solutions for those limits.

Part 1a Discussion

By analysis of how 3D printers print fast, and comparison of printer speeds, it can be concluded that DLP printing is one of the fastest printing methods. Similarly, by comparing which 3D printers have large build volumes, and by investigation of their processes, conclusions can be drawn about the suitability of those different methods and 3D printers for printing large objects. It is of vital importance to this thesis to keep in mind that 'large' is defined as having relatively big x, y, and z axis dimensions, rather than a large mass. Here, again, DLP printing shone. Finally, accuracy was examined in much the same way. Because of the difference in edge texture in the xy-axis between the scalable vector-based contouring of FDM and SLA printing, and the pixelation of projector-based approaches, this was somewhat less obvious. However, the superiority of the projected image method in the z-axis coupled with the fact that technology exists to mitigate the xy banding issue presented a clear ideal technology.

By taking these observations in aggregate, it is argued that due to the interactions between the three desirable traits, DLP becomes an obvious favourite. FDM printers can print tremendously large, but are very slow and have terrible resolution. SLA can technically print large, and at good resolution, but is slow due to the necessity of intra-layer steps. DLP printers can manage fast, large, and accurate individually. To enable simultaneity of those traits, it must be understood that there is the condition that 'large' is meant dimensionally rather than volumetrically. Preferably, that dimensionality should be in both height and width/depth, which excludes bottom-up processes like CLIP that rely on a taut membrane, which prevents large xy-axis printing.

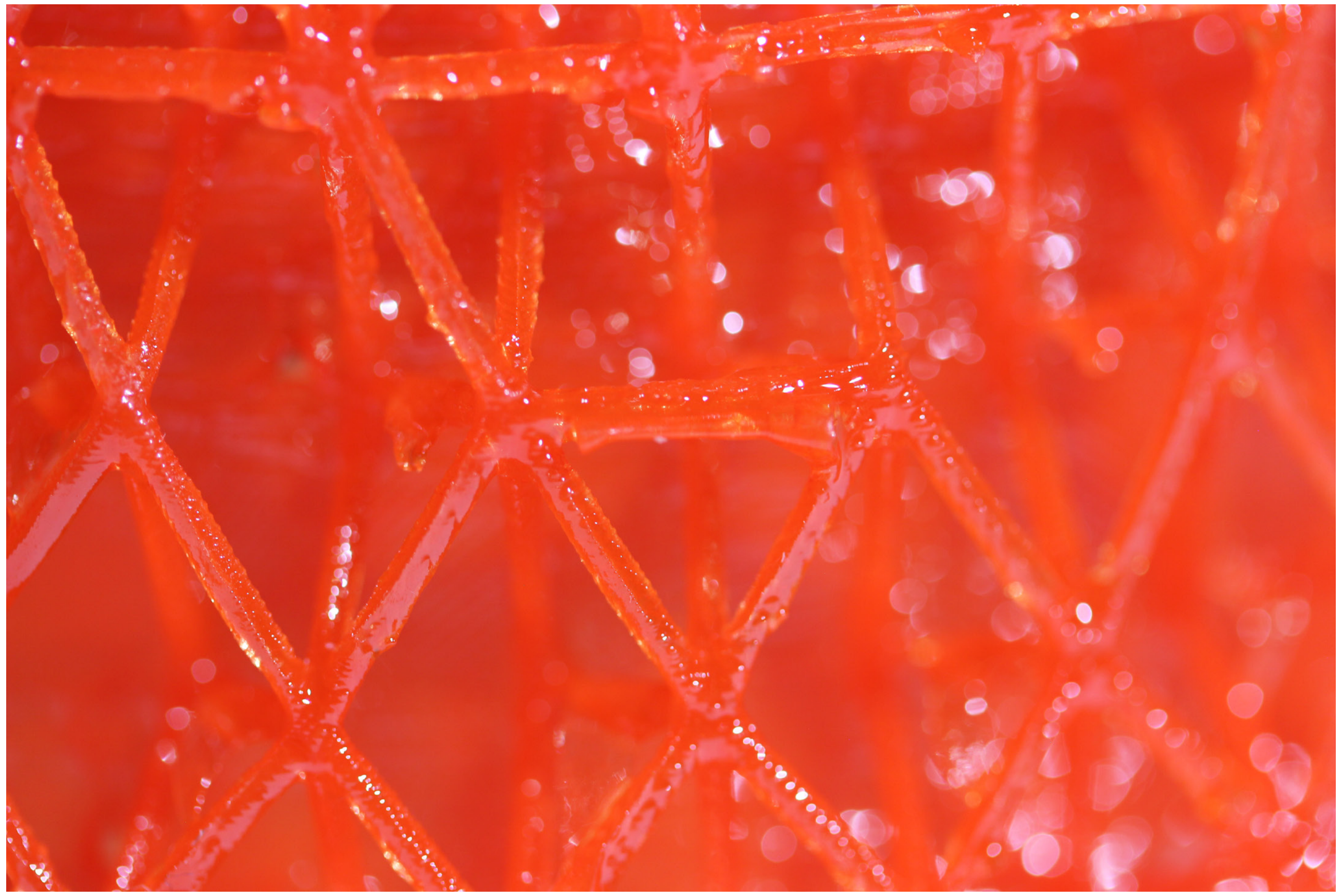

Figure 18: A comparison of DLP and FDM resolution.

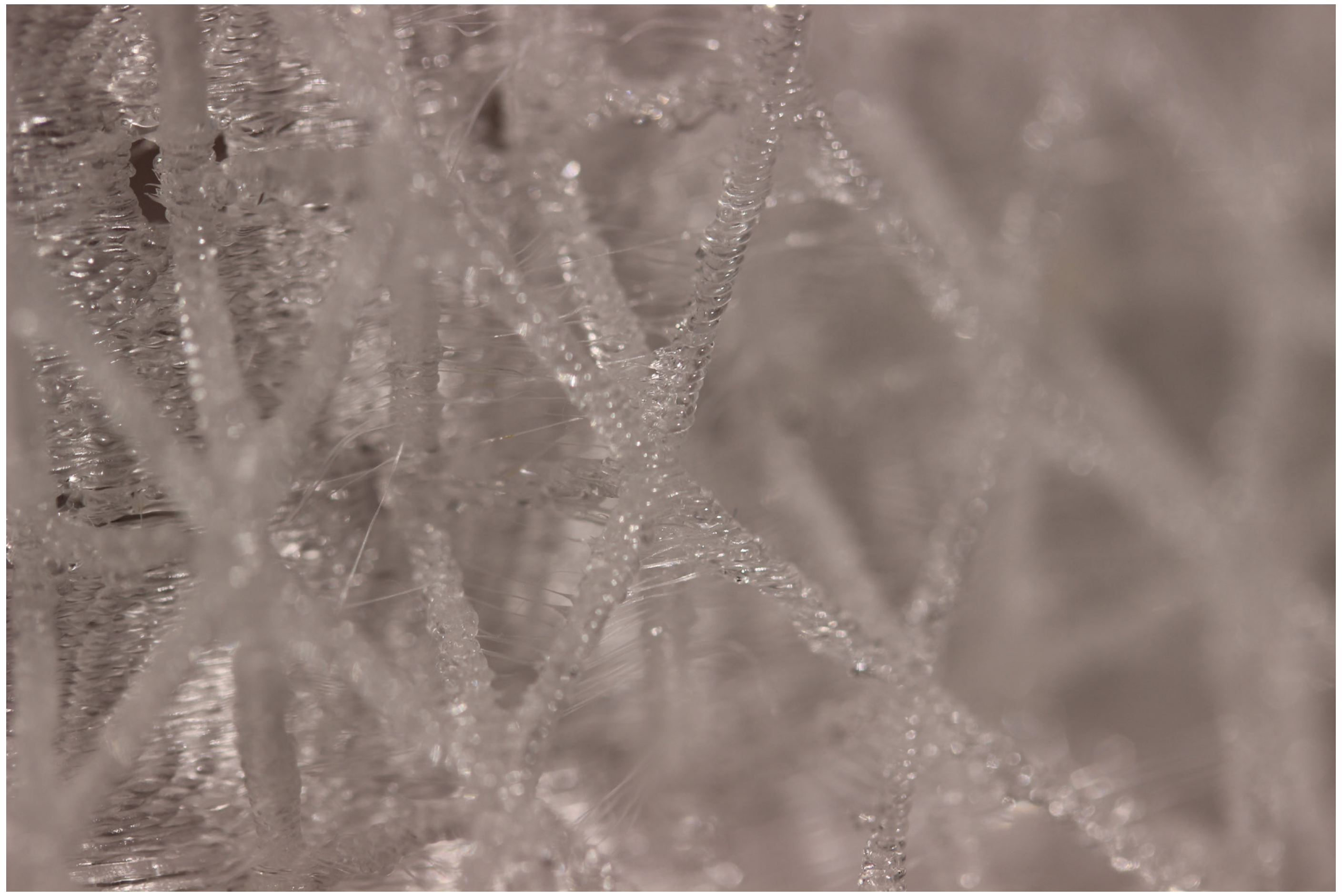

1b) Prior Art

Having encountered prior art in DLP printing, and 3D printing and additive manufacturing in general, with the perspective of trying to discover its particular strengths, and having established a body of knowledge of its basic functionality, capability, and limitations, certain design opportunities began to present themselves. Throughout investigation of the various projector-based printers for the previous section, it became obvious that lattices were a particular strength of the method. They are also a strength of other methods, particularly SLS and SLM, for at least some of the same reasons - thermodynamics being chief among them. Because complexity is free in additive processes, and taking into consideration their other qualities, lattices are an attractive prospect for the achievement of fast, large, and accurate 3D printing. Lattice structures are lightweight for their size because they are largely empty space; strong for their weight because they exploit structure for their means of strength, rather than mass.

They can be optimised for force loading from particular directions. These traits make them useful for 3D printing support, particularly for SLA and DLP methods, as commonly seen in an abundance of printer software, such as Preform, which is Formlab's program.

Figure 19: Preform generated print support trusses on a designed object.

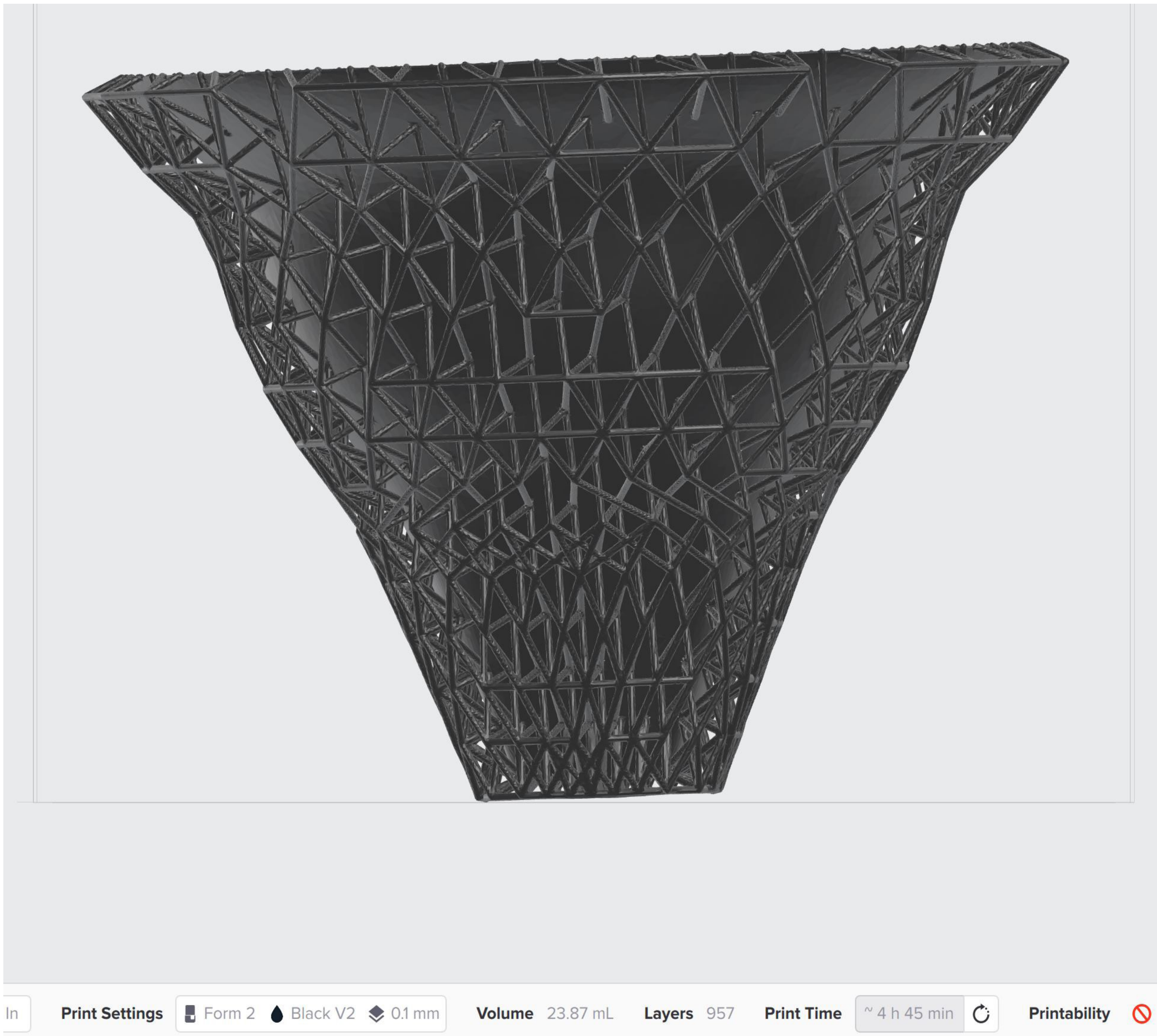

Figure 20: Designed object without support. Note volume of resin required, and print time. Object is automatically oriented on an angle to minimise surface area attached to vat membrane at the end of each layer scan.

Chapter 5) Lattices

For the purposes of this thesis, lattices must be designed as structures to simultaneously improve the strength and printability of an object, such that the object will be unacceptably weak and/or fail to print adequately without the lattice, and where improved printability means printable at higher speeds, greater dimensions, and finer resolutions concurrently. Towards this goal, it was important to gain insight into the status quo of lattices and lattice-like structures, especially as they are understood within the context of additive manufacturing and 3D printing processes.

The first observation of lattice status quo was that methods of both generating and evaluating them tend to do so nodally. That is, a single unit of the lattice is designed, based on a shape within a cubic bounding box. It can be appraised by finite analysis, as detailed by Daynes, Feih, Lu, & Wei (2017, p. 216). These node designs are based either on struts/trusses or surfaces, as documented by Panesar, Abdi, Hickman, & Ashcroft (2018, p. 85). Once the nodes are arrayed in a group a certain number of units in each of the x, y, and z directions, they form a lattice structure, which may then be attached to or bounded by a surface or 'skin'. It can then be modified in multiple ways. Azman breaks this down into six categories of variable: Pattern, Design Space, Relative Density, Progressivity, Conformality, and Joint (2017, p. 103). Pattern refers to the node type. Design space pertains to the nature of the surface the lattice is attached to. Relative density deals with the ratio of object material to space. Progressivity refers to the location of material within nodes. Conformality is a choice between the uniform or conformal style of lattice, as seen in Figure 21. Joint is about the nature of the intersections between nodes.

While Azman only offers Constant and Gradient options within the Progressivity category, Daynes et al. add spatial gradation, which might fit as a variation of the Constant option, in that there is no change to the diameter of elements in each node, only their arrangement (2017, p. 217) within nodes and throughout the object. Spatially graded lattices could also be counted as a type of conformal lattice.

Uniform lattices are generated with an orientation that can be independent of the object design. Conformal lattices, conversely, are procedurally modified in reaction to the contours of the object design. The shoe soles created out of the collaboration between Carbon and Adidas use conformal lattices, in addition to a change in pattern (Goehrke, 2018). Autodesk's Netfabb software ("Netfabb," n.d.), nTopology's Element ("Home," n.d.), and the browser-based Meshify ("Meshify," n.d.) all offer both uniform and conformal lattice generation. They often do this by replacing a certain volume of a digital object with lattice structure, as shown by Tang & Zhao (2015, p. 1381).

This lattice prior art is all highly contextual, it must

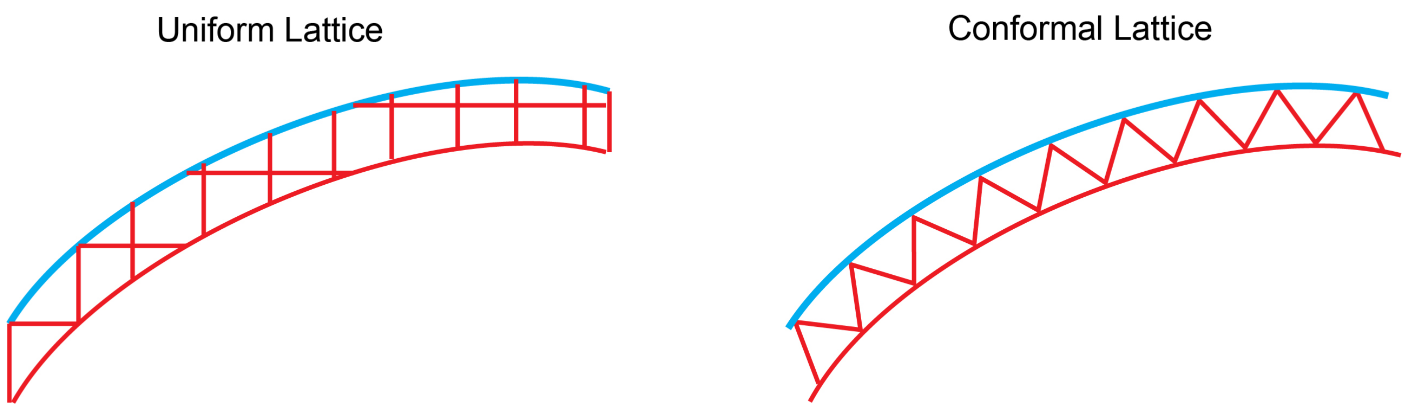

Figure 21: Lattice types. Surface, or 'skin' of the object in blue, lattice structure in red. Based on a diagram by Engelbrecht et al. (2009, p. 834).

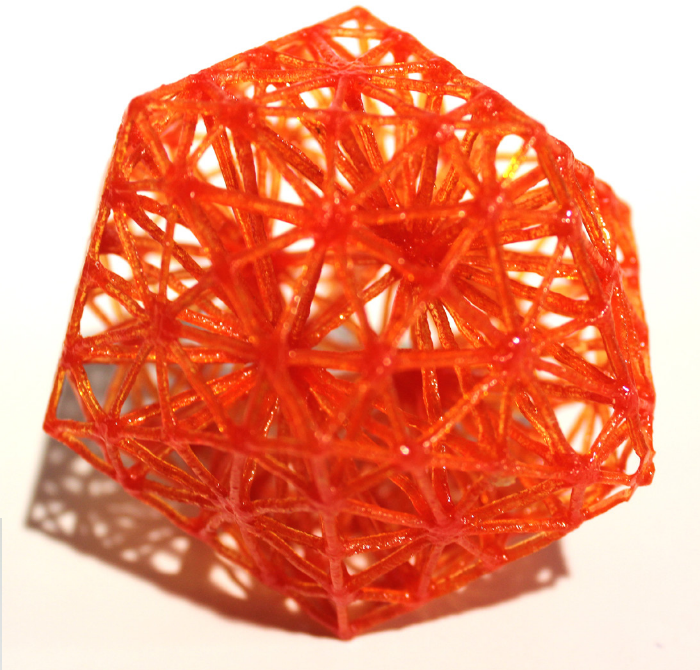

Figure 22: Strut lattice, 80mm x 55mm x 55mm, printed at 1mm/minute, at 50µm resolution - highly successful.

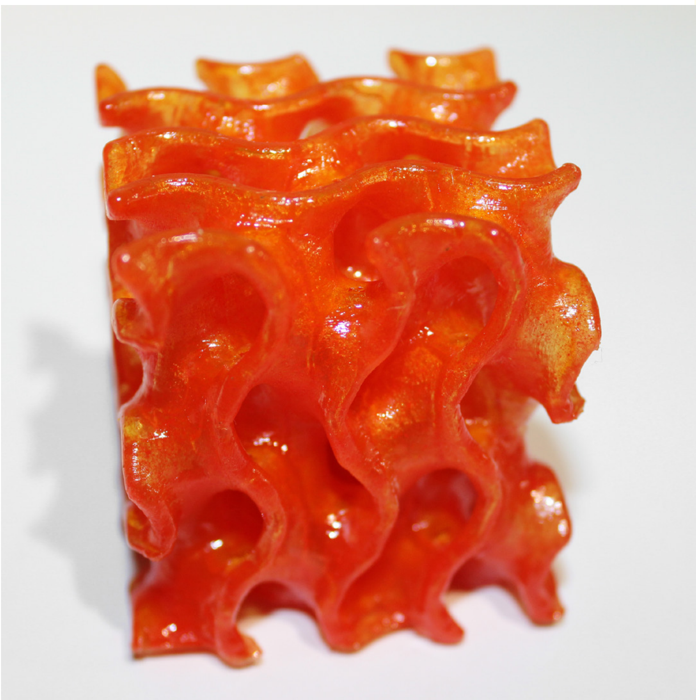

Figure 23: Gyroid continuous surface lattice, 50mm cube, printed at 0.25mm/minute, at 50µm resolution. It has small resin starvation holes on the tops of wide areas that were horizontal during printing.

be said. All of the above sources deal specifically with lattices as they pertain to additive manufacturing. Bearing in mind the constraints of top-down DLP printing, in order to maximise print speed it is important to minimise cross-sectional area of the object being printed. This is so that all of the power of the projector is concentrated, so that resin doesn't have to flow very far, and to limit thermal and curing contraction forces within the print.

Lattice structures that use continuous surfaces, such as the gyroid type (Yeo et al., 2018, p. 12) and Marc Fornes' 'structural stripes' ("Invention of Stripes," n.d.), while both extremely strong due to their exploitation of double curvature, are therefore less attractive for those reasons. They necessitate less-than maximum speed printing in order to prevent resin starvation, due to cross-sectional area at certain points, but also due to resin flow issues caused by their topography - they create areas resin can't reach while printing continuously, top-down. Strut or truss-based lattice structures work better, despite not benefiting from strength granted by things like double curvature, since they can confer their own structural strength with minimal cross-sectional area, and no topological resin starvation issues.

Chapter 6) Supports in 3D Printing

A key element of design for additive manufacturing is minimising the support required to obtain a successful print. This is because supports take time to print in most methods, making printing times longer, and require material which becomes a waste product after removal from the printed object. Strategies for support minimisation include designing objects with little or no overhanging area, which can be understood as topology optimisation for printability, and orientation-for-printing of objects that do have overhangs to minimise the area that needs to be supported. Supports are nevertheless necessary sometimes, and lattice-type structures are popular for use as support because of the properties discussed in the previous chapter.

Panesar et al. (2018, p. 92) evaluate different versions of an object based on how much support it needs to successfully print, although they have intentionally omitted the reorientation strategy, which would have significantly reduced their minimum amount of required support. They do note, however, that support requirements can be minimised "by employing self-supporting unit cells", that is, lattices whose nodal structure requires no support to print.

Current SLA/DLP support structures appear to be mostly based on simple trusses, as seen in Figure 19 and in Sculpteo's comparison of SLS and CLIP ("Compare SLS and Carbon's CLIP technolgies," n.d.). With SLA, such strategies drastically inflate both printing time and resin use; the model in Figure 20 requires ~24mL of resin, but the supported print seen in Figure 19 requires ~109mL - a 454% increase! It takes more than twice as long to print supported compared with unsupported (10hr45min vs 4hr45min), and still has red areas indicating problems. To mitigate this type of shortcoming, smarter support strategies are being explored. Mezzadri, Bouriakov, & Qian, (2018, p. 671) and Lantada, Romero, Isasi, & Bellido, (2017, p. S181) independently arrived at fractal or L-systems style support structures, which they describe as tree-like, despite the former group designing for FDM while the latter specified photopolymerisation.

Gizmetor, the software associated with readying a digital file such as an STL or OBJ for printing on a Gizmo3D printer, currently has no support-building capability, so Meshmixer was used during the research for design phase of this thesis. Meshmixer is a free Autodesk product designed for basic digital mesh manipulation ("Autodesk Meshmixer," n.d.).

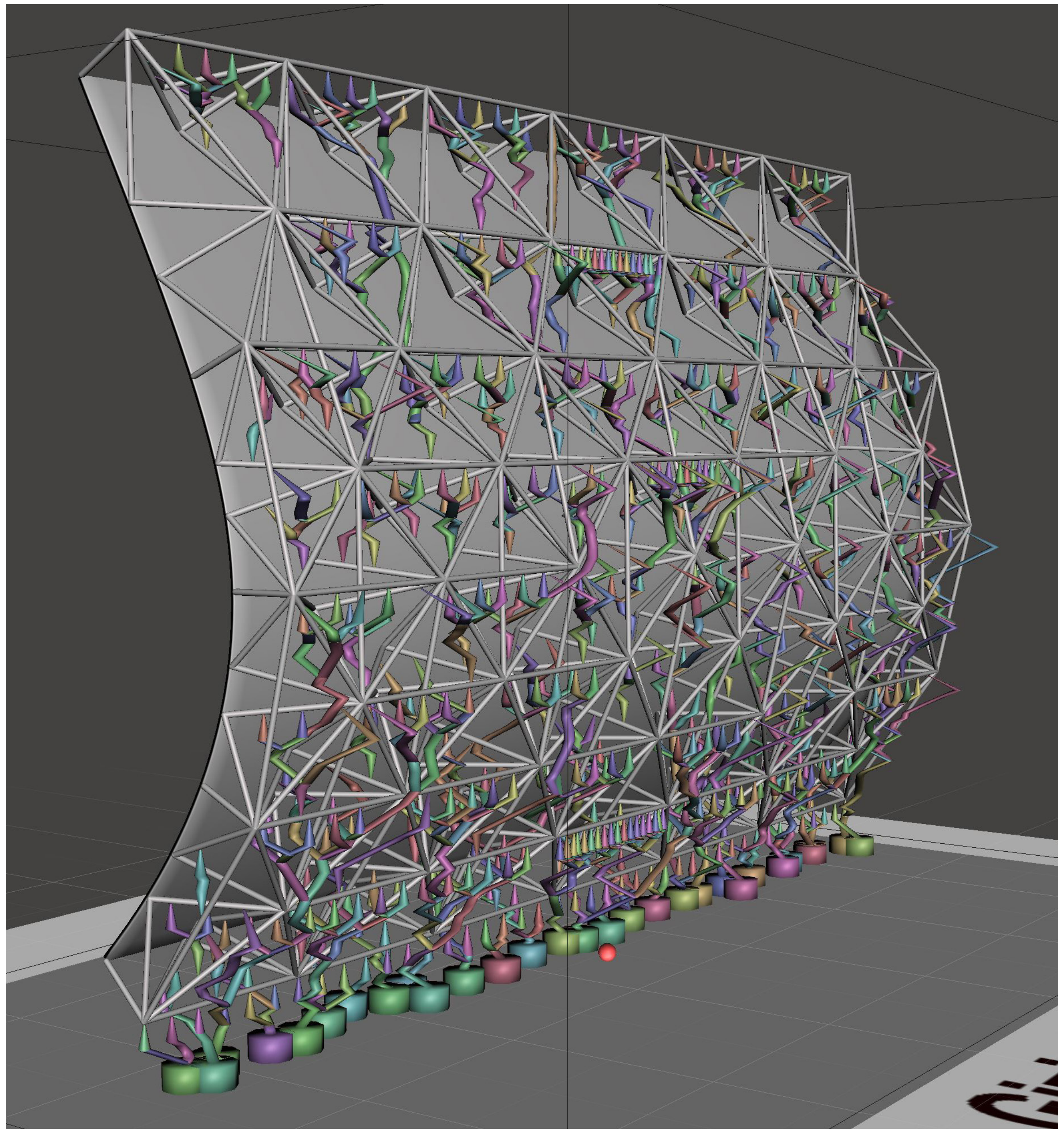

Figure 24: Support structure (multicoloured) generated by Meshmixer on lattice-reinforced object.

Chapter 7) Grasshopper Research

Grasshopper was selected as the best program to use for several reasons. First, it's a plugin for the modelling program Rhino. This meant that surfaces could be designed and visualised in Rhino, which could then have a Grasshopper-generated lattice structure applied to them. Second, because of the graphical nature of algorithm construction in Grasshopper, an algorithm 'written' by someone else can quickly be 'read' and intuited with a basic level of skill with the program, and one that you have written yourself can be deeply understood despite its complexity. Third, it is a program that is widely used for related purposes, meaning there was a body of work from which to begin iterative algorithm development. Finally, the online community around Rhino and particularly Grasshopper are very active, constantly generating tutorials and new tools, and responding to queries on highly populated and heavily used forums. These factors accumulated so that, despite the only prior knowledge of Grasshopper being an insight into its potential and power, it was the ideal choice for a program to enable highly parametric and procedural development of a new method for generating lattice structures on a surface.

Over the course of several months, a combination of specifically selected and increasingly relevant video tutorials available on YouTube, and a campaign of targeted questioning at both the official Grasshopper website (Davidson, n.d.) and the Rhino forum, which includes a dedicated Grasshopper section ("McNeel Forum," n.d.), were used to learn how to construct a Grasshopper algorithm. Specifically, how to use Rhino and Grasshopper to write an algorithm that would be powerful, adaptable, and iterative by design.

It should be noted that there is an add-on for Grasshopper called Intralattice, which functions similarly to Netfabb in that it works by converting volumes to node-unit style lattices ("INTRA|LATTICE," n.d.). In order to maximise the design done in the research for design phase, and to create an innovative and distinctive latticing technique, Intralattice was not used.

Part 1b Discussion

Lattices were researched, discovered, evaluated, and determined to be suitable for the intended purpose - enabling fast, high resolution 3D printing of large objects by reinforcing surfaces that are necessarily thin. As a universally ideal lattice for this purpose was not available, but having eliminated types of lattice that were not appropriate, it proved necessary to generate variable lattice structures on designed surfaces by first designing a method capable of doing so.

3D printing supports were an important source of inspiration in both lattice structure and 3D printing prior art. Taking design cues from support-style lattices proved valuable despite the fact they are optimised for printability in only the printed orientation rather than omnidirectional strength, like the lattices in the thesis technique.

A software suite particularly suited to the purpose, Rhino and Grasshopper, was selected and learnt in order to expedite design of a prototype algorithm that would serve to provide design capability for digital models of proof-of-concept objects to be 3D printed. It was important that it should be built from first principles, rather than using pre-existing lattice generation software like the aforementioned Netfabb or Meshify. This would ensure a lattice output designed from the ground up.

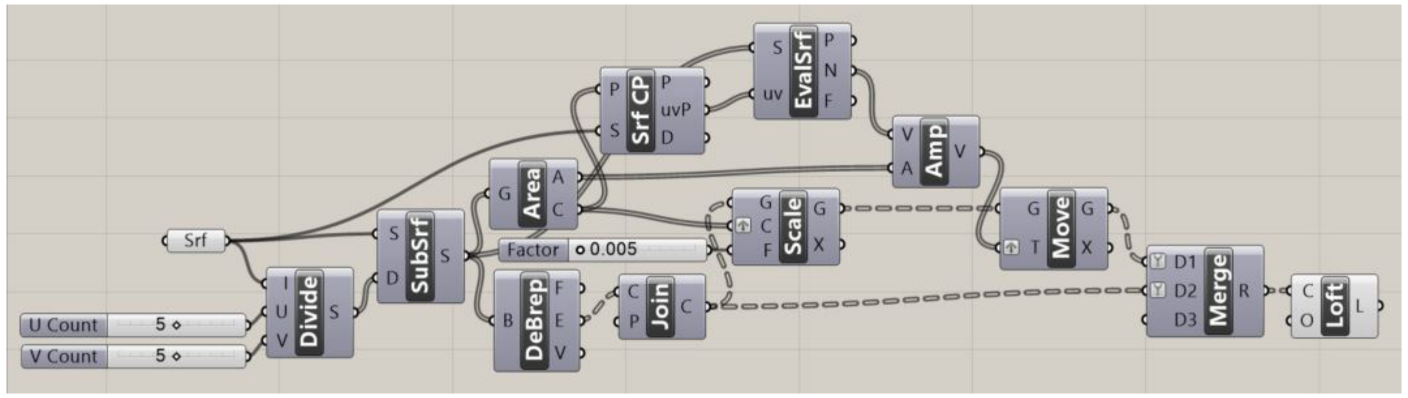

Figure 25: Grasshopper script to build structures on a surface, used as partial inspiration for a piece of the required algorithm.

Part 2: Research For Design

Part 2 of this thesis deals with the design of the algorithm for designing and applying a reinforcing lattice structure to a thin surface. As such, it is important to clarify and be explicit about why this was done.

In Chapters 2 through 4 it was established via analysis and comparison of printers that DLP printing was particularly suited to quickly and accurately printing objects with large dimensions. It was noted that it is necessary, because of the fluid behaviours and thermodynamic activity involved with printing with those three desirable traits, that certain other conditions be met. The first, that cross-sectional area of prints must be small, entails thin-walled objects. However, due to the lack of rigidity of printer-cured resin during and following a print, it is also necessary to address the weakness of thin-walled objects. This is because they can warp or distort either during or after printing, and then have those distortions worsened and made permanent during post-curing. Therefore, a method is required to impart significant strength to the object from the moment it is made manifest. An attached lattice structure, of a minimal size but appropriate sturdiness, fulfills this requirement, as seen in Figure 26. Design and iteration of the algorithm would also drive design and iteration of lattice structures. That being said, considerable inspiration was derived from the work of Wang & Rosen (2002), and Engelbrecht et al. (2009) for their use of lattices only one or two nodes deep attached to surfaces, and Kure et al. (2011) for their method of using a polygonal grid on a surface as part of the workflow towards an attached lattice.

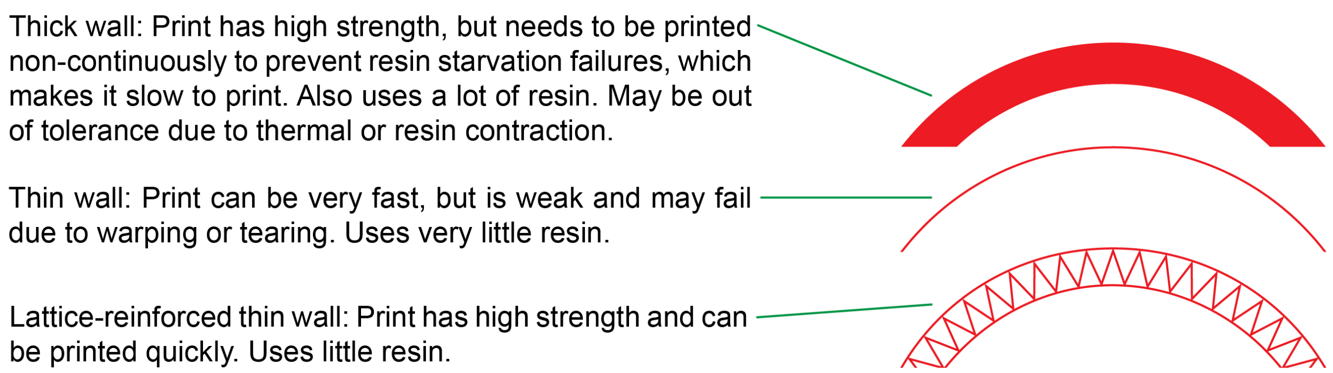

Figure 26: Diagram of thick/thin/reinforced walls to show why reinforcement of a thin-walled object is beneficial.

2a) Material Research

As DLP printing is carried out using liquid resins, which have widely varying material and printing properties, research was carried out in order to evaluate the suitability of the available resin. Research on non-FunToDo resin was conducted with the generous assistance of Whitehall Technical Services in Auckland, who provided custom-formulated resin samples to determine if a resin could be produced that would print well while being more suited to the university environment, that is, having relatively low odour and reduced toxicity.

Chapter 8) FunToDo Standard Blend Red Resin

FunToDo SB Red is the resin that ships with Gizmo3D printers, and is the resin that printing has been done with during previous research with the Gizimax at the School of Design ("FunToDo, Best 3D Dlp resins," n.d.). See Appendix A for an Material Safety Data Sheet which provides a composition list and toxicity information.

When research with the Gizimax began at the School of Design, there was not an enclosure on the machine. This necessitated the wearing of a gas mask while in the printing room, and keeping the door shut in order to contain the fumes given off by the resin, especially during printing. As an educational institution safety is a high priority. As a solution to the odor problem an enclosure, as seen in Figure 5, was designed and constructed during tenure as a research assistant for the School of Design which made the printing involved in this thesis less uncomfortable.

FunToDo Standard Blend Red is an observably low viscosity, low surface-tension resin, with a consistency at 19°C similar to canola oil. While the projectors are able to set the form of the object during high-speed printing, it emerges soft and flexible. As with the other vat polymerisation methods, it is necessary to post-cure printed objects to finalise their material properties. During post-curing, it gradually becomes less red, with full-cured objects being a dark orange. It also becomes significantly harder and less flexible, but more brittle. The red pigment rapidly settles out of FunToDo Standard Blend, but is easily mixed back in.

Chapter 9) Other Resins

Having received custom-formulated tester resins from Whitehall Tech, and having no first-hand experience with resin other than FunToDo Standard Blend Red, it was necessary to carry out some basic curing tests to enable a basic evaluation of their characteristics. As such, each of the test resins was subjected to curing for 1- and 2-second increments in order to determine an approximate curing speed.

The tests in Figure 27 were carried out by using the calibration settings in Gizmetor to display for 2 and 4 seconds for two small puddles of each resin. Resin viscosity was also observed at this time. UV3D 5S has excellent curing rate, but is slightly viscous relative to the baseline of FunToDo SB Red. Untint Gib Black-10 was quite viscous, like a molten chocolate, and cured relatively little. UV3D3H had good viscosity, but didn't cure much at all. UV Dome 5848V was extremely viscous, like treacle, and showed only slight curing.

Once the results of these tests were obtained, they showed that one resin had outstanding curing quality relative to the others - the 5S. However, upon testing it in the small vat, it was discovered that visible-light projectors cause serious unwanted curing in clear resin, due to over-penetration and refraction. This had not been covered in printer documentation. As such, due to the limited amount of the other test resins available, coupled with the abundance of FunToDo SB Red, its status as a known entity, and under University safety protocols about the maximum amount of resin allowed on site, it was decided to proceed with the standard resin rather than a specially formulated one.

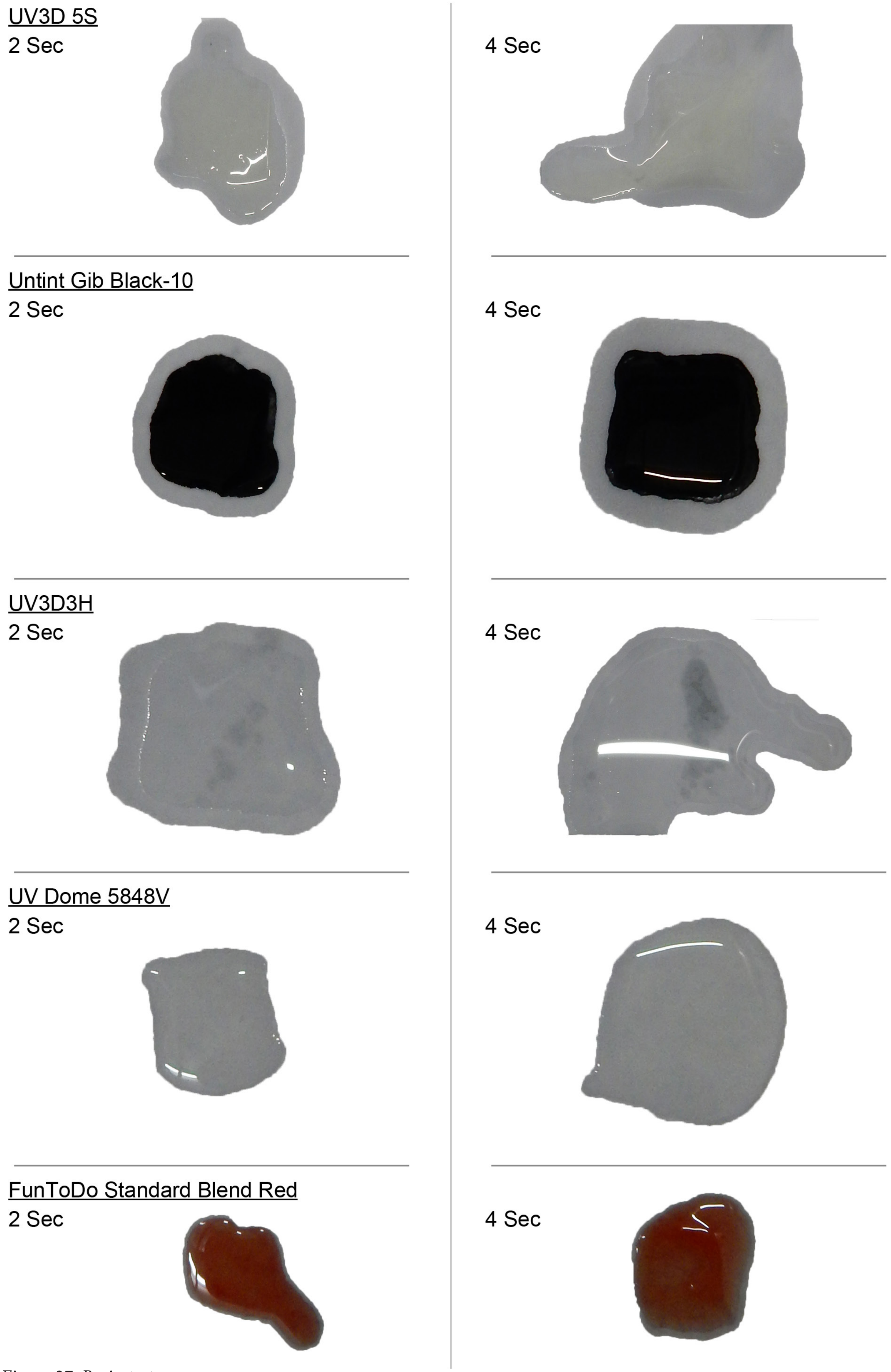

Figure 27: Resin tests.

Part 2a Discussion

The purpose of the resin research was somewhat outside the scope of the thesis - trying to find a resin that prints well but is office/educational institution friendly has a limited amount to do with printing fast, large, and accurately. However, the first-hand knowledge gained was invaluable in understanding the vagaries of UV curing and resin formulation, which also contributed to eventual success in overcoming some of the obstructions to achieving good prints. It was also helpful to know that the FunToDo resin is actually good, rather than just cheap.

2b) Software Research

In order to be able to create multiple lattice versions, that can attach to surfaces with varied numbers of edges, sizes, and degrees of curvature, it was deemed necessary to design a robust algorithm with several options for adjustment. The algorithm in Figure 25 formed the basis of a lot of future development. The method of building the algorithm was to gradually add capability, and continually refine. Any extraneous components were eventually removed, although they were useful during the development phase, for example the Text Tag 3D component allowed visual location of specific hexagons, when that was important. A few components that are not strictly necessary remain in order to maximise the clarity of the algorithm.

Chapter 10) Algorithm Development

The ability to build structures on a surface was established early in algorithm development, and the next step was to learn a method for building struts from which to build up a lattice, as seen in Figure 28 and Figure 29.

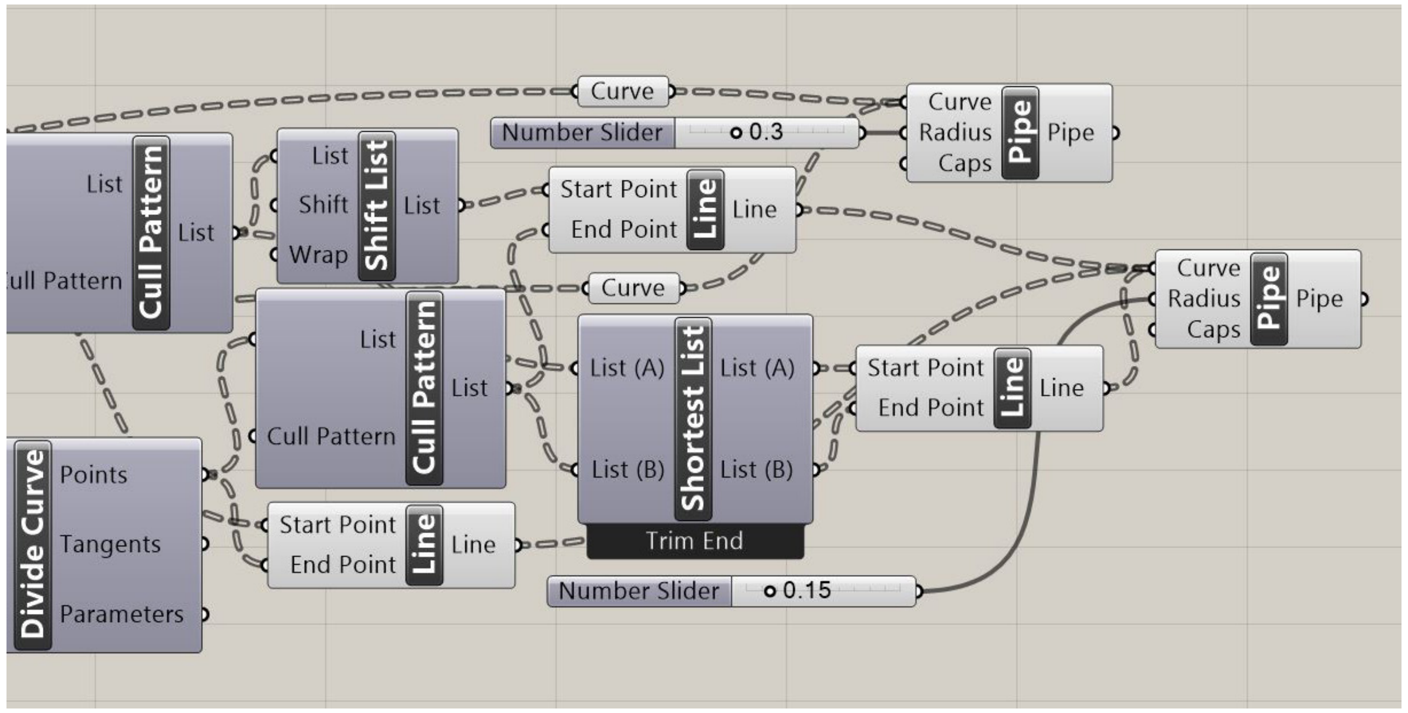

Figure 28: Choosing the correct lines to build cylindrical surfaces (pipes) around.

Having encountered architectural based Grasshopper scripts using the box morph component, which arrays a grid of predesignated shapes on a surface, a script based on a tutorial of that tool was adapted for the purpose, seen in Figure 30. However, the box morph tool was quickly found to be lacking in flexibility, as it uses a rectangular grid. Also, the fact that it is essentially a node unit arrangement tool was not missed. The result, seen in Figure 31, was a validation of the idea that a better method should be sought.

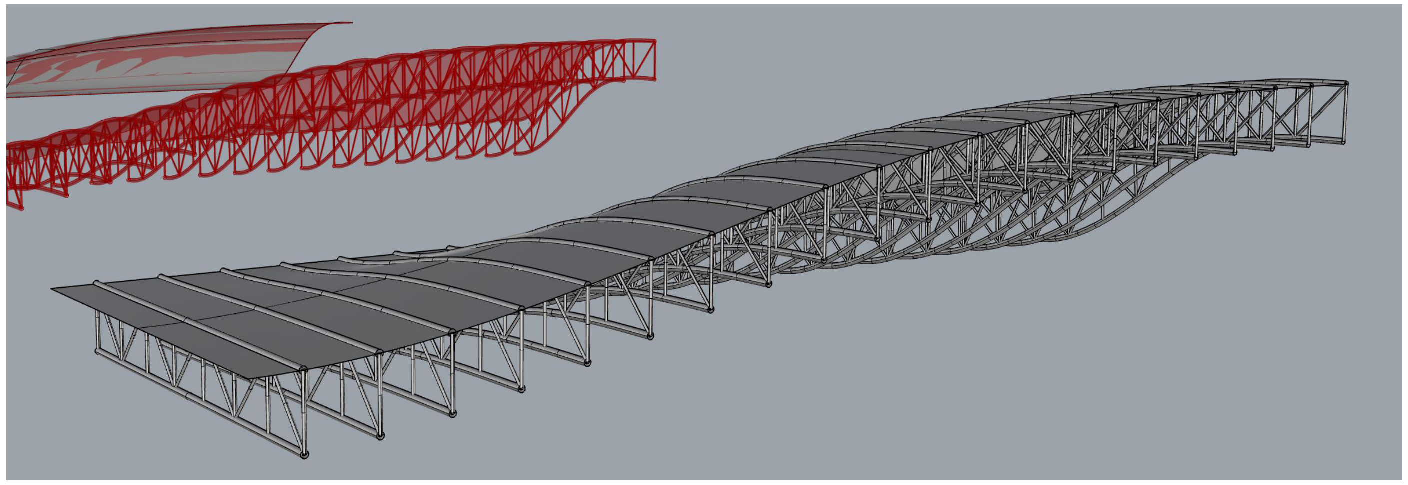

Figure 29: The truss structure as generated by the algorithm in Figure 28.

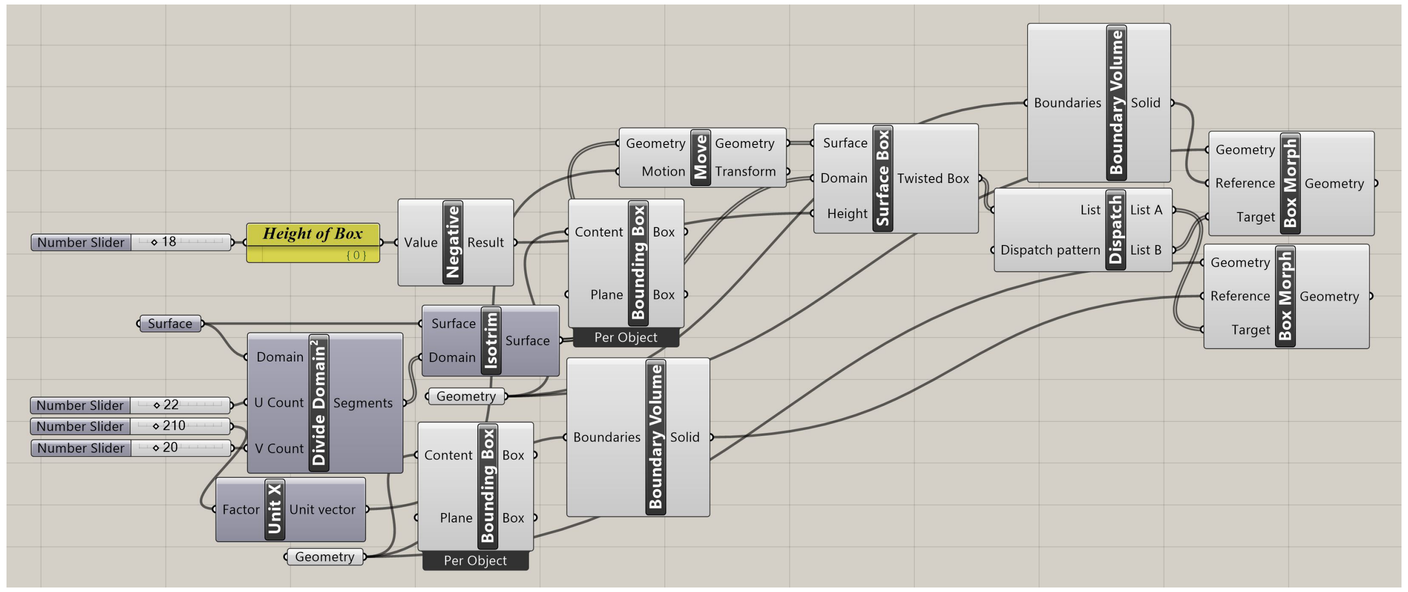

Figure 30: A box morph experiment to see if a designed node method was viable.

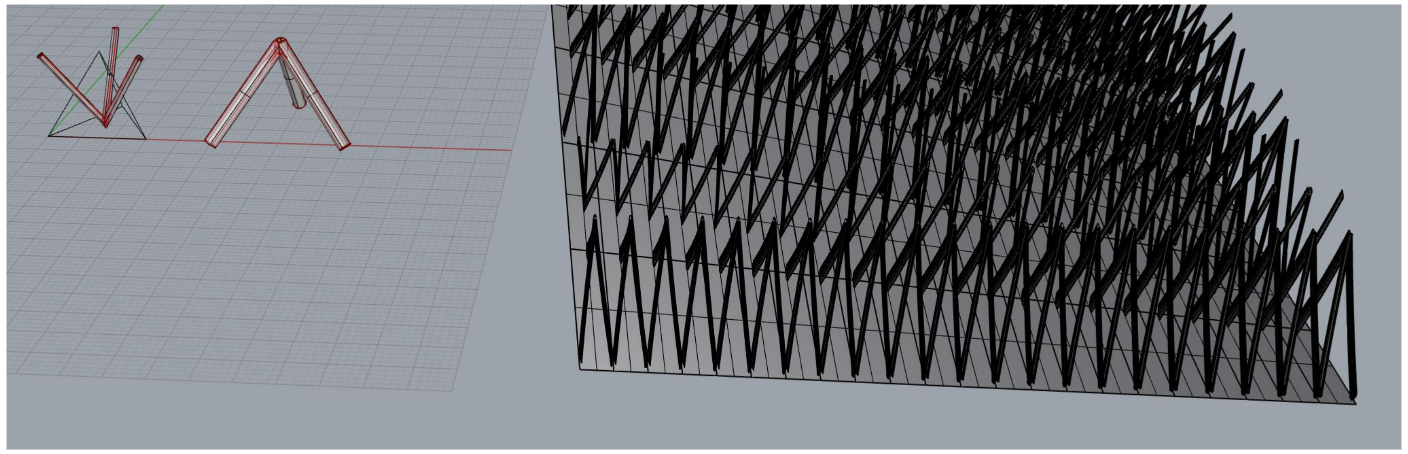

Figure 31: Box morph result.

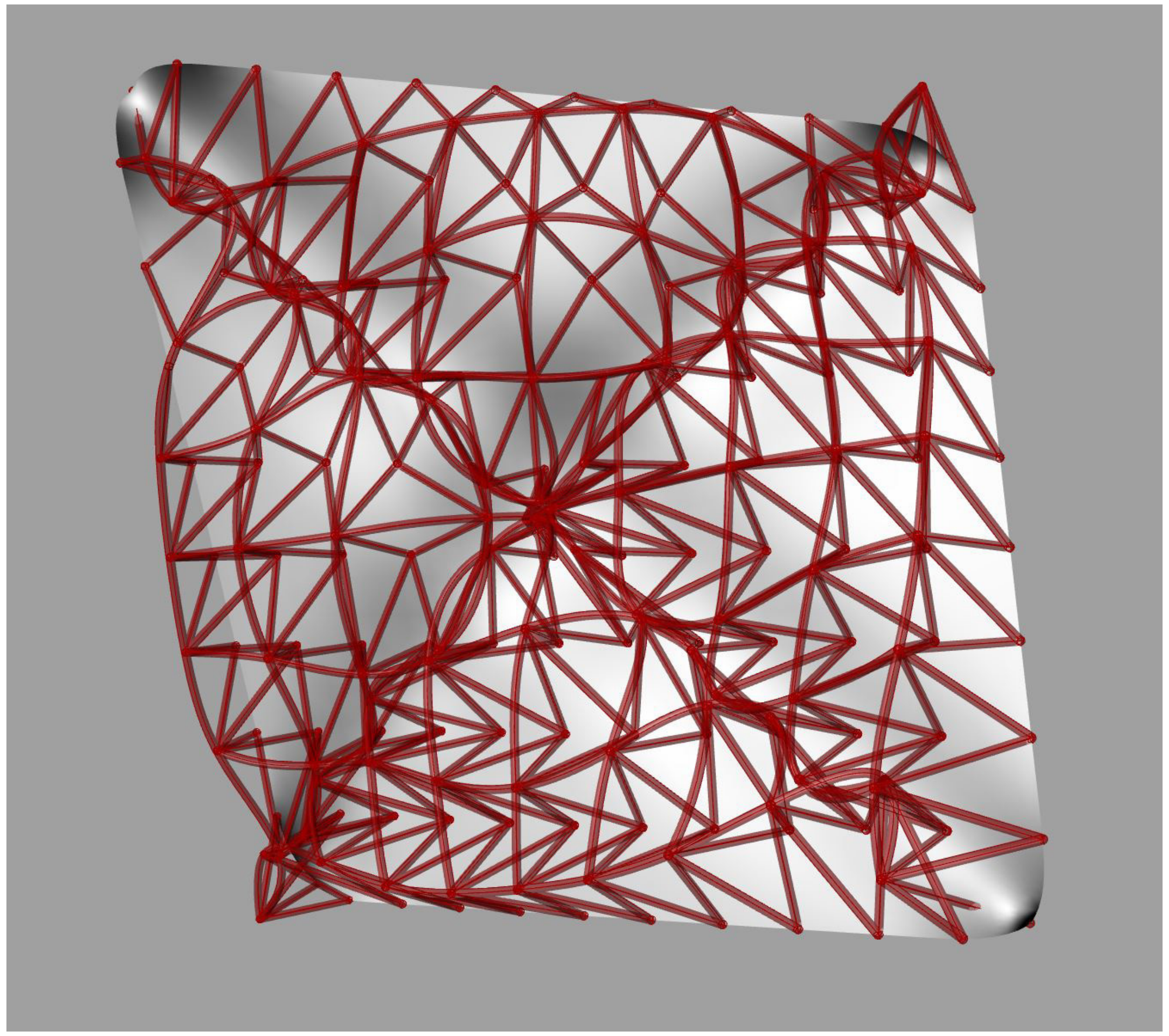

Figure 32: Building struts with points and lines, rather than set shapes.

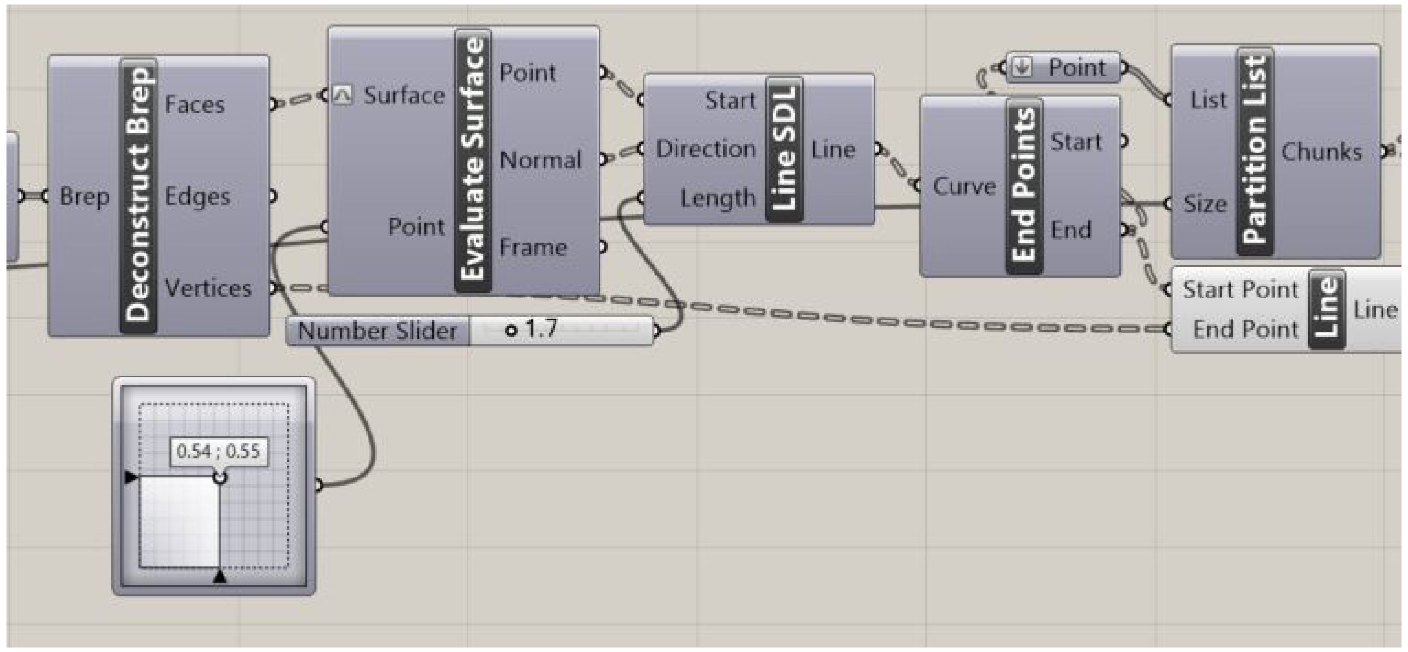

Figure 33: First parametric script. The direction the struts emerge from the surface, and their height, is adjustable.

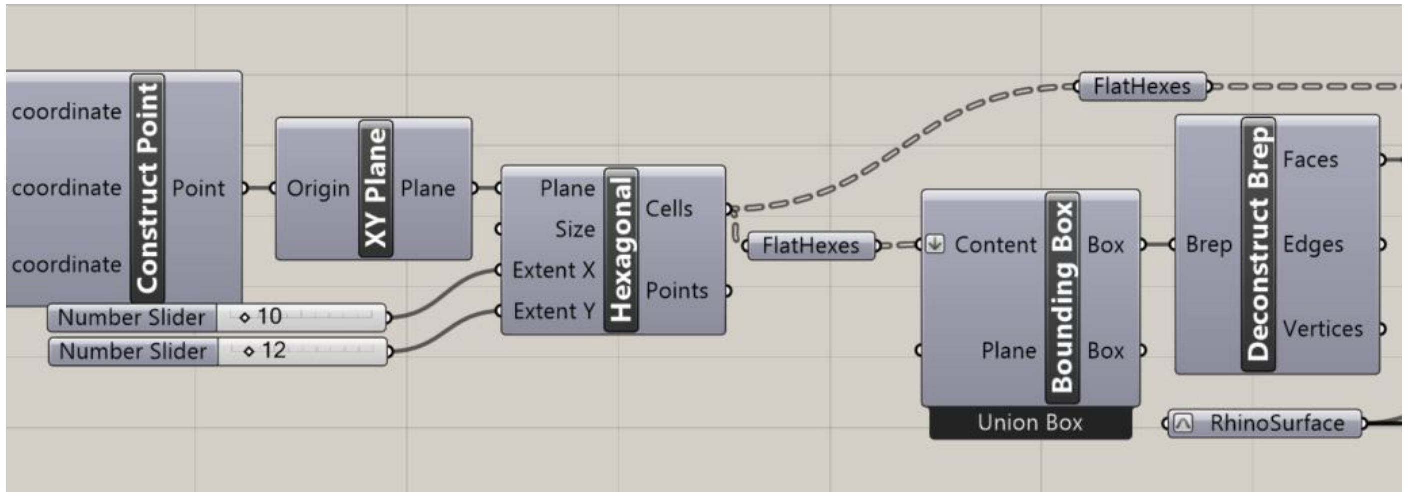

Figure 34: The 2D Hexagonal grid component being tested.

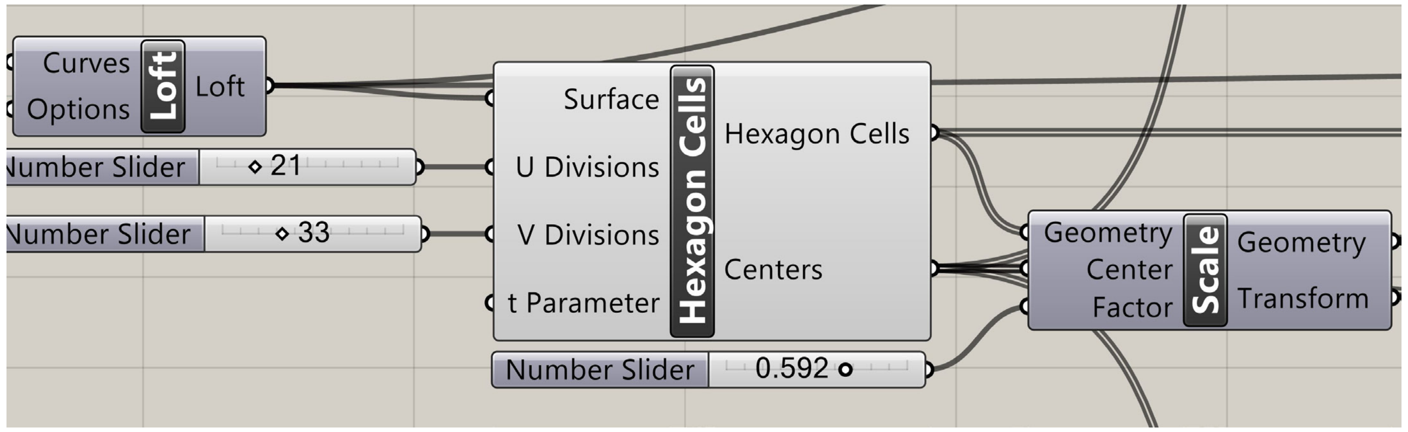

Figure 35: The Hexagon Cells component, a smarter component.

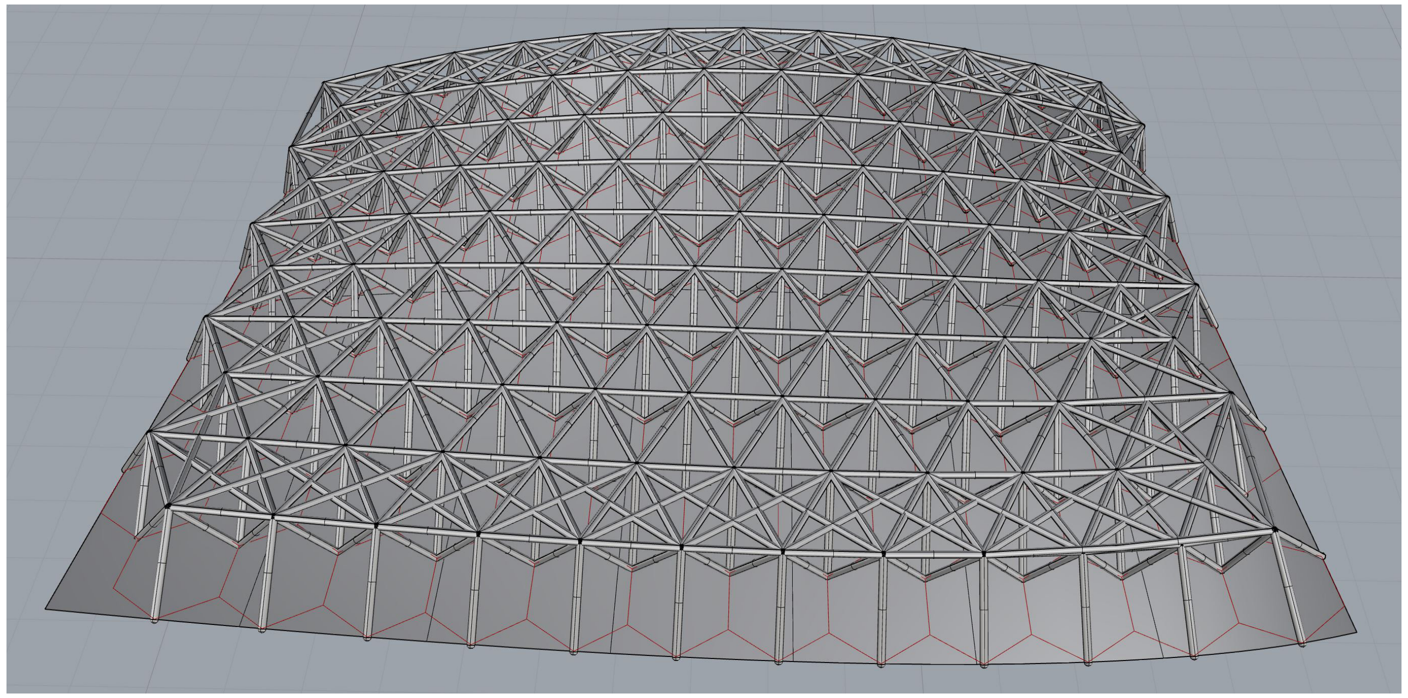

Figure 36: One of the first successful lattices based on a hexagonal grid, which is visible on the surface in red.

After the failure of the box morph method, a more advanced points-to-lines method was discovered and written, as seen in Figure 33. Unfortunately it suffered from several shortcomings, the most visually obvious being that the struts joining the apexes of the triangles followed the contour of the surface, which can be seen in Figure 32. It looks bad, and causes problems with penetration of the surface. Also, it was still based on a grid of squares, leading to possible lattice weakness along the lines of that grid.

In order to generate a tessellating grid that would not have any straight lines longer than the side of a unit shape of that grid, a method for drawing a hexagonal grid was used, as seen in Figure 34. This was eventually swapped out for the Hexagon Cells component seen in Figure 35, because it works better with 3D surfaces and allowed significant simplification of the algorithm. It also outputs the centre points of the hexagons as built on the surface. The centre points are used for establishing the apexes of the struts coming from the corners of the hexagons, perpendicular to the angle of the surface at the location of each individual hexagon.

Once the hexagonal grid method was at a satisfactory level for making a lattice on a surface, the ability of the algorithm to accept diverse surface types was expanded and assessed. This was achieved via the use of a particularly complex surface as a kind of case study - a mobius strip twisting through 360 degrees, as seen in Figure 37. Once the algorithm was able to handle building a lattice on a mobius strip the parametric features of the algorithm were built out.

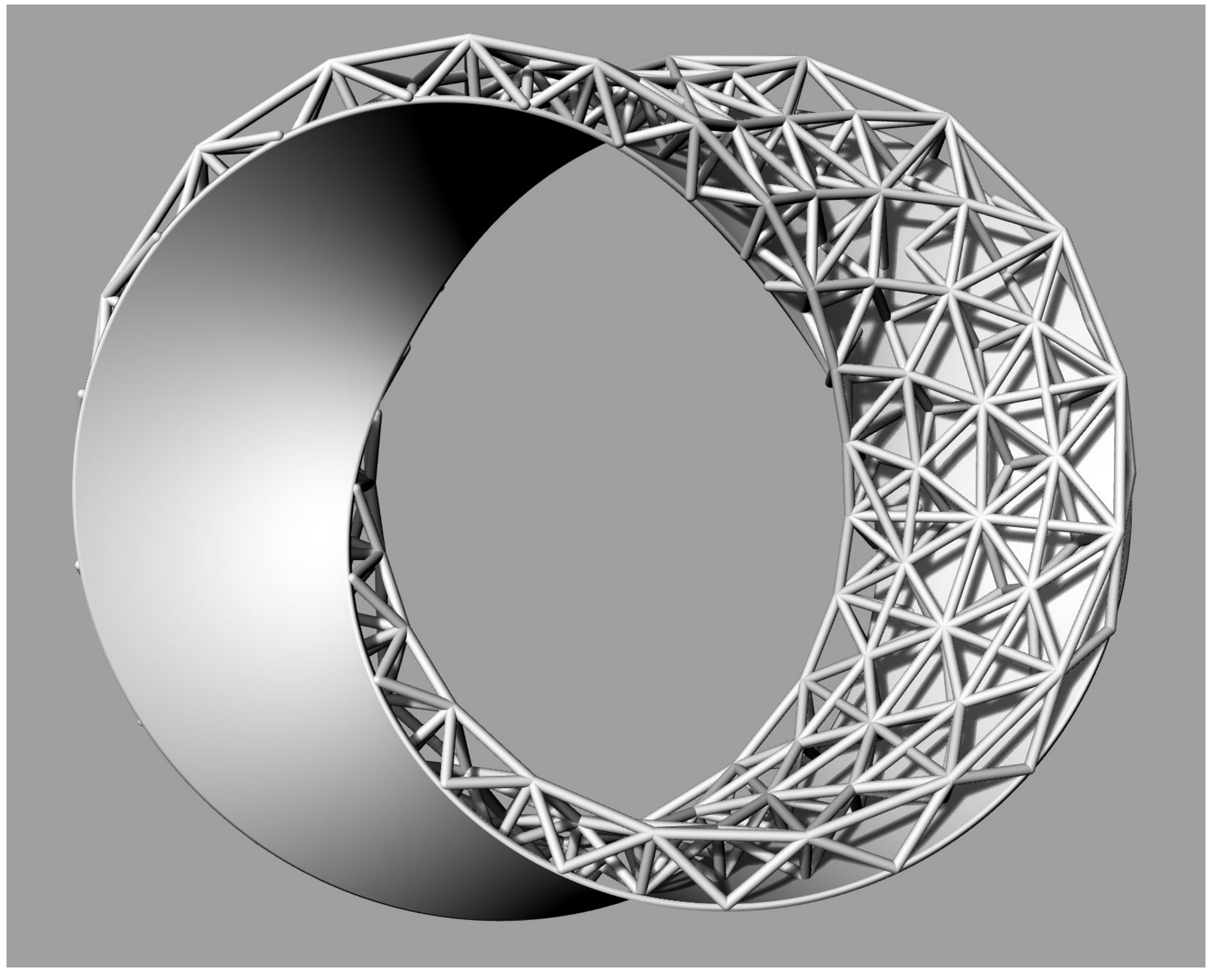

Figure 37: A lattice reinforced mobius strip.

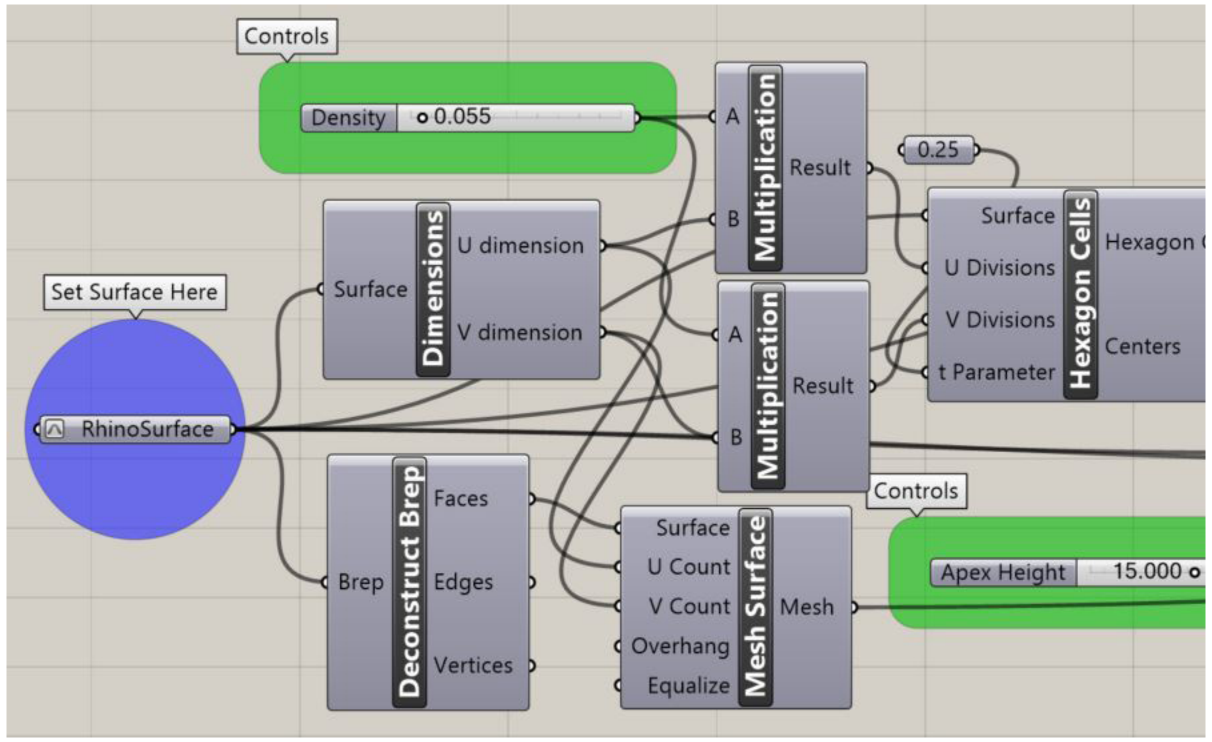

Figure 38: The beginning of the algorithm. Set Surface, Density and Apex Height controls.

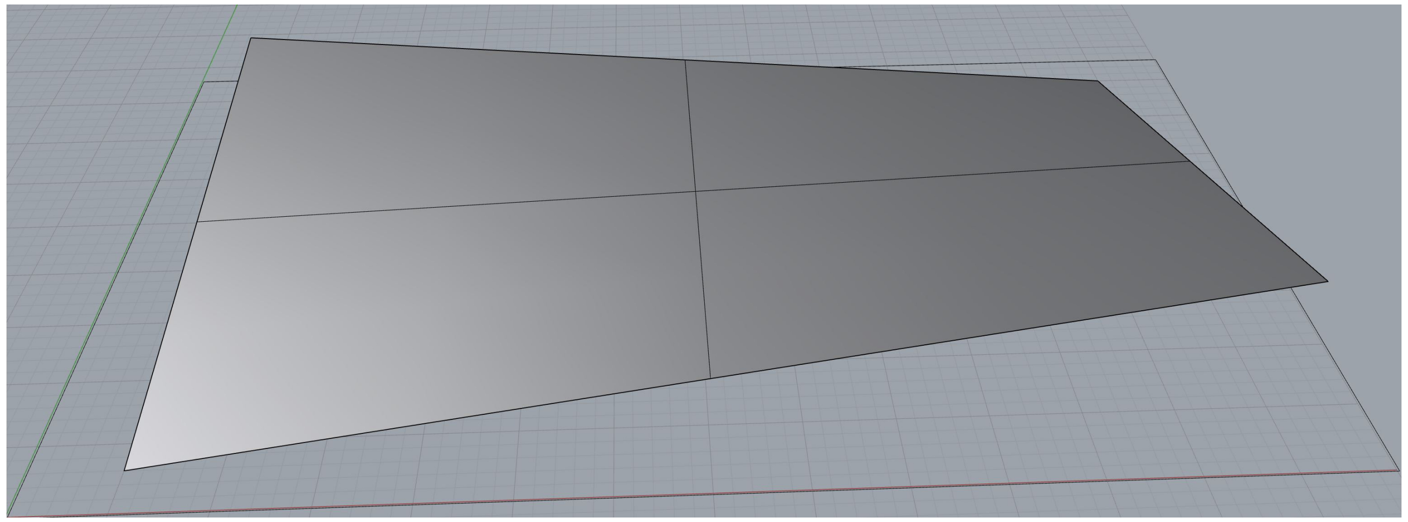

Figure 39: A surface in Rhino, ready to have algorithm applied via RhinoSurface component in Grasshopper.

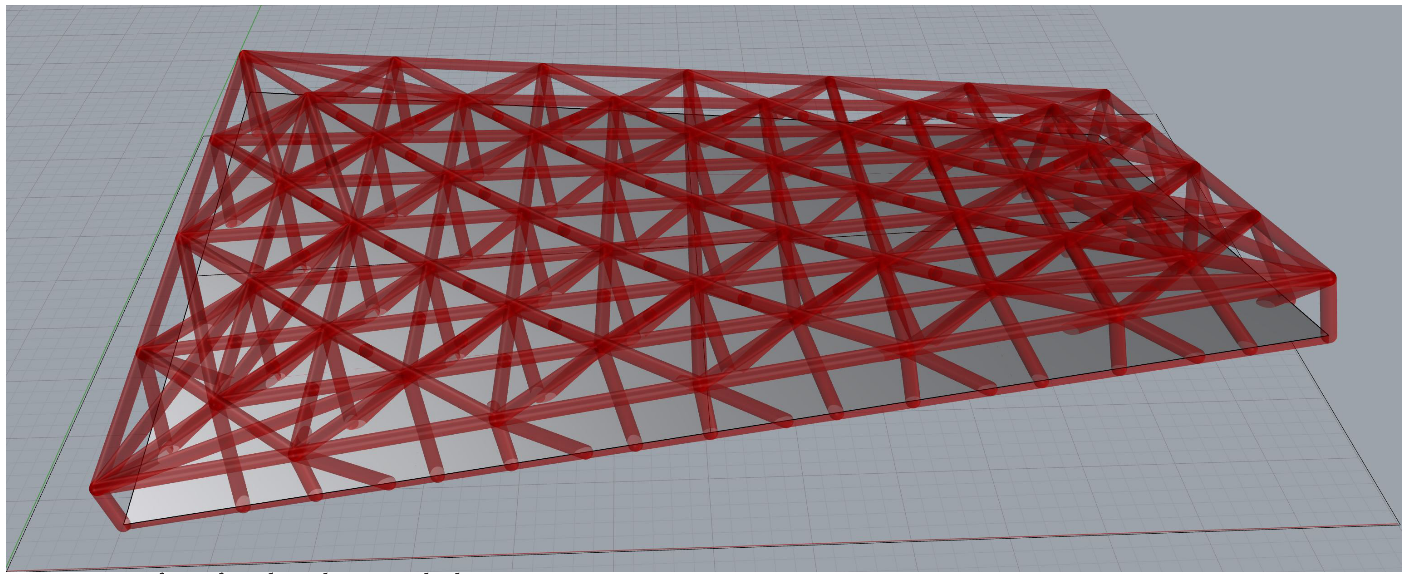

Figure 40: Surface after algorithm is applied.

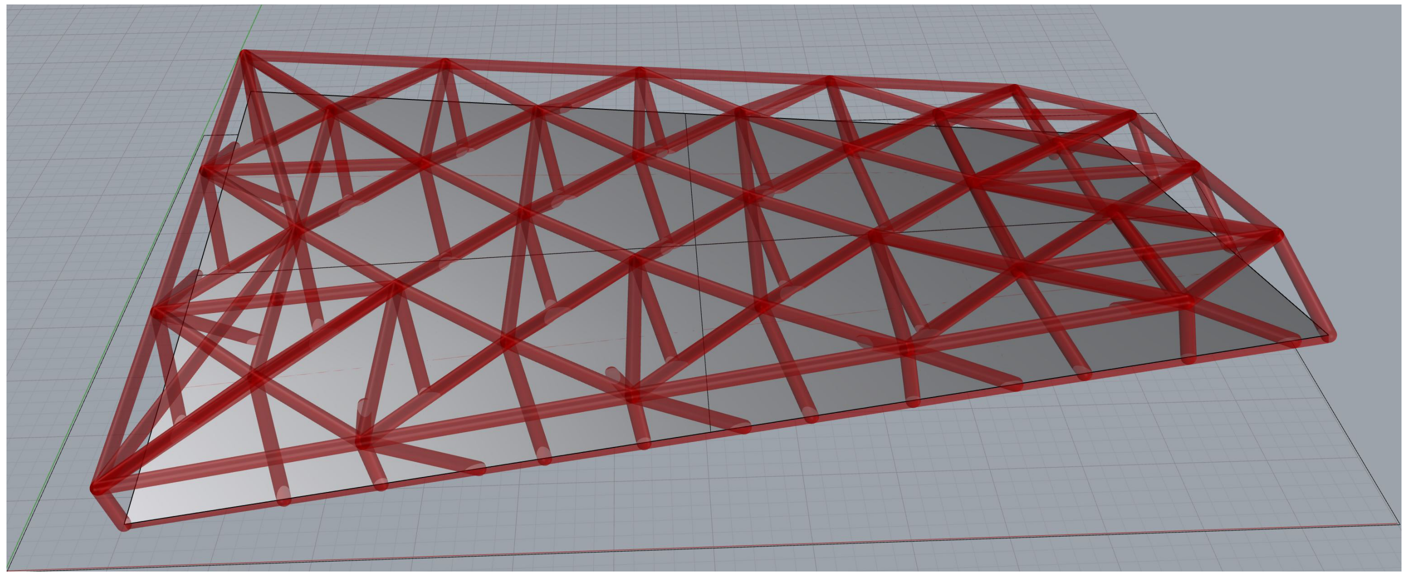

Figure 41: Density is decreased, weakening the lattice but lightening the computational load.

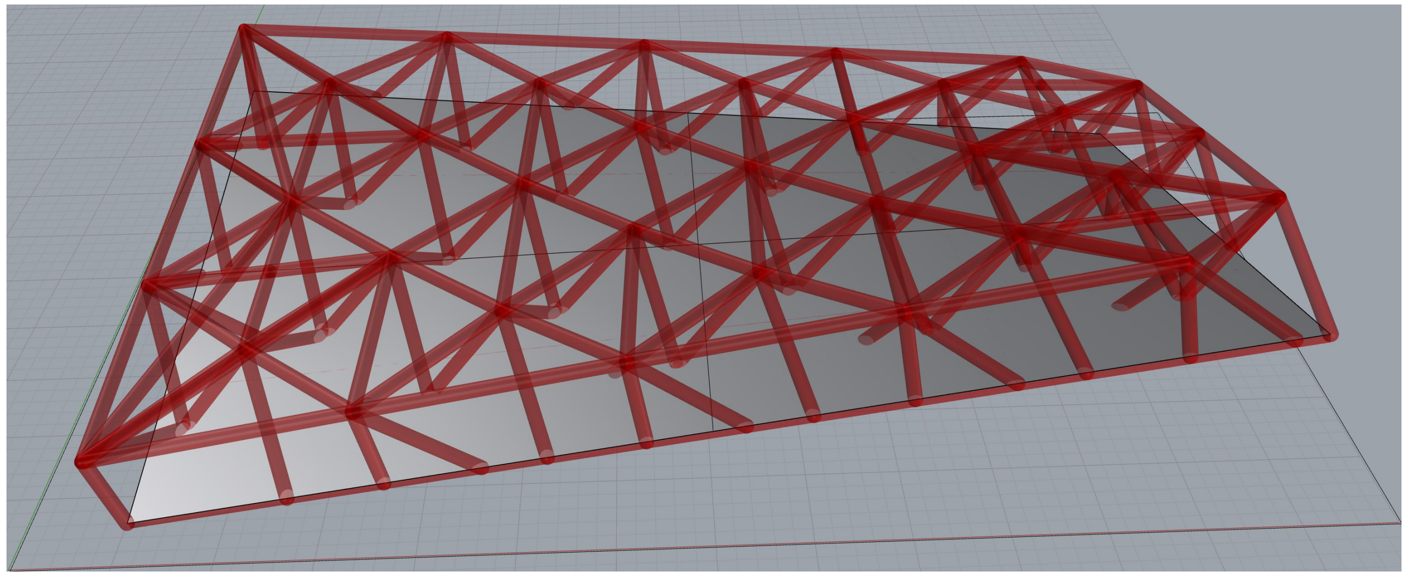

Figure 42: Apex height is increased, analogous to thickening the surface in terms of physical behaviour.

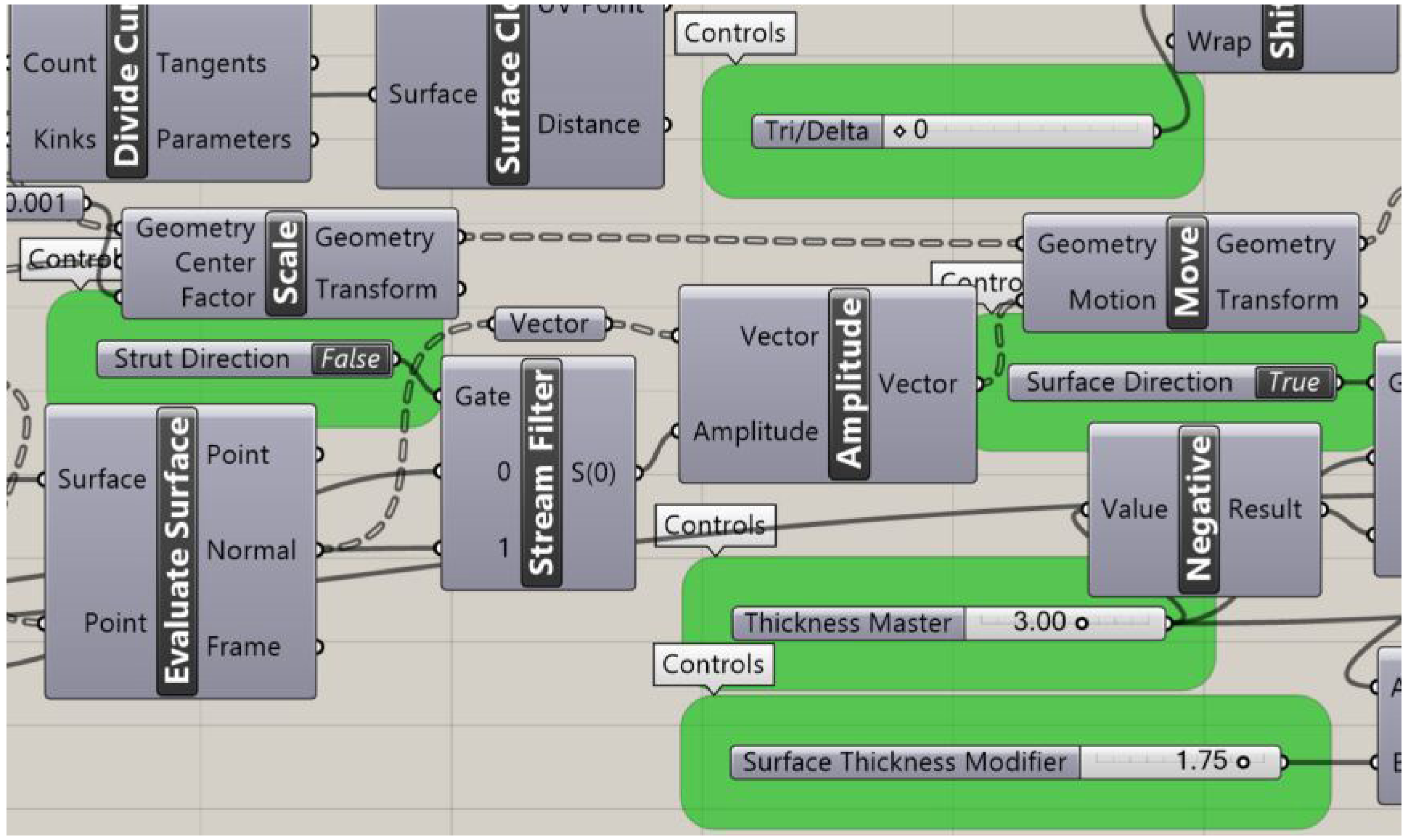

Figure 43: Strut Direction, Thickness controls, Triangle and Delta orientation 'switch', Surface Direction toggle.

Three of the most important controls are right at the beginning of the algorithm, seen in Figure 38. The component named Rhinosurface can accept a surface from Rhino, such as the one seen in Figure 39, or from within Grasshopper. It is the surface that the lattice is built on. Most surfaces have two sides, but that isn't specifically addressed until later in the algorithm. The Density control determines how many hexagonal cells are packed within the surface area, attempting to keep them relatively regular despite the shape of the surface. Apex Height controls the distance from the surface to the point the struts of an individual hexagon meet, which also determines how long the struts have to be to reach that point.

In the guts of the algorithm, seen in Figure 43 and Figure 49, there are eight more controls. First, the Strut Direction toggle. This establishes which side of the surface the lattice will be built on. The Surface Direction toggle determines which side of the surface will be thickened, taking it from 2D to 3D to enable printing. These two toggles work in tandem to prevent the bases of the struts poking through the surface. There are also the Thickness controls, Master and Modifier respectively. The Thickness Master determines the diameter of the struts, and the beams that link the apexes of the struts, and also the base thickness of the surface. The Surface Thickness Modifier is a value to divide that Master value by, if the user wants the surface thickness and the lattice member thickness to be different. The surface is thickened normal (perpendicular) to itself, rather than in an axis direction.

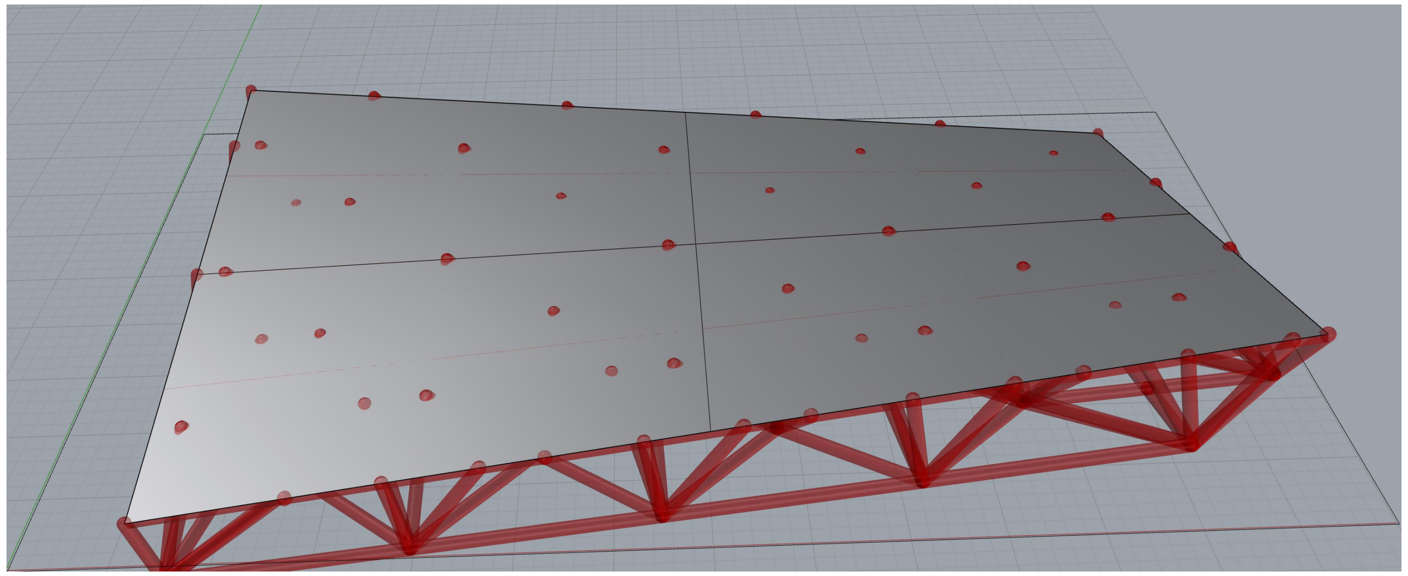

Figure 44: Strut direction is flipped, and now the bases of the struts poke through the surface.

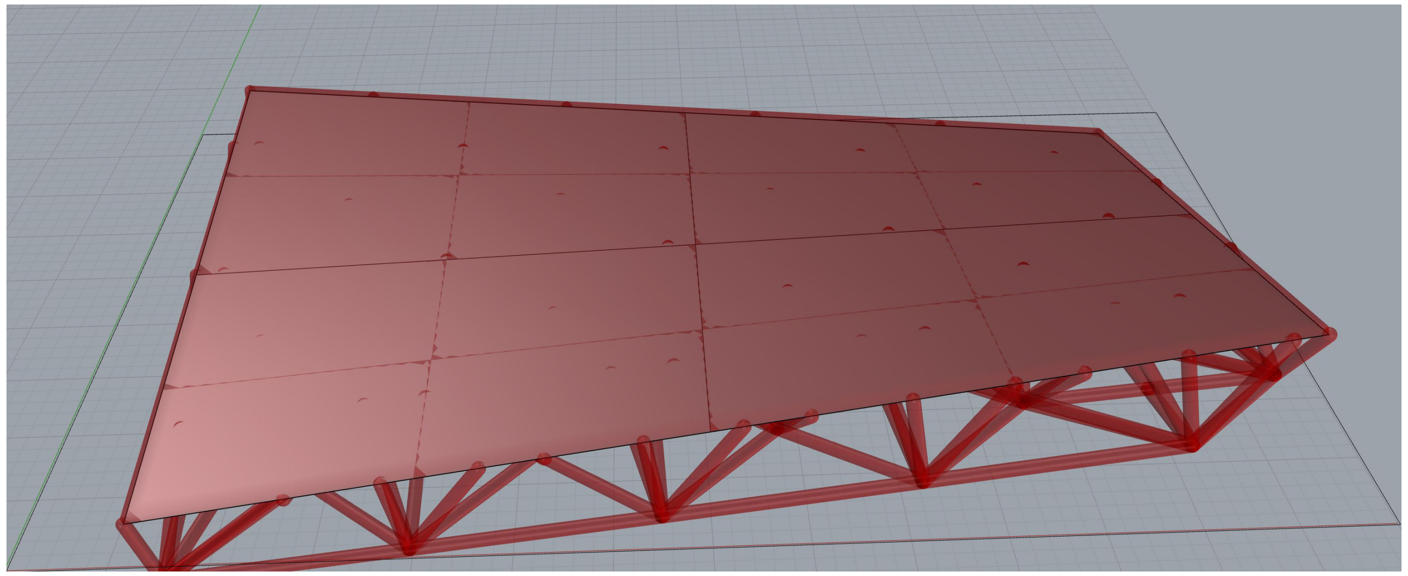

Figure 45: Surface direction is flipped to encase strut bases.

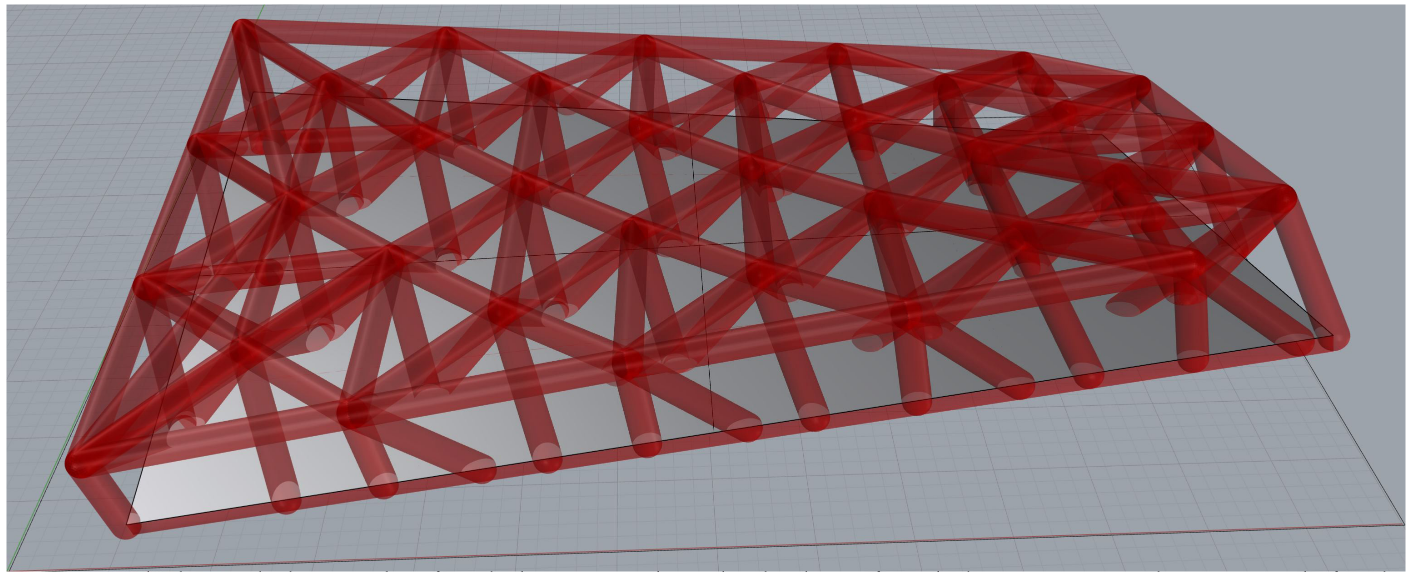

Figure 46: The lattice thickness and surface thickness are tied together by the Surface Thickness Master, and are increased after the direction of the lattice is reverted.

The Tri/Delta 'switch' and Hex Struts toggle determine the arrangement and number of struts around each hexagon in the grid. Because each hexagon has six points at its corners, there are six points struts can originate from. Taking odd points gives the delta orientation while even points gives the tri configuration. All six points at once make six lines, and therefore six struts per hexagon. Depending on the orientation in space of the surface in question during 3D printing, delta or tri may print better. Using hex struts doubles the designed number of struts, introducing a level of redundancy into the lattice as a failure to print contingency and providing a higher degree of reinforcement.

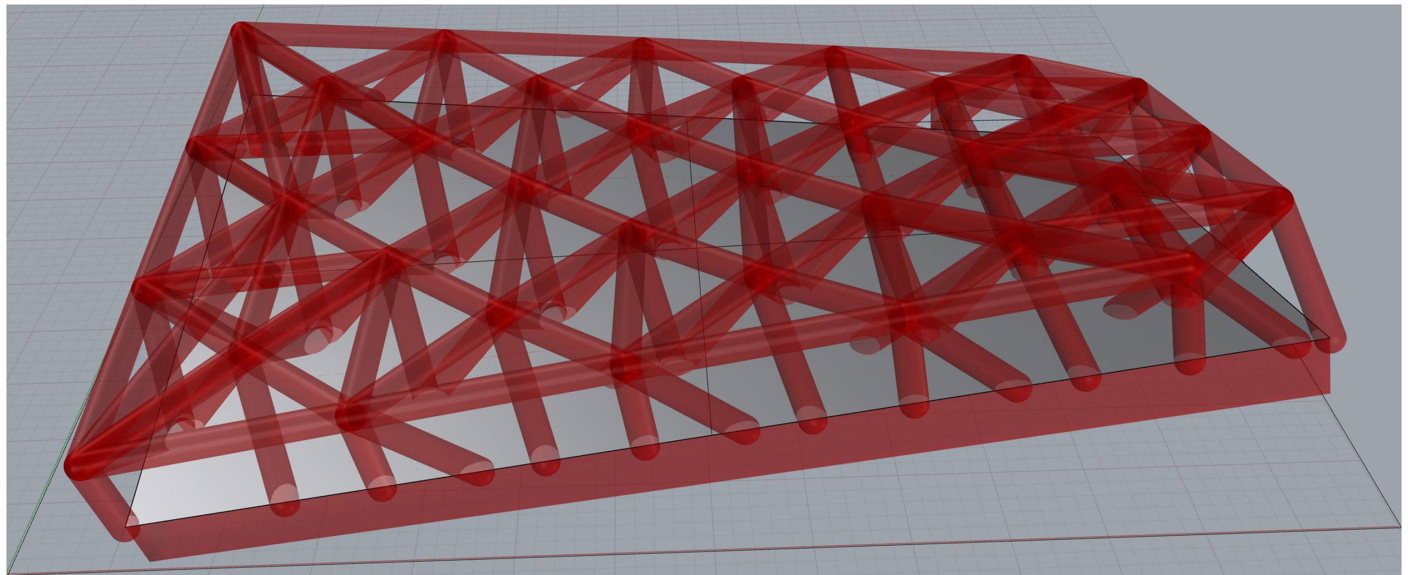

Figure 47: The thickness of the surface can be separately modified by the Surface Thickness Modifier, however.

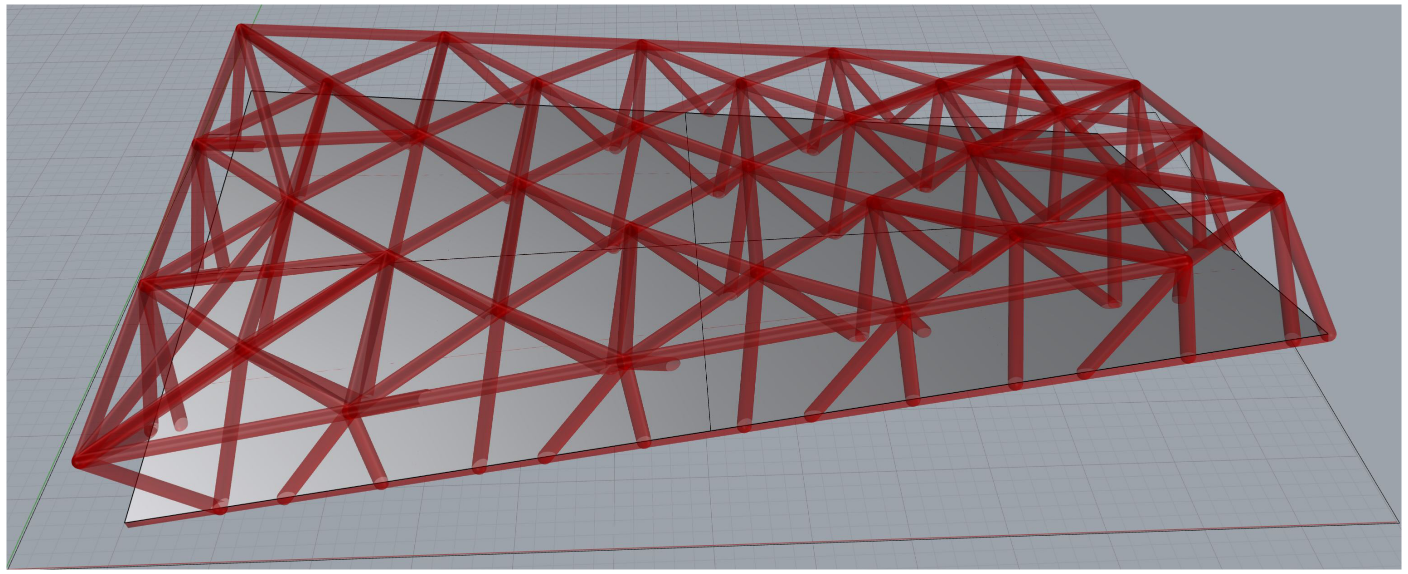

Figure 48: The strut orientation is switched to delta, after the thickness is reverted.

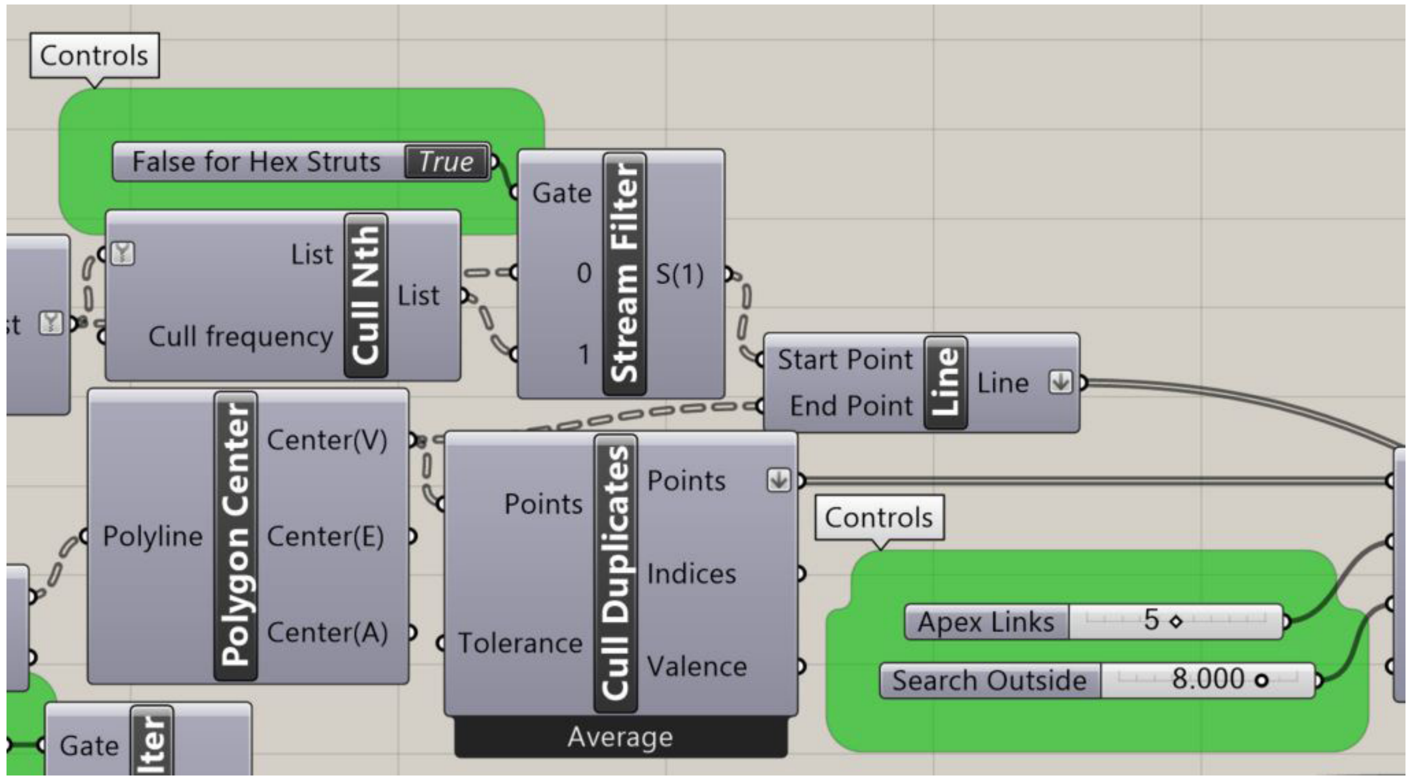

Figure 49: Hex Struts toggle, Apex Links and Search Outside controls.

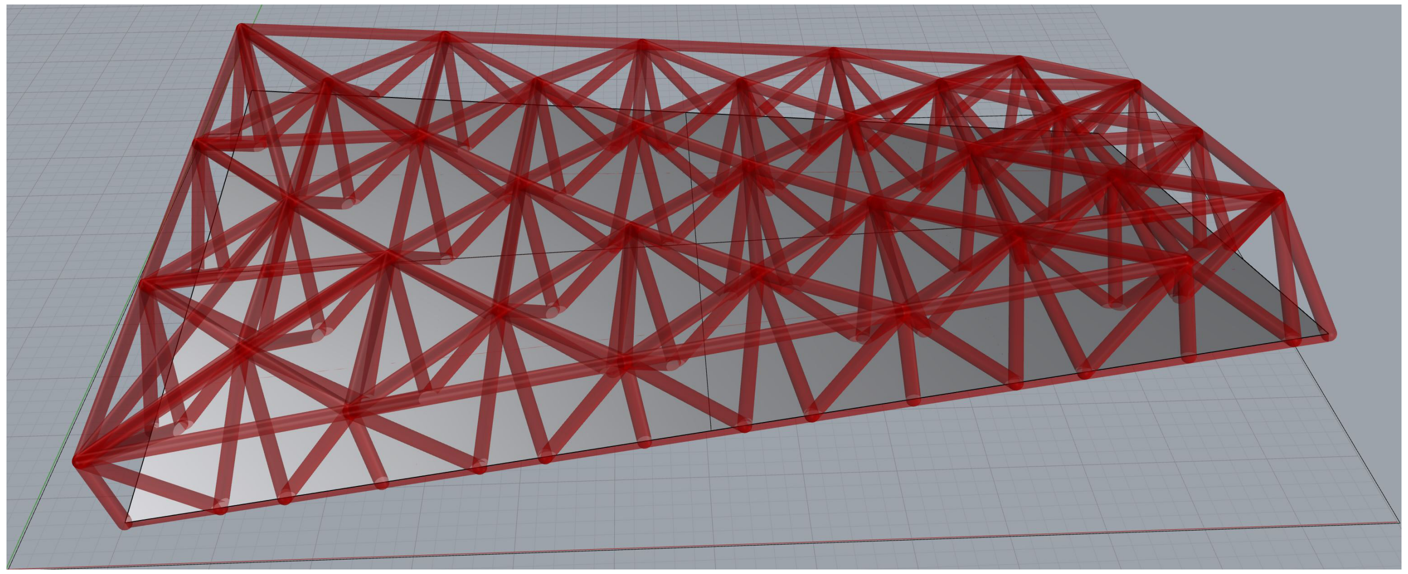

Figure 50: Hex strut toggle is flipped, so delta and tri struts are both present, which makes a stronger lattice.

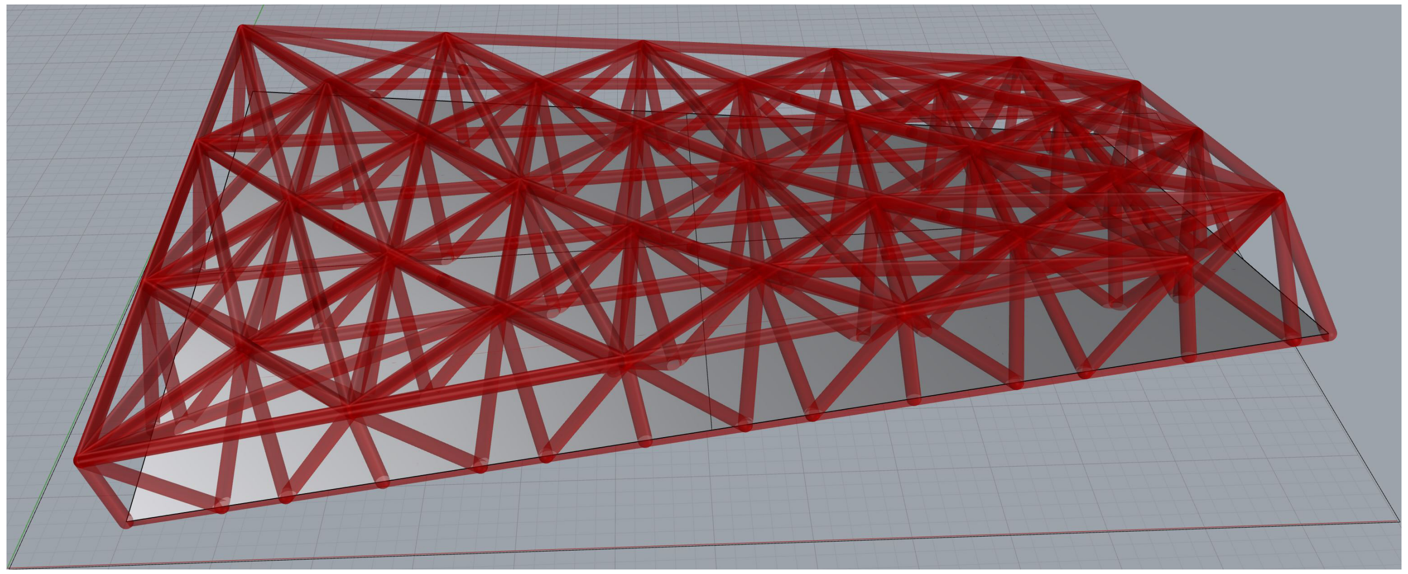

Figure 51: The Apex Links count is increased, strengthening the lattice at the expense of the pattern.

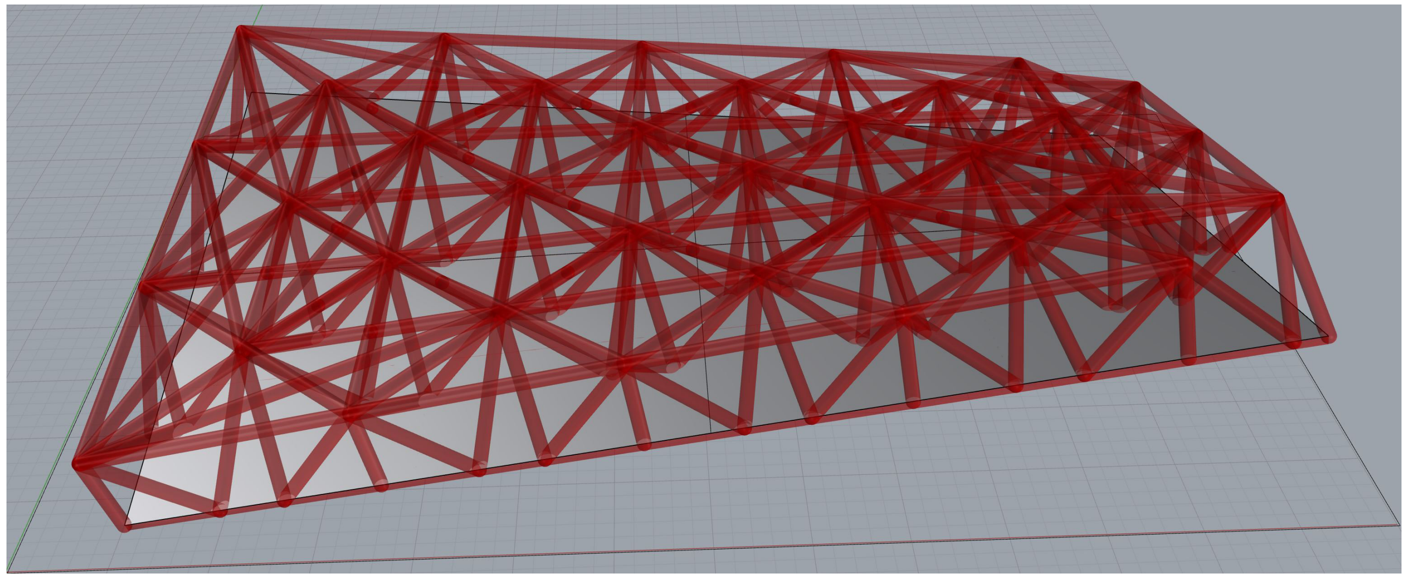

Figure 52: Search Outside radius is adjusted, preventing links within the specified radius.

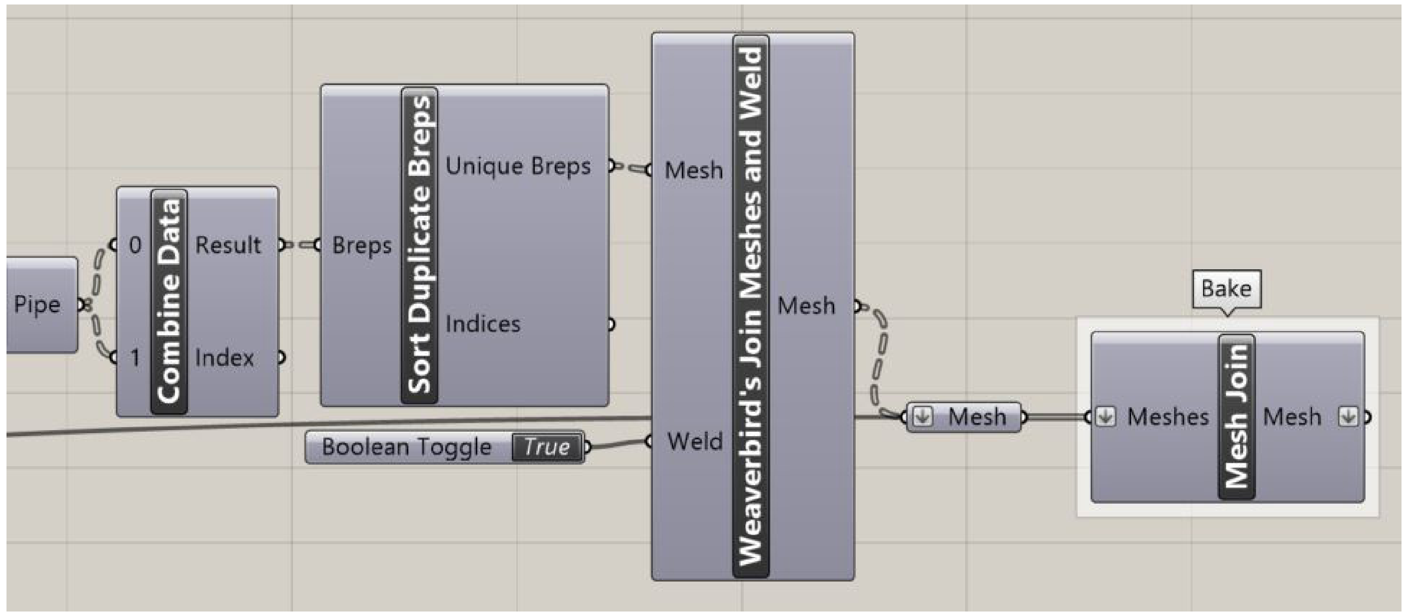

Figure 53: The end of the algorithm. Bake using the right-hand side of the component to output a single mesh.

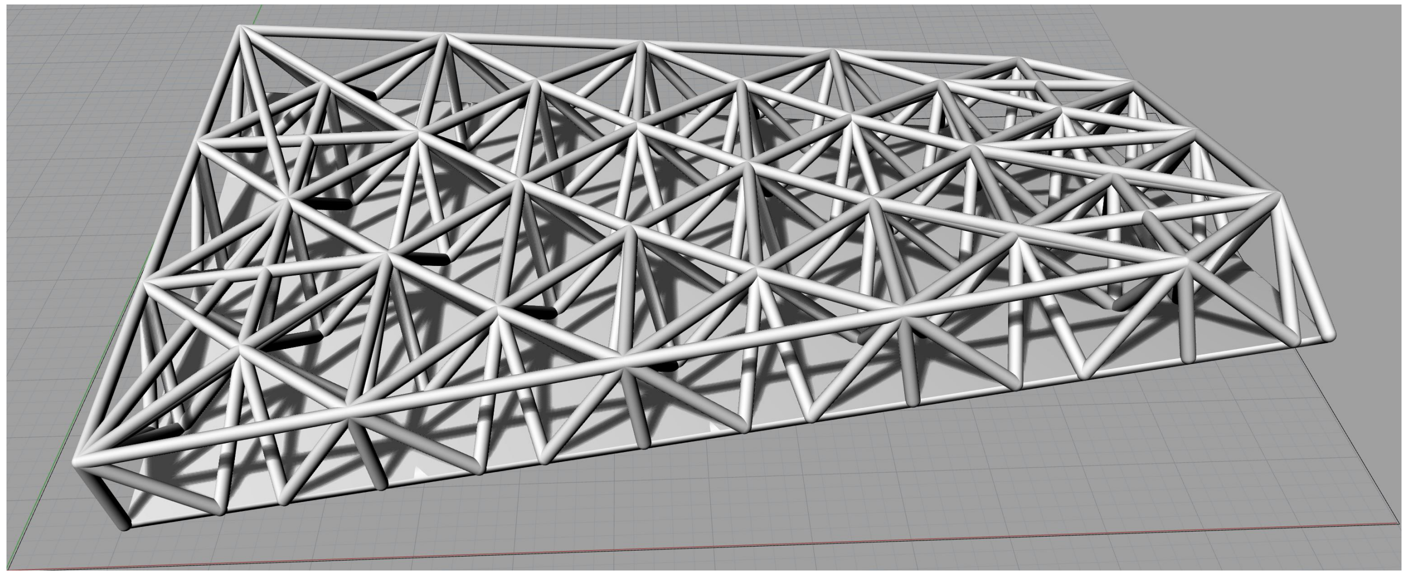

Figure 54: Once baked in Grasshopper, the mesh object is editable - and exportable - in Rhino.

Apex Links is a count of how many linking beams should be made between apexes. Search Outside is the spherical radius around each apex inside of which to not build any beams. These two controls work in tandem to generate the emergent pattern of the lattice, and are therefore also important in determining the overall
strength of the lattice.

Finally, in Figure 53, there is the final component a user needs to interact with in Grasshopper when using the algorithm. To generate the lattice and surface as a mesh in Rhino, the data entering the Mesh Join component must be Baked. After that it can be exported from Rhino as an STL file, to be cleaned and prepared for printing.

Chapter 11) Getting a Printable File: Problems With Software

Using the complexity available in Grasshopper, a great degree of parametric flexibility was built in to the algorithm via the features covered in the previous chapter, thanks in part to the open nature of the Grasshopper online community and their willingness to help. However, there were always problems to solve, and hard limits that couldn't be circumvented, only tolerated.

The first of these problems emerged during the use of the mobius strip. Because of the way Rhino thinks about surfaces, it seems that surface shapes with less than three edges have a seam. Such shapes include cones (one edge and a point, or two edges if truncated), cylinders (two edges), and mobius strips (a single edge if one has a multiple of 180º twist other than multiples of 360º, when there are two edges) among others. The seam is a line that begins at one edge and ends at the other one (or the point at the tip of a cone).

The seam problem is solvable on a case-by-case basis, but requires a lot of non-automated work in Grasshopper, which would change for each surface and many variations made in the parametric options of the algorithm. It manifests as a beginning and end of the grid of hexagons - two extra sides. This means it often interrupts the pattern, creating an eyesore. If the file was printed straight from Rhino, it would also create a line where the surface was much thinner than elsewhere, essentially a ready-made fault line ready to crack under pressure.

Secondly, the computational load for certain configurations of the algorithm and its representation in Rhino, Netfabb, and Meshmixer became untenable. The main reason for this was the density of a lattice. Working with fine, dense lattices means that there are a lot more struts and beams, and hexagons, all of which mean more triangles and vertices in the STL mesh to compute. It also generates much larger file sizes, which are awkward to load and process in programs.

The slicing software in Gizmetor had a hard time interpreting the Rhino STLs because objects in Rhino are composed of surfaces. When closed those surfaces represent solids rather than actually being solid, like in Solidworks for example. This lead to some very strange, but more importantly, time-intensive and wrong layer images being generated. In order to solve this, as well as the previously mentioned problems, Netfabb and Meshmixer were used to prepare the Rhino STL files for Gizmetor.

After export from Rhino, the first stage of preparing an STL for printing is to import it into Netfabb. In Netfabb, the mesh can be reduced, lowering the number of triangles and vertices in the STL, and allowing further steps with the computational power available. After reducing the mesh, holes in the surface are stitched. Then, self-intersections can be split from the mesh with a boolean operation, and removed. The mesh can be stitched once more to be safe, and the Netfabb repair operation completed.

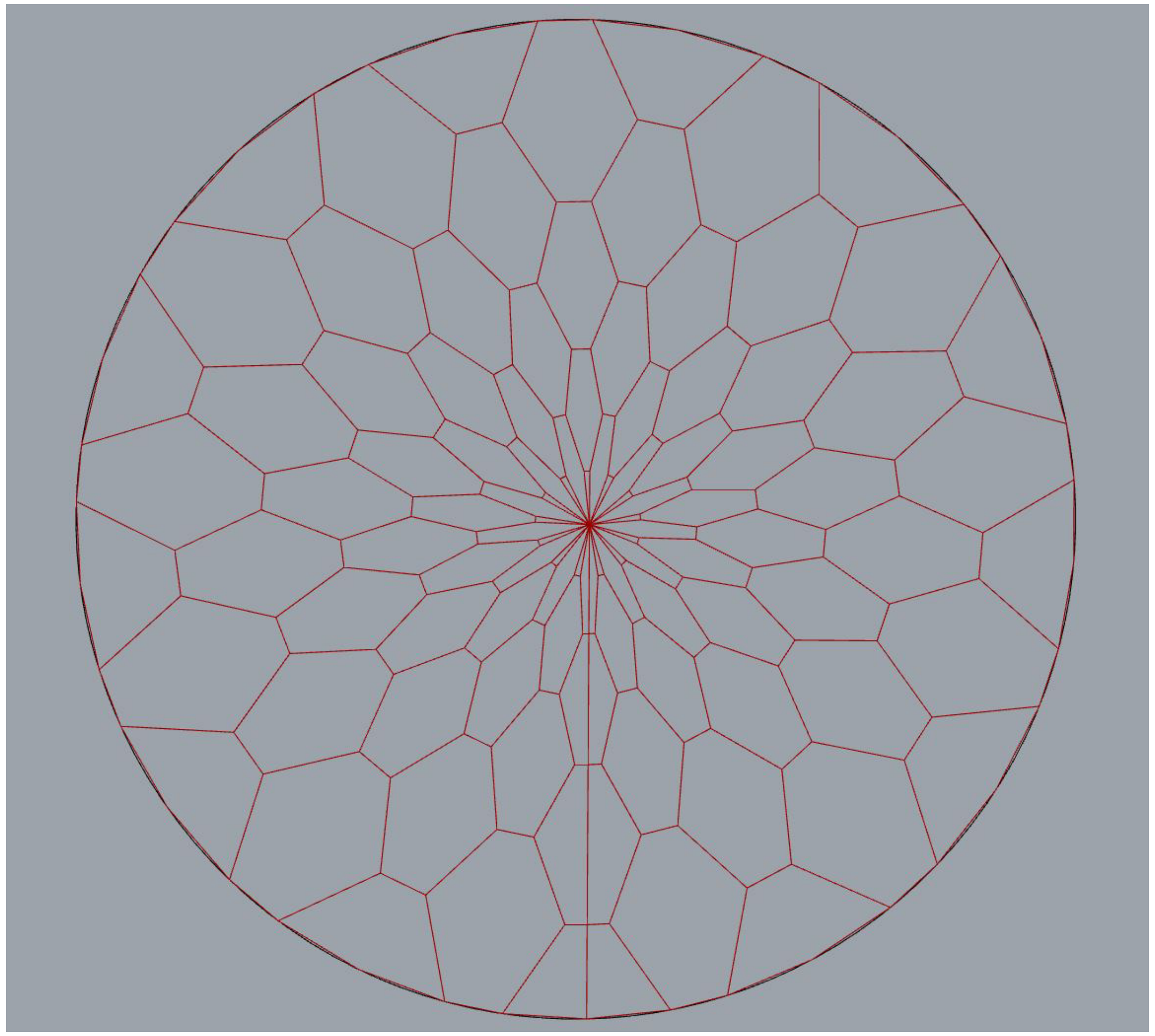

Figure 55: Top view of the hexgrid pattern on a cone, showing the seam - the long vertical line.

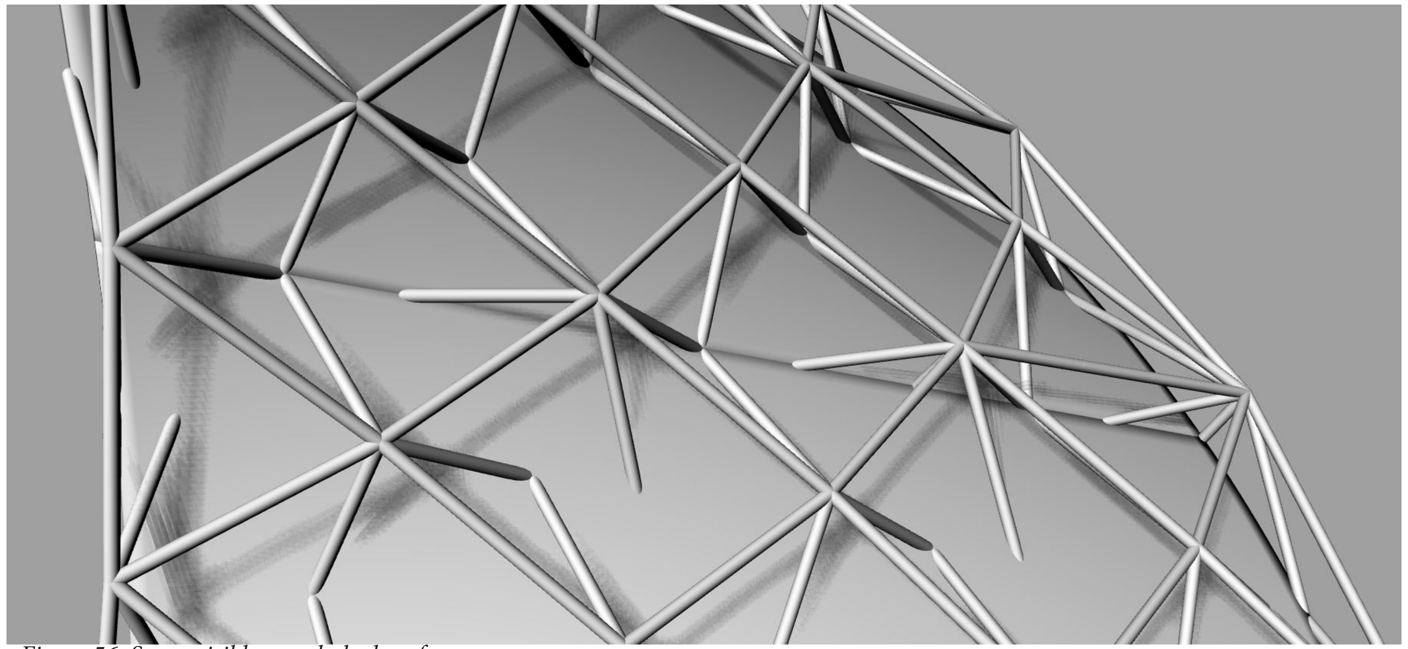

Figure 56: Seam visible on a baked surface.

After Netfabb, Meshmixer is used to transform the file from closed surfaces to a solid, using the Make Solid tool in the Edit tab. If desired, Meshmixer is the program used to add print support. During the test printing phase, supports were used in an attempt to reduce print failure. While successful, supports were deemed ultimately counterproductive to the spirit of the thesis. Supports require extra surface area to be displayed. Also, if a reinforcement lattice is applied to the inner surface of a mostly-enclosed designed object, it would be impossible to remove the supports after printing. Instead, the lattice reinforcement structure should be designed to not need extra support, during the Grasshopper stage - as per design for additive manufacturing best practice.

Once the file is exported from Meshmixer as an STL, it can be imported into Gizmetor for slicing. Gizmetor has the ability to hollow out the digital file and insert a honeycomb infill, leaving the majority of the inside of the printed object liquid until post-cured. It does drastically increase slicing time, but allows faster printing. Only the edges of the object on each layer and the infill need be displayed. In the case of the objects printed within the context of this thesis, the infill is a few ~1mm lines joining the surfaces of the object. Gizmetor also has the ability to print solid and hollow within the same print job. This is useful for ensuring the base and top of the object are solid so that the internal liquid resin of a mostly hollow print won't leak out if a small tear or hole is made during removal from the buildplate, for example.

Figure 57: Seam visible on a printed object, as a vertical line and an interruption in the pattern.

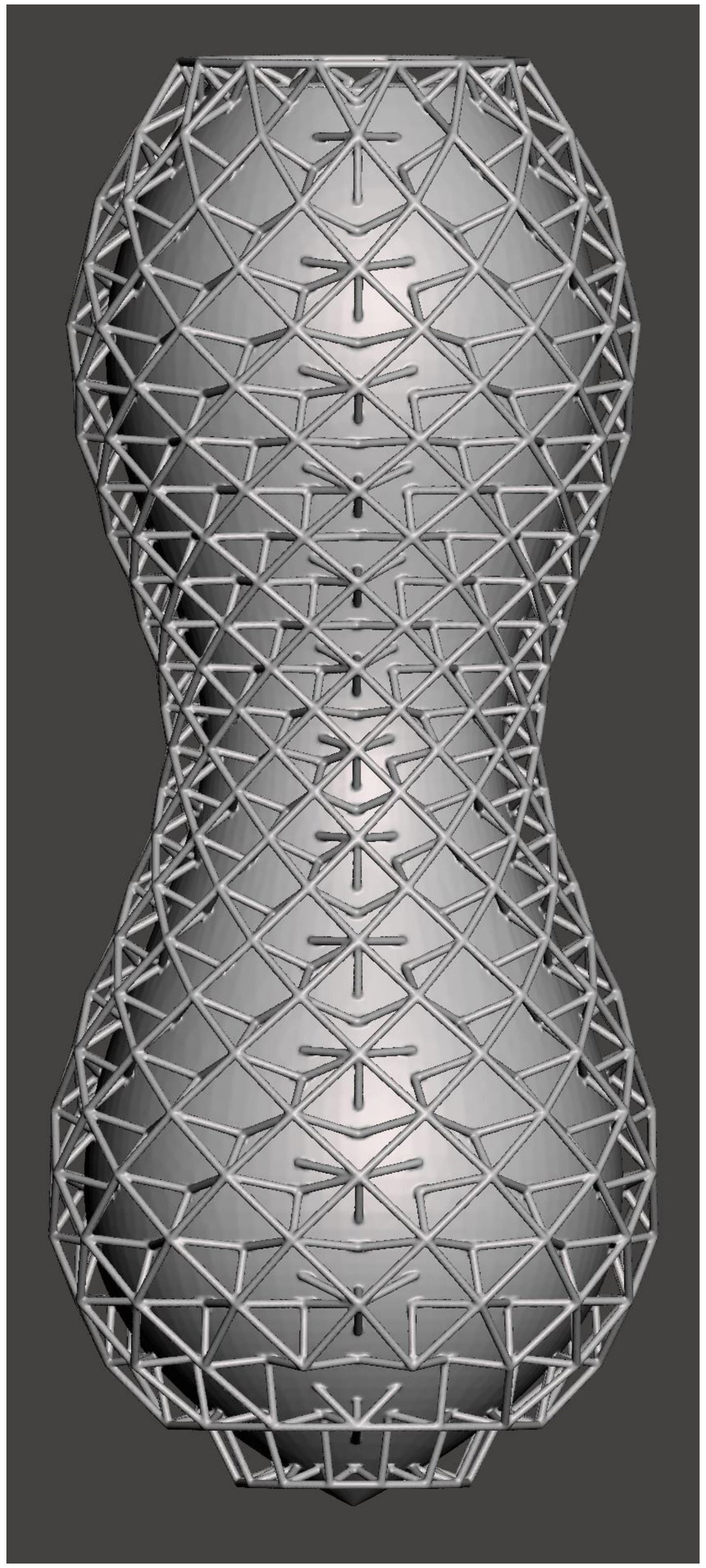

Figure 58: A vase design, with a delta lattice. Having been made solid in Meshmixer, it no longer shows a seam on the surface. The effect of the seam on the lattice pattern remains, however.

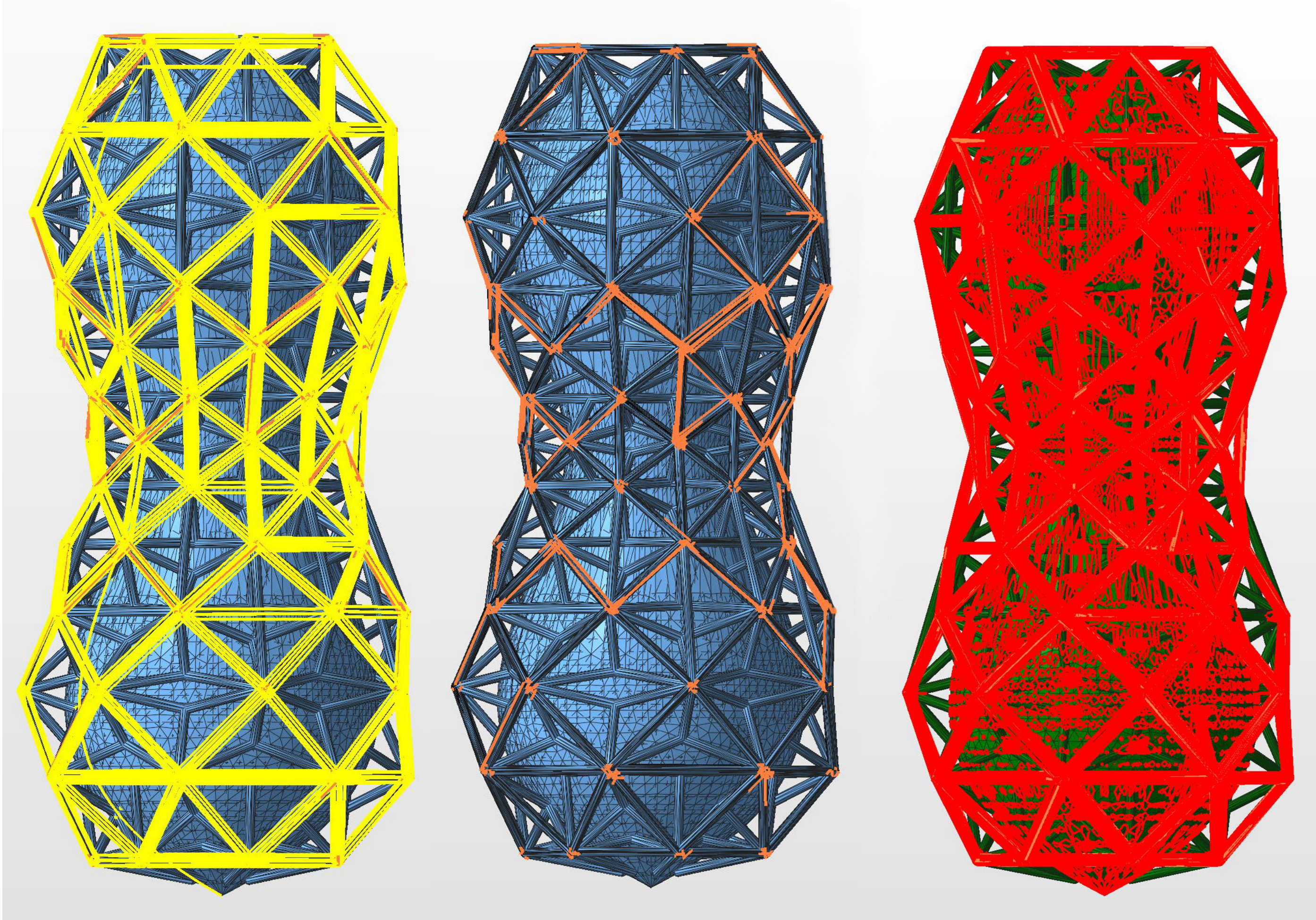

Figure 59: Three stages of the Netfabb process, readying a hex-lattice reinforced vase.

Part 2b Discussion

The design and deployment of a robust and capable algorithm was an ongoing process. It began immediately after the research on design phase was completed, and extended well into the research through design phase out of necessity. Research into using Grasshopper never really stopped, since even after the algorithm was fit for purpose it could still be streamlined and optimised, incrementally iterated to be better. Using it to design strong, highly printable, and aesthetically pleasing lattices was a satisfying method of judging it.

By using a technique that grows struts from a surface into tetrahedral pyramids and links their apexes, rather than the standard nodal unit volume replacement method, inherently conformal lattices that visually express aspects of the surface they're reinforcing in their emergent pattern became the new norm.

Overcoming the various software problems, by workaround if not within the algorithm, was admittedly frustrating. The algorithm is left in a prototypal state, meaning there is still plenty of room for added functionality. Functional grading by manipulation of lattice density, making apex link length a driving factor, and curved struts were all features considered for implementation but deemed ultimately unnecessary for enabling fast, large, and accurate 3D printing. The ultimate goal would be generation of a file able to be directly exported into Gizmetor and sliced, without the intermediate steps in Netfabb and Meshmixer.

Part 3: Research Through Design

As soon as the algorithm enabled a reinforcement lattice to be built on a surface, and adjusted to maximise printing speed and resolution, several test prints were conducted using the small vat, and a single projector. This meant that continuous printing was not possible to begin with, but also that there were no projector alignment issues. The first test prints consisted of lattice variations on business card sized rectangular surfaces. There was very little design of the cards themselves. However, iteration of lattice designs lead towards the types that would print well. Experimentation with supports progressed in parallel, ultimately leading to the conclusions that supports weren't necessary and the design of the lattice reinforcement structure should be self-supporting during printing.

Once a basic understanding of how the lattices interact with the surface they reinforce was established, the medium vat was installed into the Gizimax and the second projector added. This enabled continuous printing, and therefore progress towards the holy grail of simultaneously fast, large, and accurate 3D printing.

Chapter 12) Printing Process

The model of Gizimax Ultimate the School of Design has is very open, as are the versions of Gizmo3D's two programs, Gizmetor and Giziprint, used to slice and package files and run the printer respectively. This means that every setting can be manipulated, whether digitally in the software, or by hand on the projectors. The height, display area, and focus of both projectors must be manually adjusted. The majority of projector image alignment must currently be done using screws. Fine tuning is then done with the projector remote, by visually inspecting the calibration grids displayed on a sheet of foil floated on the resin in the vat, and trying to match them pixel-to-pixel. Once projector alignment and other settings are satisfactory, the resin is mixed and at the overflow level, with the top of the buildplate set just under the surface, the printer is physically ready to begin printing.

After importing a file into the 3D Layout in Gizmetor, it can be oriented on the virtual build platform. Multiple files can be imported and arranged in this way, to enable simultaneous printing. The platform should be set to reflect the current vat size, buildplate size, and display area settings. Once suitably placed, the next step is to slice the object into layers with the appropriate print profile and settings. Profile settings include the resin being used, and the desired z-height. Print settings account for whether the print is continuous or not, whether it should be solid or hollow, and more. There are several parameters within most of these variables, and they can all be changed. After slicing is complete, the transition from Gizmetor to Giziprint is made.

With Giziprint, the first layer can be displayed on the resin; first in non-curing red, to check the scale and display location are correct, then in white to ensure an extra well-done bond to the buildplate. After that, if everything was set up correctly, the print can begin.

Chapter 13) Problems Using the Printer

Because every variable on the printer is adjustable, the fact that no two projectors have exactly the same spectrum profile, and the fact that each resin is different and varies in its behaviour depending on its age and how well-mixed it is, problems crop up a lot. Primary among these, and one of the most difficult to resolve, is projector alignment. Given the differing keystone between projectors due to the distinct angles they are projecting at, along with their individual brightness and contrast settings, getting the images aligned is a non-trivial task, yet essential for accurate prints. Getting good alignment is probably the biggest hurdle in the process.

The colour of FunToDo Standard Blend Red resin is the result of added pigment, which settles out over relatively short periods of time - overnight, for example. Attempting to print with poorly-mixed resin will cause print failure since it amounts to using clear resin. As mentioned earlier, in Chapter 9, clear resin results in over-penetration of light into the resin, and refraction which distorts the projection and therefore the accuracy of the print. So the resin has to be re-mixed prior to printing each day. This must be done manually, by stirring or sucking up the pigment that has collected at the bottom of the vat until it is re-suspended evenly throughout the resin. There is an electric mixer built in to the bottom of the Gizimax Ultimate, featuring magnets designed to spin a metal bar inside a large acrylic vat. The motor is too weak to be effective, however, and the large vat the university received is steel, which essentially renders the mixer useless.

Another problem is due to the top-down method of printing. The curing inhibitive effect of oxygen on resin exploited by Carbon also affects resin when printing top-down. This means that the very surface of the resin doesn't cure well, and leaves the prints tacky, even after significant UV post-curing.

The resin must be kept clean. Any partially cured fragments tend to accumulate at the bottom of the vat, but may be stirred up when the resin is mixed. Additionally, dust and fluff gets into the resin. This is possibly exacerbated by the active extraction, which sucks air into the enclosure through its open base, up into the vacuum at the lid. Any of this non-liquid matter can interfere with high-resolution printing. Relatedly, dust or smudges on the projector lens can have significant detrimental effects on print quality. These problems are likely all contributing factors of persistent hole problems with the prints made during this research.

Finally, print settings and their interactions have a major effect. Overcuring, whether due to brightness settings, print speed being too slow, or poorly mixed resin, results in an exaggerated z-layering effect reminiscent of FDM z-layering. Considering the difference in actual layer height, this is a significant issue. Fortunately, anisotropy appears to remain relatively insignificant with settings that cause that level of overcuring. Some of these problems can be resolved with software, by matching printing speed to display area, for example. However, that has yet to be implemented in Gizmo3D software.

Chapter 14)
Prints and Print Evaluation

As mentioned in Chapter 11, rectangular test objects were printed using print support. These were printed at three different angles relative to the buildplate. The basic orientation was standing vertically on a long edge of the rectangle. The two variations of that were angled 45º, towards either the flat side, or the lattice-reinforced side, seen in Figure 60.

The 45º degree angle necessitated use of support, so that the printed object would not fall over during the jerky dipping movements of the buildplate during non-continuous printing. The surface-down orientation, on the left in Figure 60, was an attempt to get better resolution on the object surface. The lattice-down orientation on the right was an attempt to get better resolution on the lattice. This is because it is understood that bottom surfaces print better. Removal of print supports was tedious, and destructive to the prints; fortunately, progression to printing with supports only for the base of the object quickly established they weren't really necessary so long as the orientation angle of the object and the lattice design were both within a certain tolerance.

After the flat rectangles, attempts were made to print curved rectangles, only much thinner, with respect to both the surface and the reinforcing lattice. An example of this is seen in Figure 24. The surfaces printed, with highly visible xy-banding, but the lattice structures failed entirely, as they were too thin.

At that point the decision was made to move to continuous printing, which necessitated installing and aligning the second projector. An object was designed to have smooth, regular curves within the printing angles likely to successfully print. This evolved into the vase seen in Figures 58-60, and Figures 63-65. The issues with computational load due to lattice density, and slicing closed surfaces rather than solids emerged during the first attempts to get a reinforced vase to print.

The vase prints were a good learning experience. They indicated the apex height should be increased, and the density lowered. In order to get the full visual effect of the lattice structure, it is important that an observer be able to see underneath the beams, look through the structure, and notice the strut pattern. Even if aesthetic considerations are ignored, the physical performance, accuracy to the design, and printability all improve with slightly higher apexes. The density of the externally-reinforced vases was at 0.12, which was about as high as the hardware used to process the files before printing could handle. It needed to be lowered to allow larger objects to be prepared for printing, since with greater surface area they have correspondingly more lattice structure and are therefore more computationally intensive.

After the vase, a basic lampshade was designed, in the form of a truncated cone with a circular base and a rounded square top. Again, this was to exploit the support-less printing capability of the

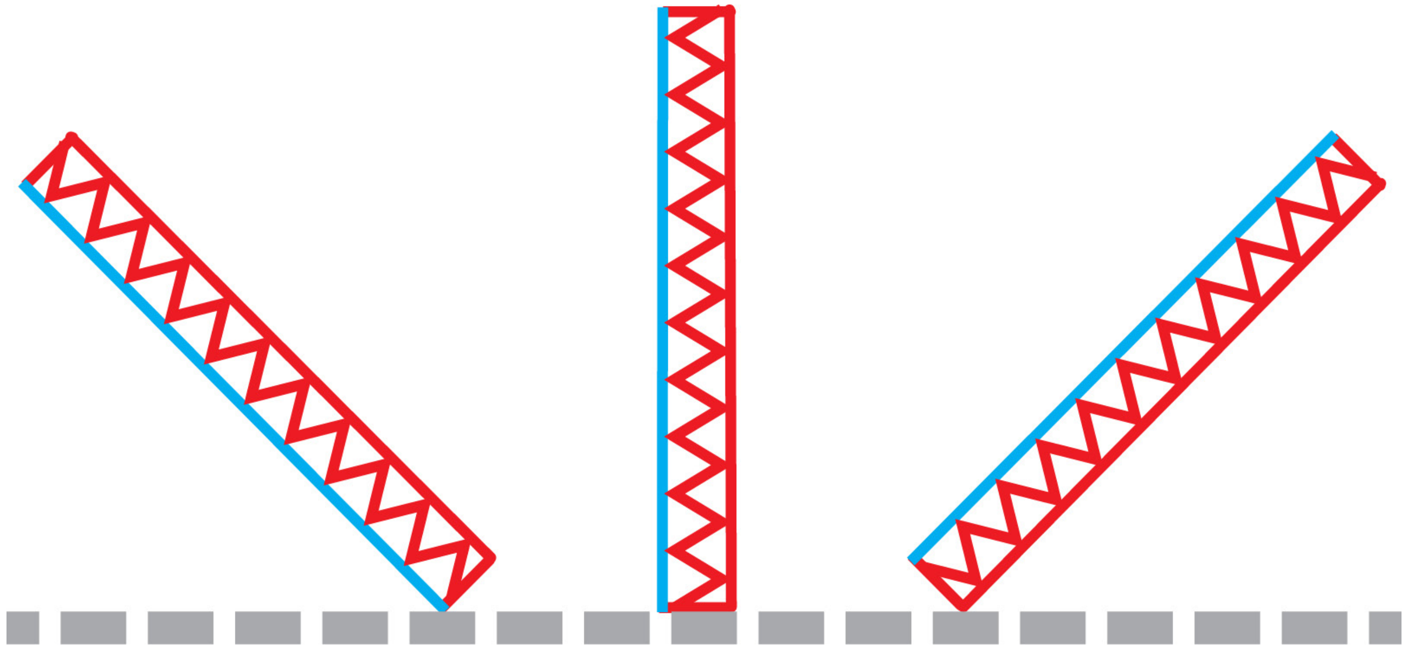

Figure 60: Side view of test print orientation on the buildplate. Surface in blue, lattice in red.

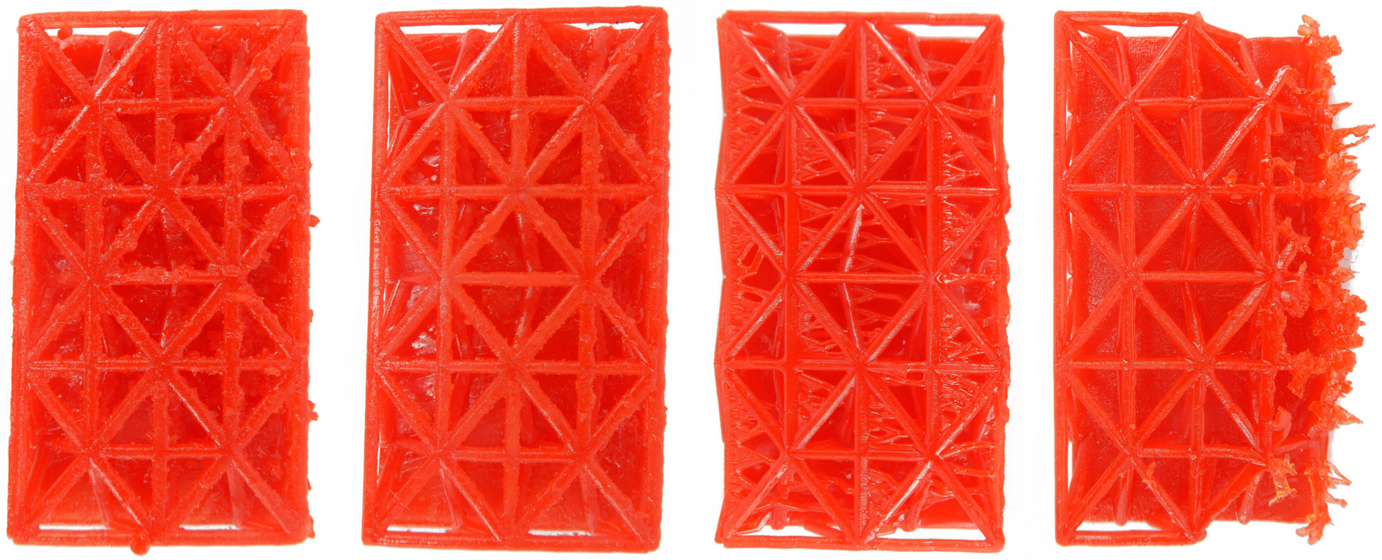

Figure 61: Four test prints, in printing order from left to right. The far right was printed without support except at the base, angled 45° towards the lattice side. The left two had their supports manually removed after printing.

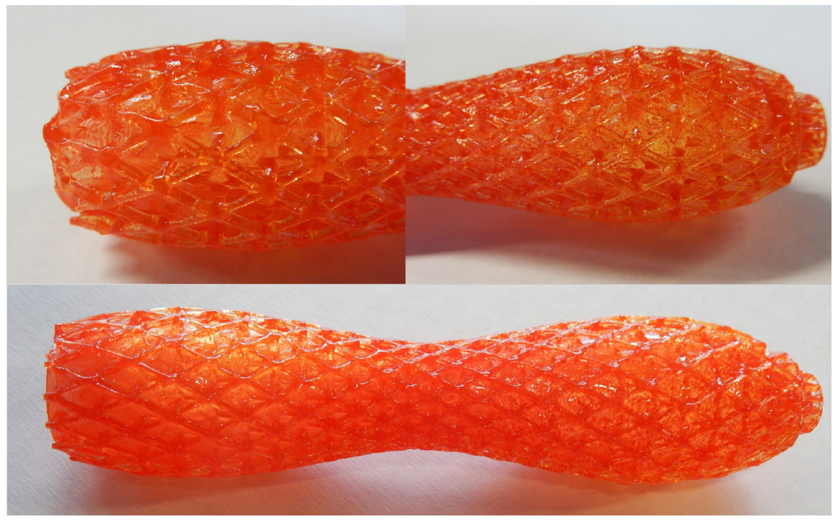

Figure 62: The first continuous print had a scaling issue; it was compressed in the xy-plane. This presents as a smaller vase stretched in the z-axis.

lattice-reinforced surface technique. By this point, and given the results with the vases and the earlier rectangular prints, it seemed like supports were more trouble than they were worth. Scaling up, with longer 'unsupported' beams linking apexes, would be an excellent thesis proof of concept.

The anticipated printability of the lattices on the basic lampshades was validated by the prints. The only internally-reinforced objects printed, their lattice quality is excellent. It's also relatively over-strong, being much thicker than it needs to be. However, in contrast to the lattice structures, the surface quality of the internally-reinforced lampshades, seen in Figures 67-70, was unacceptably bad. While the textures may have aesthetic value, they were not designed, and are an expression of incorrect print settings and inaccurate manifestation of the digital into reality. Therefore, considerable effort was made to eliminate such unanticipated printing side-effects.

Incorporating the revised higher degree of control over surface thickness, another lamp was designed, by iterating from the first. It was bulged in the middle and flared at the base, to introduce curvature similar to that seen in the vases. The variation in the normal vector from base to top creates a higher degree of deviation in the lattice pattern, leading to interesting emergent perturbations. The structure is technically weaker, but the lattice remains more than fit for purpose.

Printing the thinner surfaces with better projector alignment lead to drastically improved print quality, although new print inaccuracies surfaced too. These include extended holes resembling tears, and narrow vertical lines where the surface is thinner. Small resin starvation holes at the attachment points of a few lattice struts also continued through several print setting alterations.

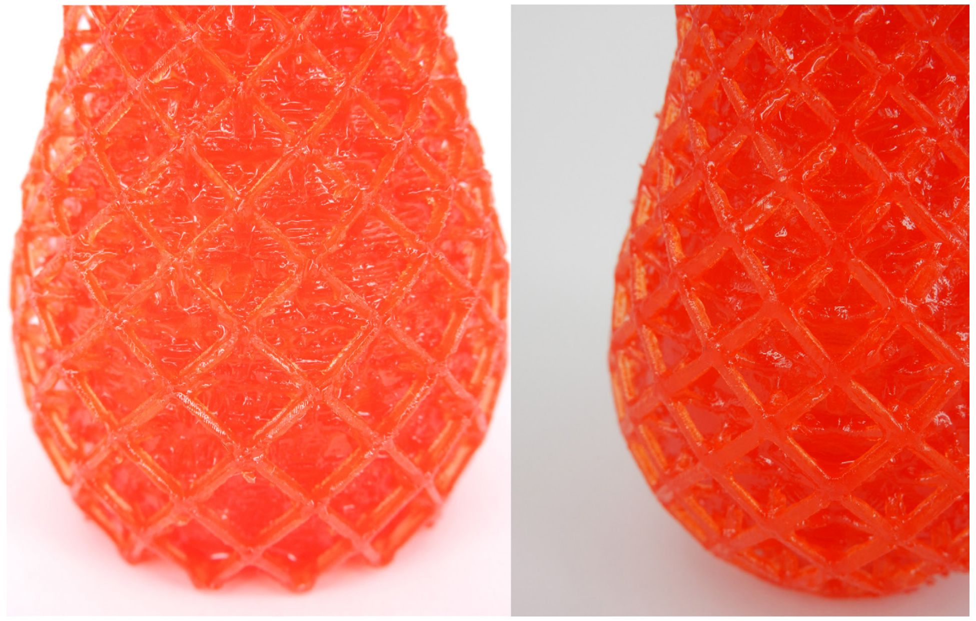

Figure 63: The vase prints had an apex height of 3mm, which is only just enough to keep the struts and beams distinct from the surface.

Figure 64: Vase. External reinforcement for visibility's sake; internal lattice structure would be excellent trellis for plant roots, if an environmentally friendly resin was used.

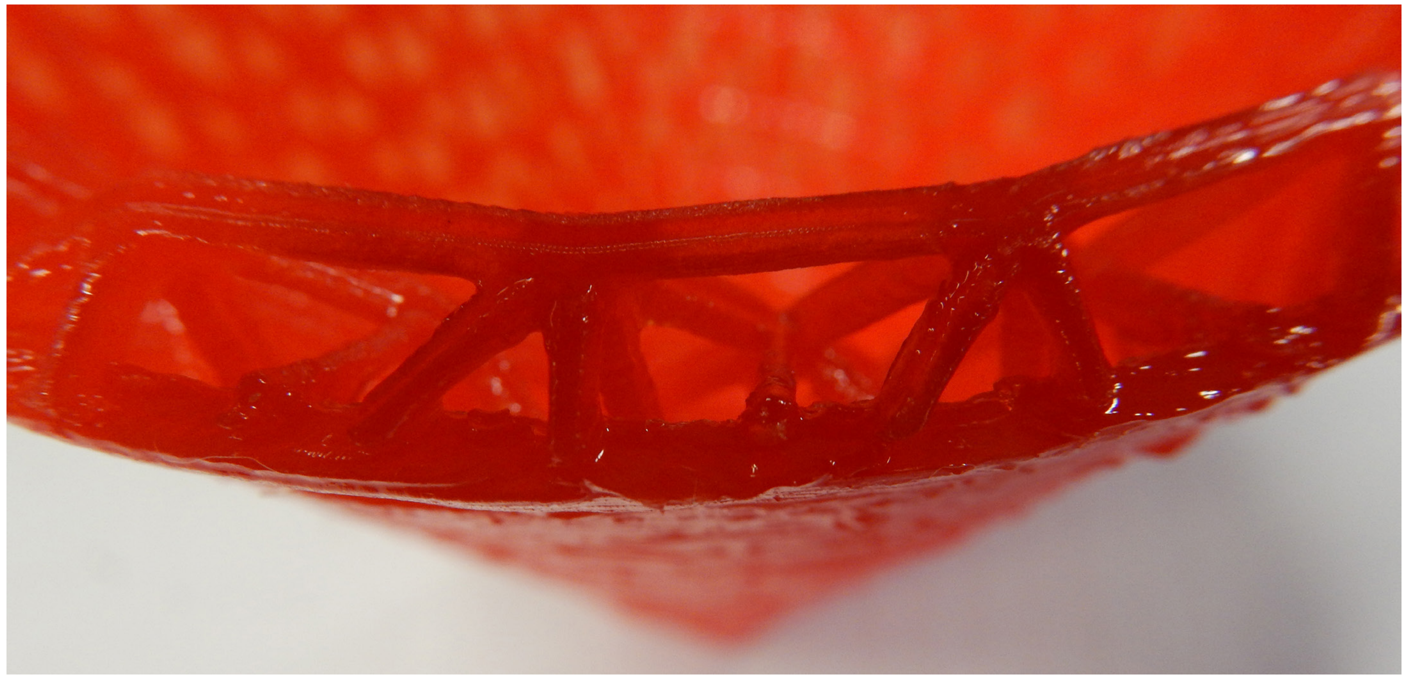

Figure 65: Apex height was increased to 5.5mm. This gives a more easily discernible separation between the lattice structure and the surface.

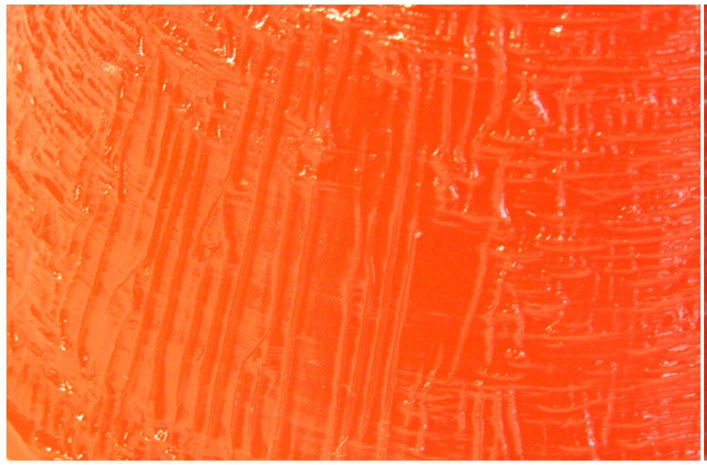

Figure 66: Odd streaks on the outside surface of an internally reinforced basic lampshade.

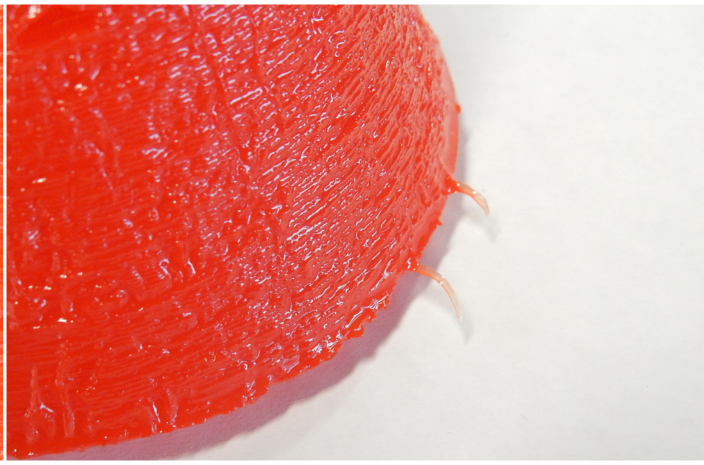

Figure 67: Strange whiskers, possibly a result of refraction through poorly mixed resin.

Figure 68: A texture transition, with resin starvation holes at the right and top right.

Figure 69: A basic lampshade print, showing surface texturing due to poor projector alignment.

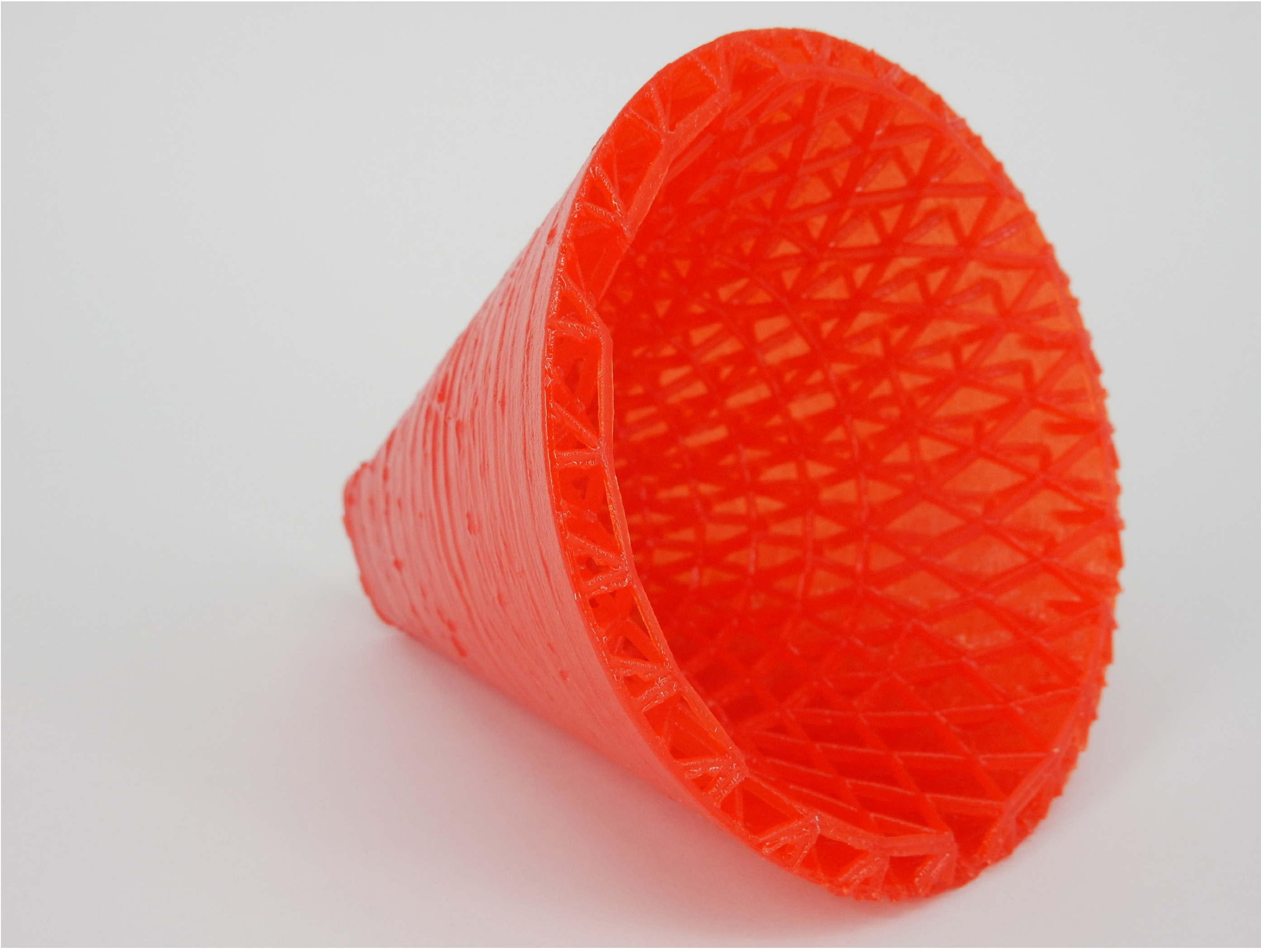

Figure 70: The basic lampshades were printed with different thickness settings.

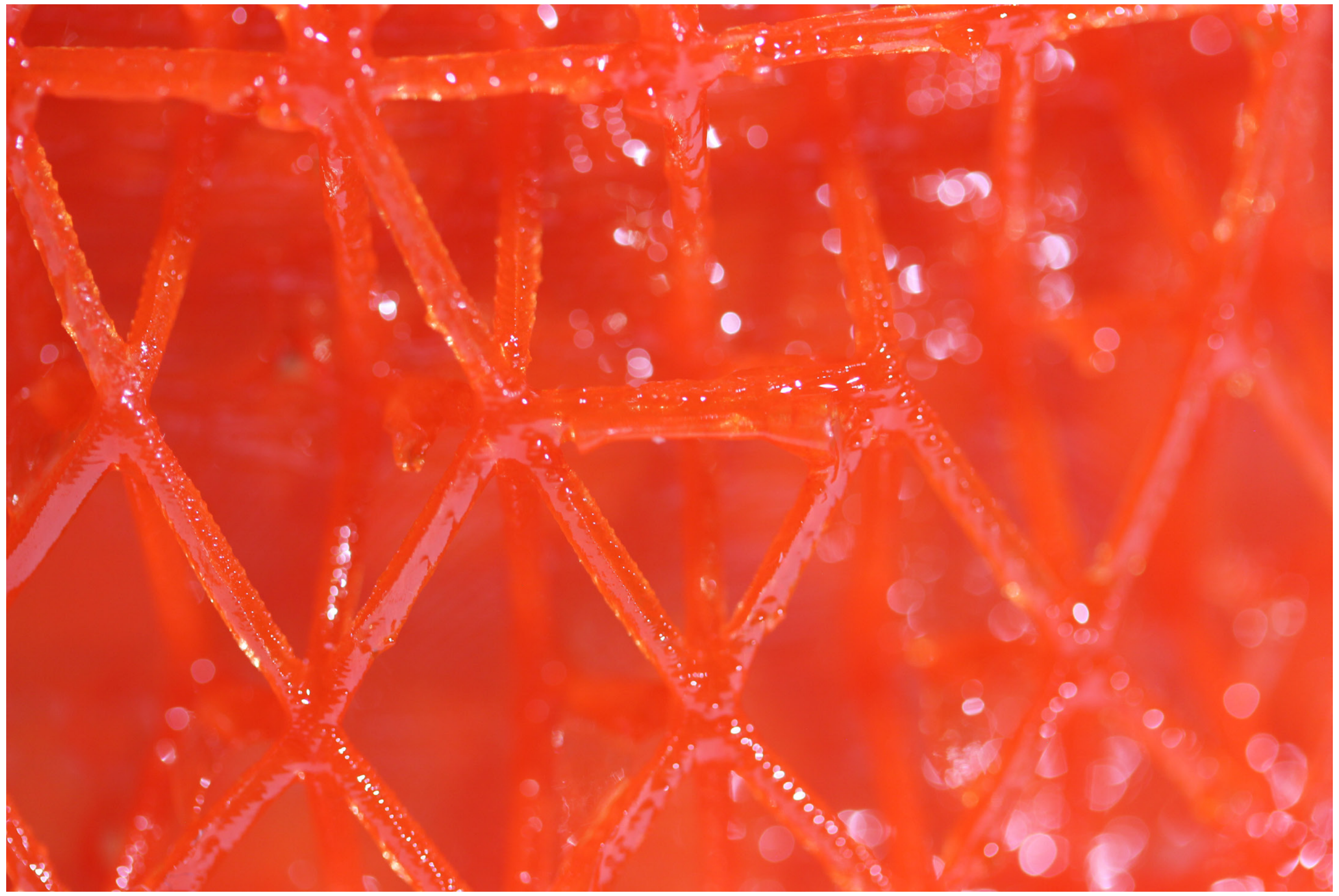

Figure 71: Once projector alignment was corrected, print resolution drastically improved.

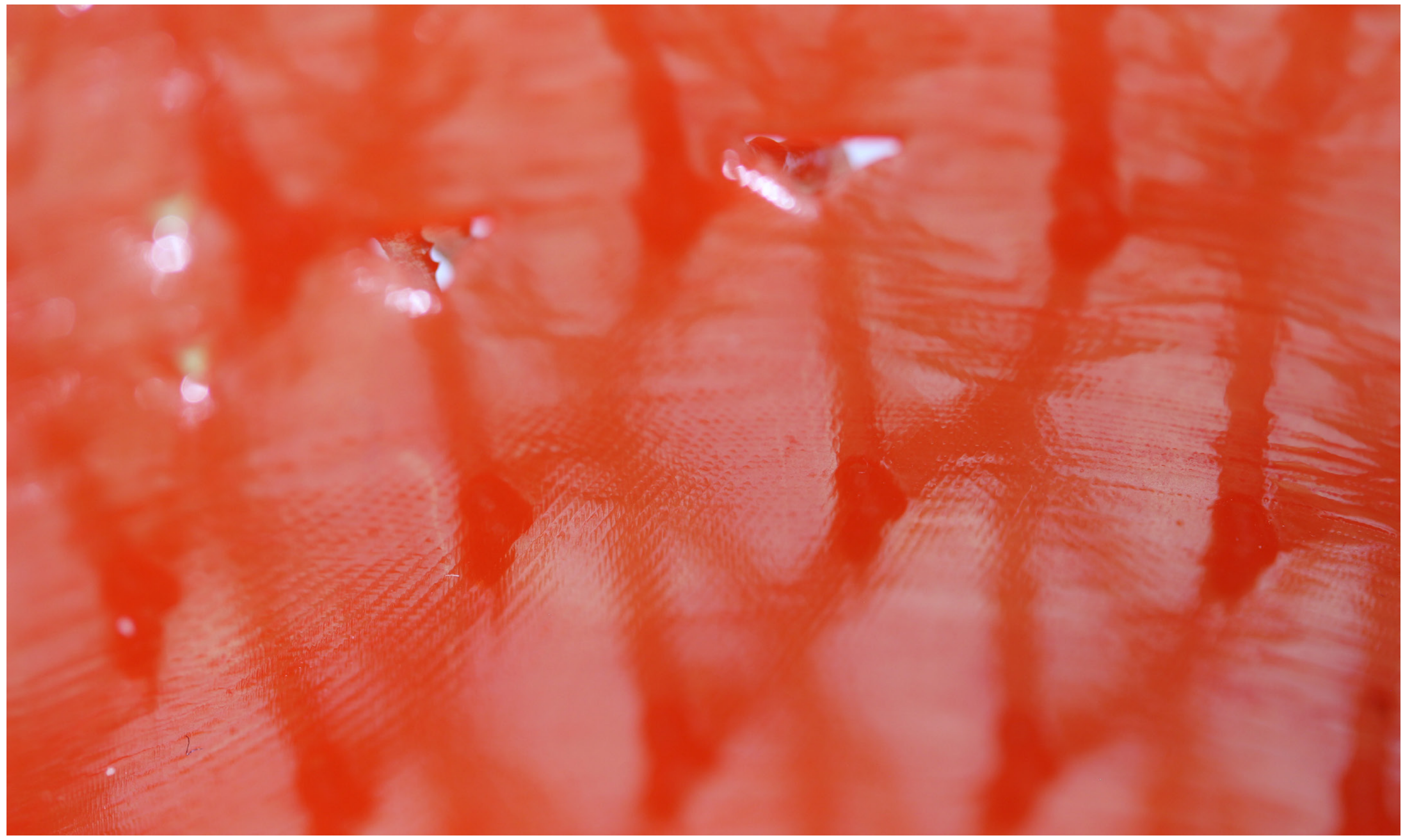

Figure 72: Projector settings alone aren't enough to resolve all issues, so resin starvation holes persisted.

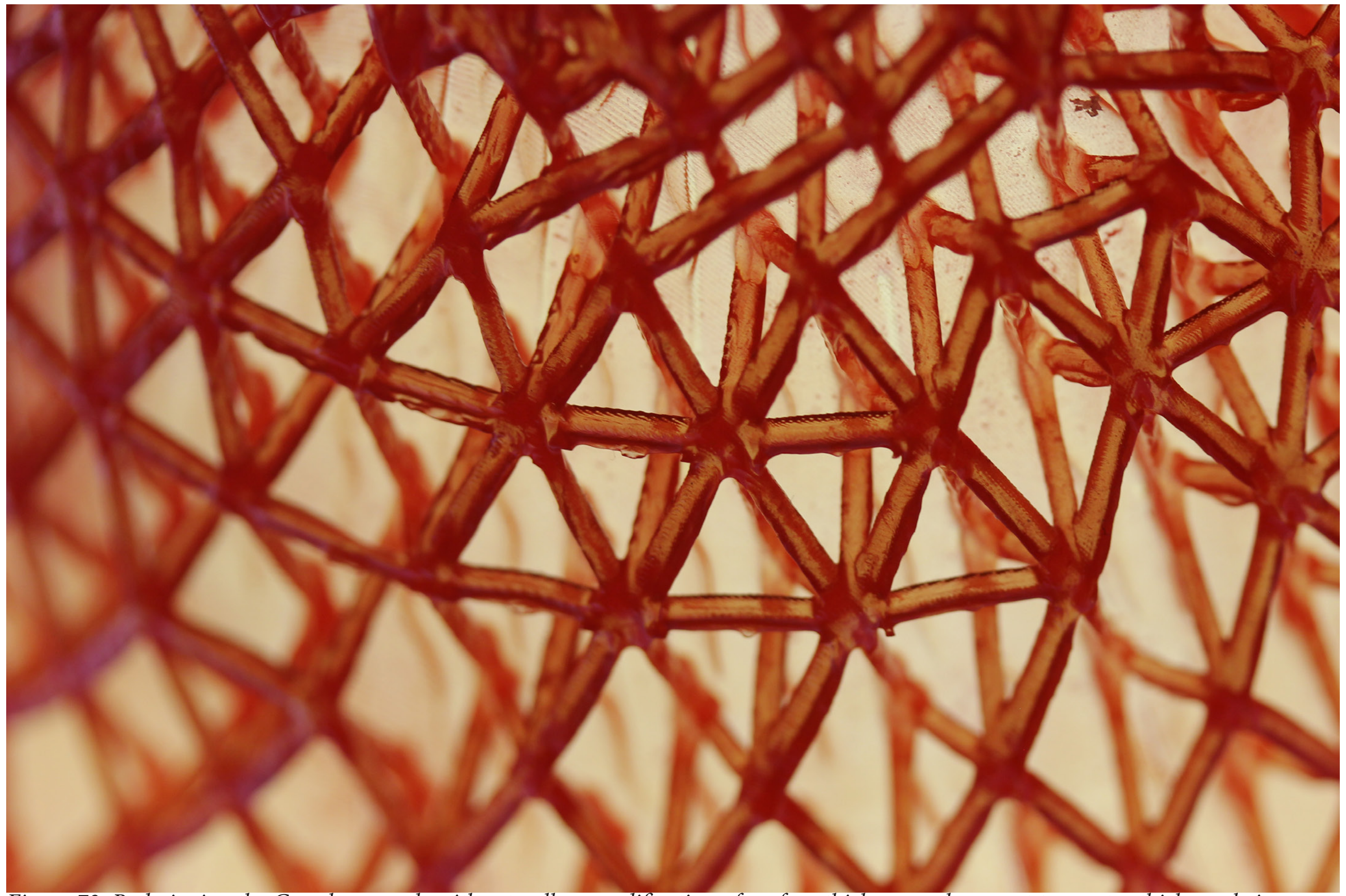
Figure 73: Redesigning the Grasshopper algorithm to allow modification of surface thickness, subsequent to master thickness being set, lead to printability gains via better ratio of surface to lattice mass.


Figure 74: Printing hollow, at 10µm z-layer thickness, lead to superlative quality, at undiminished print speed and size. Visual qualities likewise gained value from increased transparency.

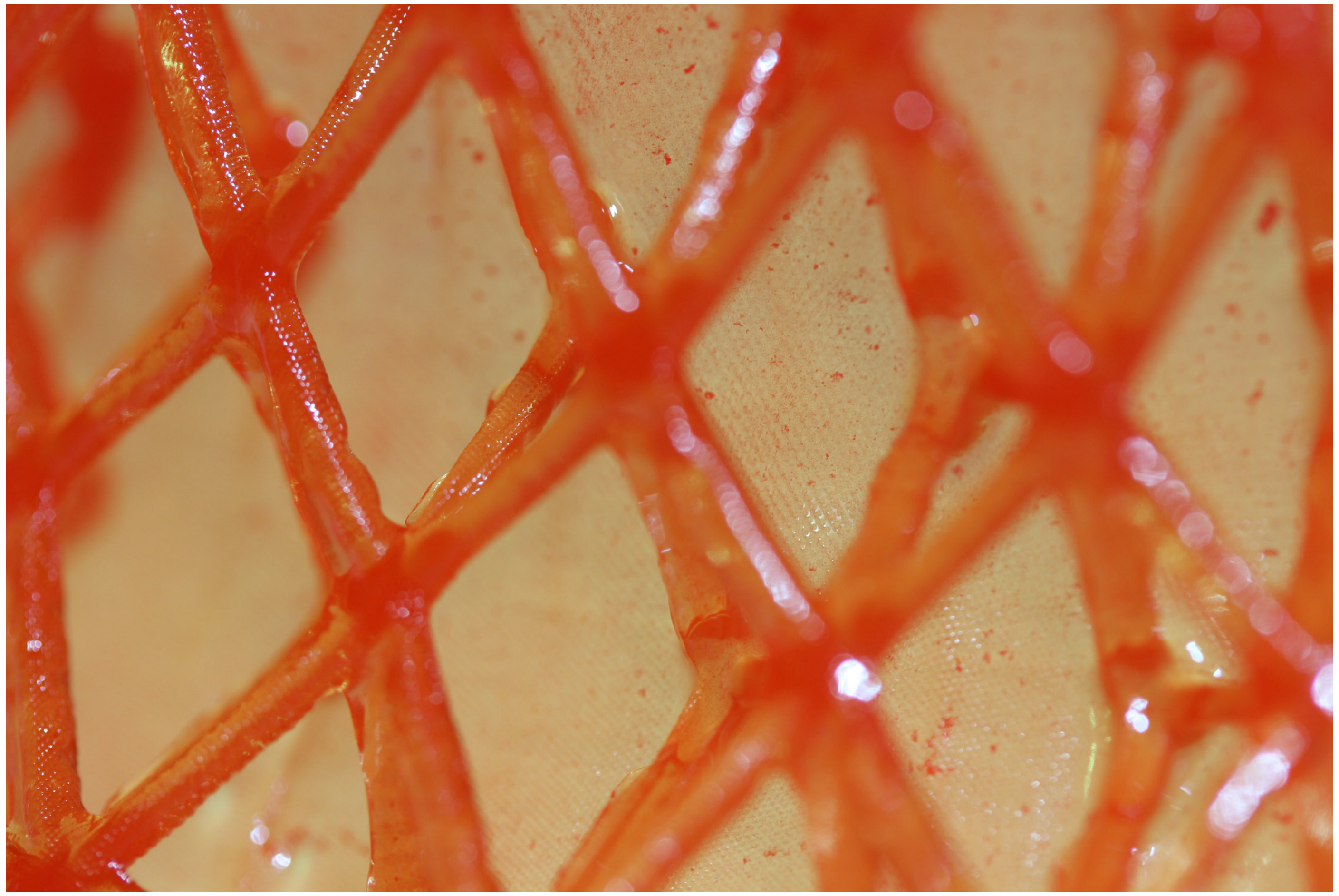
Figure 75: Contrast between a highly translucent surface and more pigmented lattice emphasises the pattern.

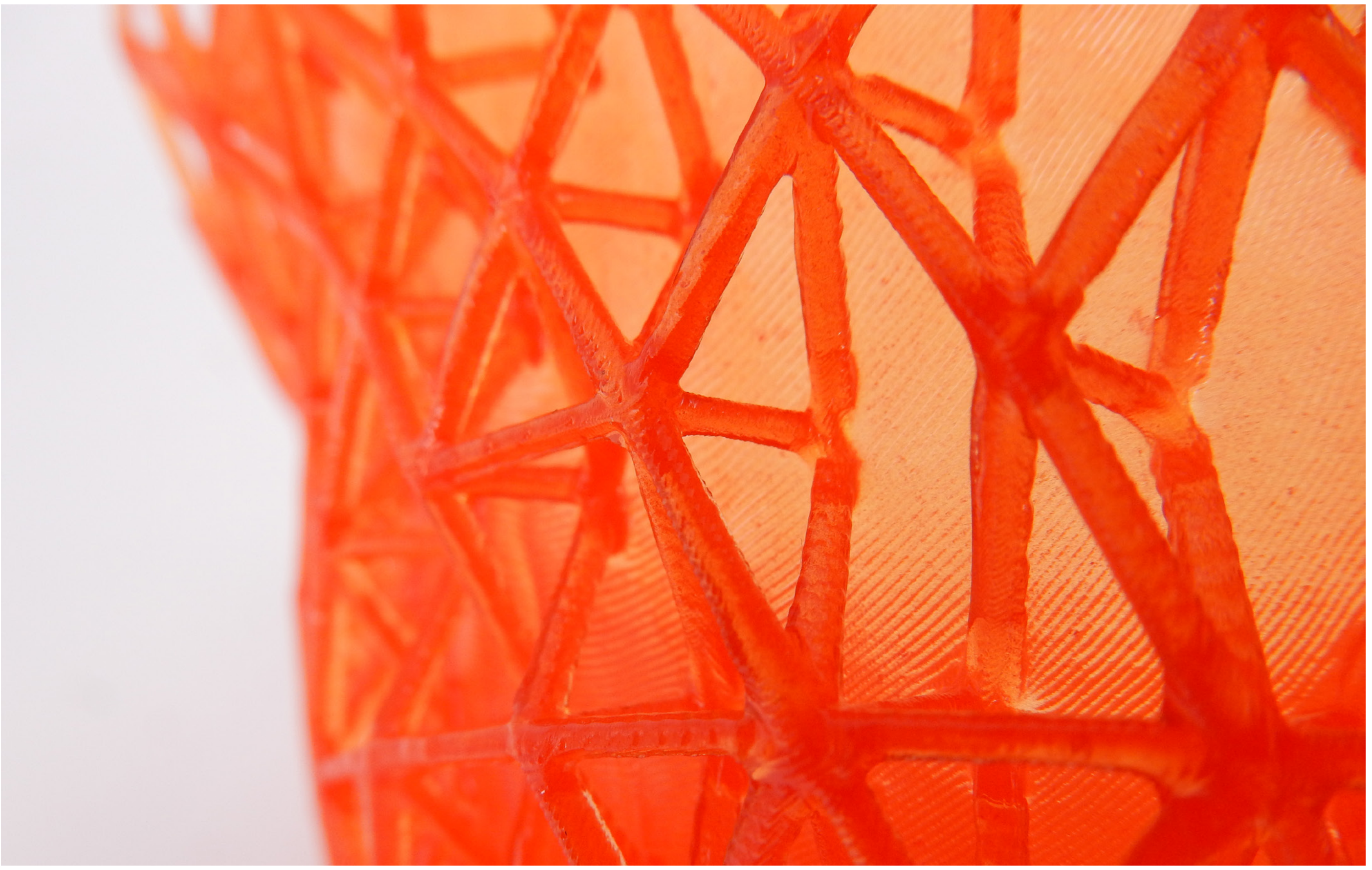
Figure 76: Future implementation of 4K UV projectors, pixel-shifting, and grey-scaling will allow the elimination of xy-banding as seen here, if desired.

Part 3 Discussion

The profusion of variables and their highly complicated relationships make printing varied objects with the Gizimax difficult. The settings an orthodontist uses, for example, will remain the same for every print, since the variety within teeth and jaw models is limited. The orthodontist can zero in on settings that work and then simply reuse them for every print. Printing iteratively, on the other hand, requires continual adoption of revised printer settings. It is mainly for this reason that certain print flaws, although disappointing, remain in end-stage prints, because the proof-of-concept is valid. The massive increase in print quality after the projectors were realigned, and the ability to print hollow with 10μm layer thicknesses, is a strong signal for accuracy. The speed of every print was a conservative 1mm/minute, and while holes in the prints could have been a symptom of speed, there is also the likelihood that they were at least partially caused by dust on the projector lens and introduced into the resin by the unfiltered air intake for the active extraction. Keeping the print speed at a fast-yet-reliable level meant there was one less variable in the web.

Although it is a subordinate consideration to fast, large, and accurate 3D printing, the aesthetic quality of the prints can also be counted as a point in this technique's favour. The ability to quickly print large objects with predictable translucency at high resolution is a welcome one.

Figure 77: Reminiscent of embers, the glowing geometry of the flared lampshade brings something new to the latticed aesthetic.

Conclusion

The idea of this thesis was to design a technique that could demonstrate the fundamental principles of fast, large, and accurate 3D printing simultaneously, and to show that the technique will continue to improve, especially with attention from engineers, chemical and materials scientists, and software developers.

In order to do that, it was shown that DLP printing was already capable of printing fast, or large, or accurate, or any two at once. It was also shown that, because of the limitations of other methods of printing, including bottom-up DLP-style methods, top-down continuous DLP printing is the only way for this method to achieve all three traits at once.

There has been a vast amount of structural engineering-based research into lattice structures in the last twenty years. As a design thesis, it was important for the research to have a solid grounding in the engineering behind the scenes, without itself relying on finite analysis or physical quantification. Similarly, the comprehension and rejection of contemporary state of the art elsewhere - using supports, printing slowly and with high part volume for strength, and nodal unit volume replacement lattice generation - enforced innovation.

Conversely, as a design thesis rather than a materials science one, resin research was somewhat limited. It was required to show that a cheap, standard resin could still be highly functional and effective. Problematic due to its fumes, tendency to get everywhere, and to become temporarily unusable because of pigment settling, it was nevertheless able to be cured at speed and high resolution, over a wide area, which is a massive point in its favour.

For the purposes of this research, in order to design a tool for designing highly customisable and, at the time, undescribed objects, a powerful program like Grasshopper was indispensable. The fact that it is ridiculously complex and has an exponential learning curve served to make using it all the more rewarding. The potential of the algorithm to undergo further development in Grasshopper is vast. What was achieved was limited in scope, but effective and efficient. The variables encoded - density, apex height, thickness, arrangement, links, and mesh export - were collectively sufficient.

Seeing the prints grow in size and complexity as research through design progressed was highly validating. Having tangible results supporting what was otherwise largely a theoretical hypothesis meant that printer limitations and problems were surmountable. The continuing development of printer hardware and methods will eventually render this technique somewhat redundant or less required, but all of that has yet to materialise.

In the meantime, the technique - printing the surface of an object as thin as possible and strengthening it on the non-cosmetically required side with a procedurally generated structural reinforcement lattice that is similarly low-volume - is a prototype. It has been developed to show that fast, large, and accurate are not absolutely mutually exclusive. It has been applied to basic objects, consisting of individual two-sided surfaces due to the Grasshopper algorithm having an input for only one surface at a time. Those basic objects were printed at a speed that would usually exclude one of the other two traits, but didn't.

All figures created by the author.

BIBLIOGRAPHY

3D Printing Technology Comparison: SLA vs. DLP. (n.d.). Retrieved July 10, 2018, from https://formlabs.com/blog/3d-printing-technology-comparison-sla-dlp/

Autodesk Meshmixer. (n.d.). Retrieved July 7, 2018, from http://www.meshmixer.com/

Azman, A. H. (2017). *Method for integration of lattice structures in design for additive manufacturing* (PhD thesis). Université Grenoble Alpes. Retrieved from https://tel.archives-ouvertes.fr/tel-01688758/document

Bartolo, P. J. da S. (2007). Photo-curing modelling: direct irradiation. *The International Journal of Advanced Manufacturing Technology*, *32*(5–6), 480–491. https://doi.org/10.1007/s00170-005-0374-5

BigRep ONE. (n.d.). Retrieved July 2, 2018, from https://bigrep.com/bigrep-one/

Brigante Design. (n.d.). *3D DLP printer success*. Retrieved from https://youtu.be/fPx9K_CLZqM?t=7m20s

Busetti, B., Lutzer, B., & Stampfl, J. (2018). Development of a hybrid exposure system for lithography-based additive manufacturing technologies. In *Laser 3D Manufacturing V* (Vol. 10523, p. 1052305). International Society for Optics and Photonics. https://doi.org/10.1117/12.2286637

Carbon M1 & M2 Build Specs. (n.d.). Retrieved July 3, 2018, from https://www.midwestproto.com/Technologies/clip-build-specs

Compare 3D Printers. (n.d.). Retrieved July 1, 2018, from https://3dprinting.com/pricewatch/

Compare SLS and Carbon's CLIP technolgies. (n.d.). Retrieved July 7, 2018, from https://www.sculpteo.com/blog/2016/09/14/sls-vs-clip/

D'Amico, A. A., Debaie, A., & Peterson, A. M. (2017). Effect of layer thickness on irreversible thermal expansion and interlayer strength in fused deposition modeling. *Rapid Prototyping Journal*, *23*(5), 943–953. https://doi.org/10.1108/RPJ-05-2016-0077

Davidson, S. (n.d.). Grasshopper. Retrieved July 7, 2018, from https://www.grasshopper3d.com/

Daynes, S., Feih, S., Lu, W. F., & Wei, J. (2017). Optimisation of functionally graded lattice structures using isostatic lines. *Materials & Design*, *127*, 215–223. https://doi.org/10.1016/j.matdes.2017.04.082

Desimone, J. M., ERMOSHKIN, A., ERMOSHKIN, N., & Samulski, E. T. (2014). *WO2014126837A2*. World Intellectual Property Organization. Retrieved from https://patents.google.com/patent/WO2014126837A2/en

Du, T. K. (2016). *WO2016179661A1*. World Intellectual Property Organization. Retrieved from https://patents.google.com/patent/WO2016179661A1/en

Effect of Preheating on Microhardness and Viscosity of 4 Resin Composites | jcda. (n.d.). Retrieved June 30, 2018, from http://www.jcda.ca/article/e12

Engelbrecht, S., Folgar, L., Rosen, D. W., Schulberger, G., & Williams, J. (2009). Cellular structures for optimal performance. In *Proc. SFF Symposium. Austin* (pp. 831-842).

Frequently Asked Questions | Formlabs. (n.d.). Retrieved June 27, 2018, from https://formlabs.com/it/support/faq/

Gizmo 3D Printers. (n.d.). Retrieved June 26, 2018, from https://www.gizmo3dprinters.com.au/3d-printers

Goehrke, S. (2018, April 19). Carbon and the "New Future Additive Will Bring": Exclusive Interview. Retrieved July 6, 2018, from https://3dprint.com/210527/carbon-site-interview/

H6510BD. (n.d.). Retrieved June 28, 2018, from https://www.acer.com/ac/en/AU/content/model/MR.JFZ11.00E

Home. (n.d.). Retrieved July 6, 2018, from https://www.ntopology.com/

Hull, C. W. (1986). *US4575330A*. United States. Retrieved from https://patents.google.com/patent/US4575330A/en

INTRA|LATTICE. (n.d.). Retrieved July 11, 2018, from http://intralattice.com/

Invention of Stripes. (n.d.). Retrieved July 6, 2018, from https://theverymany.com/invention-of-stripes/

Janusziewicz, R., Tumbleston, J. R., Quintanilla, A. L., Mecham, S. J., & DeSimone, J. M. (2016). Layerless fabrication with continuous liquid interface production. *Proceedings of the National Academy of Sciences*, *113*(42), 11703–11708. https://doi.org/10.1073/pnas.1605271113

Kantaros, A., & Karalekas, D. (2013). Fiber Bragg grating based investigation of residual strains in ABS parts fabricated by fused deposition modeling process. *Materials & Design*, *50*, 44–50. https://doi.org/10.1016/j.matdes.2013.02.067

Kure, J., Manickam, T., Usto, K., Clausen, K., Chen, D., & Pugnale, A. (2011). Parametric Design and Construction Optimization of a Freeform Roof Structure. In *Computational Design Modelling* (pp. 137–144). Springer, Berlin, Heidelberg. https://doi.org/10.1007/978-3-642-23435-4_16

Lantada, A. D., Romero, A. de B., Isasi, Á. S., & Bellido, D. G. (2017). Design and Performance Assessment of Innovative Eco-Efficient Support Structures for Additive Manufacturing by Photopolymerization. *Journal of Industrial Ecology*, *21*(S1), S179–S190. https://doi.org/10.1111/jiec.12660

Ligon, S. C., Liska, R., Stampfl, J., Gurr, M., & Mülhaupt, R. (2017). Polymers for 3D Printing and Customized Additive Manufacturing. *Chemical Reviews*, *117*(15), 10212–10290. https://doi.org/10.1021/acs.chemrev.7b00074

Lipson, H. (2012, October). Design in the age of 3-D printing. *Mechanical Engineering; New York*, *134*(10), 30–35.

Meshify. (n.d.). Retrieved July 6, 2018, from https://meshify.dk/meshify/

Mezzadri, F., Bouriakov, V., & Qian, X. (2018). Topology optimization of self-supporting support structures for additive manufacturing. Additive Manufacturing, 21, (pp. 666-682).

mUVe 3D DLP ULTIPro 4K Printer and Upgrade Kit. (2017, October 22). Retrieved July 4, 2018, from https://www.muve3d.net/press/product/muve-3d-dlp-ultipro-4k-printer-and-upgrade-kit/

Netfabb. (n.d.). Retrieved July 6, 2018, from https://www.autodesk.com/products/netfabb/overview

NewPro 3D. (n.d.). Retrieved July 2, 2018, from https://newpro3d.com/

Panesar, A., Abdi, M., Hickman, D., & Ashcroft, I. (2018). Strategies for functionally graded lattice structures derived using topology optimisation for Additive Manufacturing. *Additive Manufacturing*, *19*, 81–94. https://doi.org/10.1016/j.addma.2017.11.008

Process. (n.d.). Retrieved June 27, 2018, from https://www.carbon3d.com/process/

ProMaker L7000 D. (n.d.). Retrieved July 2, 2018, from https://www.prodways.com/en/industrial-3D-printers/promaker-l7000-d/

Rethinking foam—Carbon's lattice innovation. (n.d.). Retrieved June 21, 2018, from https://www.carbon3d.com/stories/rethinking-foam-carbons-lattice-innovation/

Sprybuild. (n.d.). Retrieved July 2, 2018, from http://www.sprybuild.com/

Tang, Y., & Zhao, Y. F. (2015). Lattice-skin structures design with orientation optimization. In *Proc. SFF Symposium* (pp. 1378-1393).

Tauböck, T. T., Tarle, Z., Marovic, D., & Attin, T. (2015). Pre-heating of high-viscosity bulk-fill resin composites: Effects on shrinkage force and monomer conversion. *Journal of Dentistry*, *43*(11), 1358–1364. https://doi.org/10.1016/j.jdent.2015.07.014

Tech Specs for the Form 2 | Formlabs. (n.d.). Retrieved July 3, 2018, from https://formlabs.com/3d-printers/form-2/tech-specs/

Testing of Glycerin/Glycerol/Glycerine. (n.d.). Retrieved July 2, 2018, from https://www.gizmo3dprinters.com.au/single-post/2017/01/18/Testing-of-GlycerinGlycerolGlycerine

Thinner 3Dresyn H "Hard diluent." (n.d.). Retrieved June 30, 2018, from https://www.3dresyns.com/products/thinner-3dresyn-uhtf-hard-dilutant

Tiertime UP BOX+ 3D Printer. (n.d.). Retrieved June 25, 2018, from https://3dprinting.com/pricewatch/3d-printer/tiertime-up-box-plus/

Tumbleston, J. R., Shirvanyants, D., Ermoshkin, N., Januszewicz, R., Johnson, A. R., Kelly, D., … DeSimone, J. M. (2015). Continuous liquid interface production of 3D objects. *Science*, *347*(6228), 1349–1352. https://doi.org/10.1126/science.aaa2397

Understanding Our Advanced DLP | 3D Printing. (2017, September 3). Retrieved June 28, 2018, from https://envisiontec.com/better3dprintingtechnology/

UP BOX+. (n.d.). Retrieved July 3, 2018, from https://www.tiertime.com/up-box-plus/

Wang, H., & Rosen, D. (2002). Parametric Modeling Method for Truss Structures. Retrieved July 4, 2018, from https://www.researchgate.net/publication/247110836_Parametric_Modeling_Method_for_Truss_Structures

Yeo, J., Jung, G. S., Martín-Martínez, F. J., Ling, S., Gu, G. X., Qin, Z., & Buehler, M. J. (2018). Materials-by-design: computation, synthesis, and characterization from atoms to structures. *Physica Scripta*, *93*(5), 053003. https://doi.org/10.1088/1402-4896/aab4e2

Zhou, C., Ye, H., & Zhang, F. (2015). A Novel Low-Cost Stereolithography Process Based on Vector Scanning and Mask Projection for High-Accuracy, High-Speed, High-Throughput, and Large-Area Fabrication. *Journal of Computing and Information Science in Engineering*, *15*(1), 011003-011003–011008. https://doi.org/10.1115/1.4028848

Appendix A: FunToDo MSDS

SAFETY DATA SHEET
Fun To Do
Standard Blend

SECTION 1: IDENTIFICATION OF THE SUBSTANCE/MIXTURE AND OF THE COMPANY/UNDERTAKING

1.1. Product identifier

Product name	Fun To Do – Standard Blend
Product No.	FTD SB

1.2. Relevant identified uses of the substance or mixture and uses advised against

1.3. Details of the supplier of the safety data sheet

Supplier
Fun To Do.
Vossenkoog 2-4
1822BG ALKMAAR
Info@funtodo.net

Phonenumber: +31 (0)6542233739

SECTION 2: HAZARDS IDENTIFICATION

2.1. Classification of the substance or mixture

Classification (EC 1272/2008)

	Physical and Chemical Hazards	Not classified.
	Human health	Skin Irrit. 2 - H315;Eye Irrit. 2 - H319;STOT SE 3 - H335
	Environment	Not classified.
Classification (1999/45/EEC)	Xi;R36/37/38.	

The Full Text for all R-Phrases and Hazard Statements are Displayed in Section 16.

2.2. Label elements

Label In Accordance With (EC) No. 1272/2008

Signal Word	Warning	
Hazard Statements		
	H315	Causes skin irritation.
	H319	Causes serious eye irritation.
	H335	May cause respiratory irritation.
Precautionary Statements		
	P271	Use only outdoors or in a well-ventilated area.
	P280	Wear protective gloves/protective clothing/eye protection/face protection.
	P305+351+338	IF IN EYES: Rinse cautiously with water for several minutes. Remove contact lenses, if present and easy to do. Continue rinsing.
	P313	Get medical advice/attention.
	P501	Dispose of contents/container in accordance with national regulations.
Supplementary Precautionary Statements		
	P261	Avoid breathing vapor/spray.
	P264	Wash contaminated skin thoroughly after handling.
	P321	Specific treatment (see medical advice on this label).

P302+352	IF ON SKIN: Wash with plenty of soap and water.
P304+340	IF INHALED: Remove victim to fresh air and keep at rest in a position comfortable for breathing.
P312	Call a POISON CENTER or doctor/physician if you feel unwell.
P332+313	If skin irritation occurs: Get medical advice/attention.
P337	If eye irritation persists:
P362	Take off contaminated clothing and wash before reuse.
P403+233	Store in a well-ventilated place. Keep container tightly closed.
P405	Store locked up.

2.3. Other hazards

SECTION 3: COMPOSITION/INFORMATION ON INGREDIENTS

3.2. Mixtures

Acrylate Monomers Glycol Diacrylate Monomers Phosphine oxide based photo Initiator	
Classification (EC 1272/2008) Skin Irrit. 2 - H315 Eye Irrit. 2 - H319 STOT SE 3 - H335	Classification (67/548/EEC) Xi;R36/37/38.

The Full Text for all R-Phrases and Hazard Statements are Displayed in Section 16.

SECTION 4: FIRST AID MEASURES

4.1. Description of first aid measures

General information

Get medical attention if any discomfort continues.

Inhalation

Move the exposed person to fresh air at once. Get medical attention if any discomfort continues.

Ingestion

Do not induce vomiting. If vomiting occurs, the head should be kept low so that stomach vomit doesn't enter the lungs. Get medical attention. Never give liquid to an unconscious person.

Skin contact

Remove contaminated clothing immediately and wash skin with soap and water. Get medical attention if any discomfort continues.

Eye contact

Immediately flush with plenty of water for up to 15 minutes. Remove any contact lenses and open eyes wide apart. To hospital or eye specialist.

4.2. Most important symptoms and effects, both acute and delayed

Inhalation.

May cause irritation to the respiratory system. No specific health warnings noted.

Ingestion

There may be irritation of the throat

Skin contact

May cause skin irritation/eczema.

Eye contact

Irritating and may cause redness and pain.

4.3. Indication of any immediate medical attention and special treatment needed

SECTION 5: FIREFIGHTING MEASURES

5.1. Extinguishing media

Extinguishing media

Water spray, foam, dry powder or carbon dioxide.

5.2. Special hazards arising from the substance or mixture

5.3. Advice for firefighters

Special Fire Fighting Procedures

Use pressurised air mask if product is involved in a fire. Water spray should be used to cool containers.

SECTION 6: ACCIDENTAL RELEASE MEASURES

6.1. Personal precautions, protective equipment and emergency procedures

Wear protective clothing as described in Section 8 of this safety data sheet.

6.2. Environmental precautions

Avoid discharge to the aquatic environment. Do not discharge into drains, water courses or onto the ground.

6.3. Methods and material for containment and cleaning up

Absorb spillage with suitable absorbent material. Transfer to a container for disposal.

6.4. Reference to other sections

SECTION 7: HANDLING AND STORAGE

7.1. Precautions for safe handling

7.2. Conditions for safe storage, including any incompatibilities

Store in tightly closed original container in a dry and cool place. Protect from freezing and direct sunlight. Keep away from heat, sparks and open flame. Keep away from food, drink and animal feeding stuffs. > 4 °C (39.2 °F), < 27 °C (80.6 °F)

7.3. Specific end use(s)

SECTION 8: EXPOSURE CONTROLS/PERSONAL PROTECTION

8.1. Control parameters

8.2. Exposure controls

Protective equipment

Engineering measures

Provide adequate ventilation.

Respiratory equipment

Wear suitable respiratory protection.

Hand protection

Neoprene gloves are recommended.

Eye protection

Wear tight-fitting goggles or face shield.

Other Protection

Provide eyewash station and safety shower. Wear appropriate clothing to prevent any possibility of skin contact. Wear air-supplied mask in confined areas.

Hygiene measures

Wash hands after contact. Wash hands after handling. Wash promptly with soap & water if skin becomes contaminated. Change work clothing daily if there is any possibility of contamination. Provide shower facilities near the work place. Shower after work. Eating, smoking and water fountains prohibited in immediate work area. DO NOT SMOKE IN WORK AREA!

Skin protection

Protection suit must be worn.

Environmental Exposure Controls

Residues and empty containers should be taken care of as hazardous waste according to local and national provisions.

SECTION 9: PHYSICAL AND CHEMICAL PROPERTIES

9.1. Information on basic physical and chemical properties

Appearance	Viscous liquid.+/- 100mpas

Solubility	Insoluble in water
Relative density	1.13
Vapour pressure	< 0.1 mbar
Flash point	> 93 C > 200 F P/M Pensky-Martens.

9.2. Other information

SECTION 10: STABILITY AND REACTIVITY

10.1. Reactivity

10.2. Chemical stability

Stable under normal temperature conditions and recommended use.

10.3. Possibility of hazardous reactions

Hazardous Polymerization

May polymerize.

10.4. Conditions to avoid

Avoid radical forming substances (metal-ions, peroxides)

10.5. Incompatible materials

Materials To Avoid

Strong acids. Strong alkalis. Amines. Organic peroxides/hydroperoxides.

10.6. Hazardous decomposition products

SECTION 11: TOXICOLOGICAL INFORMATION

11.1. Information on toxicological effects

Toxicological information

No data recorded.

Inhalation

May cause irritation to the respiratory system. No specific health warnings noted.

Eye contact

Irritating to eyes.

Route of entry

Inhalation. Skin absorption. Ingestion.

Specific effects

Dermatitis

SECTION 12: ECOLOGICAL INFORMATION

Ecotoxicity

Dangerous for the environment if discharged into watercourses.

12.1. Toxicity

12.2. Persistence and degradability

12.3. Bioaccumulative potential

12.4. Mobility in soil

12.5. Results of PBT and vPvB assessment

12.6. Other adverse effects

SECTION 13: DISPOSAL CONSIDERATIONS

13.1. Waste treatment methods

Dispose of waste and residues in accordance with local authority requirements.

SECTION 14: TRANSPORT INFORMATION

General — The product is not covered by international regulation on the transport of dangerous goods (IMDG, IATA, ADR/RID).

14.1. UN number

Not applicable.

14.2. UN proper shipping name

Not applicable.

14.3. Transport hazard class(es)

Transport Labels

No transport warning sign required.

14.4. Packing group

Not applicable.

14.5. Environmental hazards

Environmentally Hazardous Substance/Marine Pollutant

No.

14.6. Special precautions for user

Not applicable.

14.7. Transport in bulk according to Annex II of MARPOL73/78 and the IBC Code

Not applicable.

SECTION 15: REGULATORY INFORMATION

15.1. Safety, health and environmental regulations/legislation specific for the substance or mixture

EU Legislation

Regulation (EC) No 1907/2006 of the European Parliament and of the Council of 18 December 2006 concerning the Registration, Evaluation, Authorization and Restriction of Chemicals (REACH), establishing a European Chemicals Agency, amending Directive 1999/45/EC and repealing Council Regulation (EEC) No 793/93 and Commission Regulation (EC) No 1488/94 as well as Council Directive 76/769/EEC and Commission Directives 91/155/EEC, 93/67/EEC, 93/105/EC and 2000/21/EC, including amendments.

15.2. Chemical Safety Assessment

SECTION 16: OTHER INFORMATION

Risk Phrases In Full	
R36/37/38	Irritating to eyes, respiratory system and skin.
Hazard Statements In Full	
H319	Causes serious eye irritation.
R52/53	Harmful to aquatic organisms, may cause long-term adverse effects in the aquatic environment
H315	Causes skin irritation.
H335	May cause respiratory irritation.

Disclaimer

This information relates only to the specific material designated and may not be valid for such material used in combination with any other materials or in any process. Such information is, to the best of the company's knowledge and belief, accurate and reliable as of the date indicated. However, no warranty guarantee or representation is made to its accuracy, reliability or completeness. It is the user's responsibility to satisfy himself as to the suitability of such information for his own particular use.

Appendix B: Grasshopper Algorithm

https://drive.google.com/open?id=1B20qaKIVhx_jV0gwm5_FQH35Fe-pXk1O